



Politecnico
di Bari

Repository Istituzionale dei Prodotti della Ricerca del Politecnico di Bari

Earth-abundant transition metal-based catalysts for sustainable reactions

This is a PhD Thesis

Original Citation:

Availability:

This version is available at <http://hdl.handle.net/11589/248240> since: 2023-03-07

Published version

<http://hdl.handle.net/11589/248240>
DOI: 10.60576/poliba/iris/petrelli-valentina_phd2023

Terms of use:

Altro tipo di accesso

(Article begins on next page)



POLITECNICO DI BARI

D.R.R.S

10

Doctor of Philosophy in Environmental and Building Risk and Development

2022

Coordinator: Prof. Michele Mossa

XXXIV CYCLE
Curriculum: CHIM/07

DICATECh
Department of Civil, Environmental, Building Engineering and Chemistry

Earth-abundant transition metal-based catalysts for sustainable reactions

Prof. Piero Mastrorilli
DICATECh
Polytechnic University of Bari

Prof. Giuseppe Romanazzi
DICATECh
Polytechnic University of Bari

Valentina Petrelli



D.R.R.S

POLITECNICO DI BARI

10

Dottorato di ricerca in Rischio e Sviluppo ambientale,
territoriale ed edilizio

2022

Coordinatore: Prof. Michele Mossa

XXXIV CICLO
Curriculum: CHIM/07

DICATECh

Dipartimento di Ingegneria Civile, Ambientale, del
Territorio, Edile e di Chimica

**Catalizzatori a base di metalli di
transizione abbondanti sulla Terra per
reazioni sostenibili**

Prof. Piero Mastrorilli
DICATECh
Politecnico di Bari

Prof. Giuseppe Romanazzi
DICATECh
Politecnico di Bari

Valentina Petrelli

EXTENDED ABSTRACT

Noble metal nanoparticles have long been playing a central role as heterogeneous catalysts but due to their high cost, their toxicity and scarce availability, they have always been less attractive for industrial application. Moreover, the immediacy of global climate change and the need for a greener chemistry have intensified the efforts in the research of sustainable alternatives. One of the most promising ones, is represented by the use of earth-abundant transition metals that are much more available and offer appealing properties able to overcome the disadvantages of the precious metals.

In this context, the objective of this research thesis has been to develop and optimize innovative procedures for the preparation of new polymer supported transition metal nanoparticles to employ as catalysts for selected model reactions.

In particular, the first part of the work has been focused on the synthesis of cobalt catalysts obtained by copolymerizing the metal-containing monomer $\text{Co}(\text{AAEMA})_2$ with suitable comonomers. The obtained catalyst was tested in the reduction of nitroarenes to the corresponding anilines, showing good capabilities and avoiding the formation of side products. The reactions were performed under mild conditions and the catalyst was easily removed from the reaction products and reused.

The second part of this work deals with the preparation of supported nickel nanoparticles following different procedures, differing from each other for the calcination conditions or for the matrix employed. All materials were characterized by advanced techniques such as transmission of electron microscopy (TEM) demonstrating that the variation of experimental conditions leads to the formation of nanoparticles with different morphology. This feature resulted in different catalytic behavior that permitted to develop a highly selective reduction system for a variety of structurally different nitroarenes towards azoxyarenes. Under optimized reaction conditions, more than twenty azoxyarenes were obtained in good or excellent yields with wide functional group compatibility. The recovery and reuse of the catalytic system were also achieved for up to five runs without appreciable Ni leaching, loss of activity and selectivity as well as nickel nanoparticles agglomeration.

Key words

Earth-abundant transition metals, sustainable chemistry, heterogeneous catalysis, polymer supported nanoparticles, selective reduction, azoxyarenes.

EXTENDED ABSTRACT (Italian version)

Le nanoparticelle di metalli nobili hanno giocato a lungo un ruolo centrale come catalizzatori eterogenei, ma a causa del loro alto costo, della loro tossicità e della scarsa disponibilità, sono sempre state meno attraenti per l'applicazione industriale. Inoltre, l'immediatezza del cambiamento climatico globale e la necessità di una chimica più verde hanno intensificato gli sforzi nella ricerca di alternative sostenibili. Una delle più promettenti è rappresentata dall'uso di metalli di transizione terrestri che sono molto più disponibili e offrono proprietà interessanti in grado di superare gli svantaggi dei metalli preziosi.

In questo contesto, l'obiettivo di questa tesi di ricerca è stato quello di sviluppare e ottimizzare procedure innovative per la preparazione di nuove nanoparticelle di metalli di transizione supportate da polimeri da impiegare come catalizzatori per reazioni modello selezionate.

In particolare, la prima parte del lavoro si è concentrata sulla sintesi di catalizzatori di cobalto ottenuti copolimerizzando il monomero contenente metallo $\text{Co}(\text{AAEMA})_2$ con opportuni comonomeri. I catalizzatori ottenuti sono stati testati nella riduzione di nitroareni alle corrispondenti aniline, mostrando buone capacità ed evitando la formazione di prodotti collaterali. Le reazioni sono state eseguite in condizioni blande e il catalizzatore è stato facilmente rimosso dai prodotti di reazione e riutilizzato.

La seconda parte di questo lavoro si occupa della preparazione di nanoparticelle di nichel supportate seguendo diverse procedure, che differiscono tra loro per le condizioni di calcinazione o per la matrice impiegata. Tutti i materiali sono stati caratterizzati con tecniche avanzate come la trasmissione di microscopia elettronica (TEM) dimostrando che la variazione delle condizioni sperimentali porta alla formazione di nanoparticelle con diversa morfologia. Questa caratteristica ha portato a un diverso comportamento catalitico che ha permesso di sviluppare un sistema di riduzione altamente selettivo per una varietà di nitroareni strutturalmente diversi verso gli azossiareni. In condizioni di reazione ottimizzate, più di venti azossiareni sono stati ottenuti in buone o eccellenti rese con ampia compatibilità dei gruppi funzionali. Il recupero e il riutilizzo del sistema catalitico sono stati raggiunti anche per un massimo

di cinque corse senza apprezzabile lisciviazione di Ni, perdita di attività e selettività così come agglomerazione di nanoparticelle di nichel.

Parole chiave

Metalli di transizione abbondanti sulla Terra, chimica sostenibile, catalisi eterogenea, polimero supportante nanoparticelle, riduzione selettiva, azossiareni.

GENERAL INDEX

<i>1.0</i>	<i>General introduction</i>	<i>9</i>
<i>2.0</i>	<i>Chapter II – Polymer supported cobalt nanoparticles as efficient and recyclable catalyst for the reduction of nitroarenes to anilines</i>	<i>47</i>
<i>3.0</i>	<i>Chapter III – Nickel based catalyst</i>	<i>79</i>
<i>4.0</i>	<i>Chapter IV – Experimental section</i>	<i>121</i>
<i>5.0</i>	<i>Conclusions</i>	<i>133</i>
<i>6.0</i>	<i>Curriculum</i>	<i>137</i>
<i>7.0</i>	<i>References</i>	<i>143</i>

INDEX

<i>1.0 General introduction</i>	11
1.1 Catalysis in green chemistry.....	11
1.2 Chemistry of catalysis.....	15
1.2.1 Activity.....	17
1.2.2 Selectivity.....	17
1.2.3 Stability.....	18
1.3 Homogeneous catalysts.....	19
1.4 Heterogeneous catalysts.....	20
1.5 Nanoparticles: bridging the gap between homogeneous and heterogeneous catalyst.....	23
1.6 Application of nanomaterials: Nanocatalysis.....	27
1.7 Metal nanoparticles.....	30
1.8 The role of support.....	32
1.9 Polymer supported metal nanoparticles.....	34
1.10 Aim of this work.....	45
<i>2.0 Polymer supported cobalt nanoparticles as efficient and recyclable catalyst for the reduction of nitroarenes to anilines</i>	49
2.1 Cobalt Chemistry and major catalytic application.....	49
2.2 Synthesis and characterization of cobalt (II)- containing monomer: Co(AAEMA) ₂	51
2.3 Synthesis and characterization of a cobalt-containing polymer from Co(AAEMA) ₂ : Co(AAEMA) ₂ -pol and Co-pol.....	56
2.3.1 TEM analysis.....	60
2.4 Catalytic activity of Co-pol in the reduction of nitroarenes to anilines.....	65
2.4.1 Overview on the reduction of nitroarenes to corresponding anilines.....	65
2.4.2 Optimal reaction conditions for the reduction of nitroarenes to anilines mediated by Co-containing polymers.....	67
2.4.3 Scope and general applicability of Co-pol catalytic system.....	72
2.4.4 Recyclability of Co-pol.....	74
2.4.5 Analysis of Co-pol recovered after reduction.....	75
2.5 Conclusions.....	77
<i>3.0 Nickel based catalyst</i>	81
3.1 Chemistry of nickel and major catalytic application.....	81
3.2 Influence on catalytic activity of different morphologies.....	86

3.2.1 Synthesis and characterization of Ni(II)complex: Ni(AAEMA) ₂	87
3.2.2 Synthesis of Ni-res1 and Ni-res2	89
3.2.3 Characterization of Ni-res1 and Ni-res2: TEM analysis in STEM mode	90
3.2.4 Catalytic activity of Ni-res1 and Ni-res2.....	92
3.2.5 Concluding remarks on Ni-res1 and Ni-res2	93
3.3 Efficient and selective reduction of nitroarenes towards azoxyarenes catalysed by Ni nanoparticles supported on an acrylamide-based resin	94
3.3.1 Importance of azoxyarenes	94
3.3.2 Synthesis of Ni-cat and Ni-cat1	98
3.3.3 Characterization of Ni-cat and Ni-cat2	99
3.3.4 Catalytic activity of Ni-cat and Ni-cat2 in the selective reduction of nitrobenzenes towards azoxyarenes	110
3.3.5 Recyclability	117
3.4 Conclusions	118
4.0 Experimental section.....	122
4.1 Materials for the synthesis of Co-pol and Ni-pol.....	122
4.1.1 Co(AAEMA) ₂	124
4.1.2 Co(AAEMA) ₂ -pol	124
4.1.3 Co-pol catalyst.....	125
4.1.4 Ni(AAEMA) ₂	125
4.1.5 Ni(AAEMA) ₂ -res	126
4.1.6 Ni(AAEMA) ₂ -res1	126
4.1.7 Ni(AAEMA) ₂ -res2.....	126
4.1.8 Ni(AAEMA) ₂ -cat.....	126
4.1.9 Ni-cat.....	127
4.1.10 Ni-cat2.....	127
4.2 Materials and procedure for catalytic reaction.....	127
4.2.1 Typical experimental procedure for the reduction of nitroarenes with Co-pol catalyst	128
4.2.2 Recycling of Co-catalysts	129
4.2.3 Typical experimental procedure for the reduction of nitrobenzene with Ni-res ₁ and Ni-res ₂	129
4.2.4 Typical experimental procedure for the selective reduction of nitroarenes by using Ni-cat2	129
4.2.5 Recycling of catalyst Ni-cat2	130
Conclusions	134
Curriculum vitae	138
References.....	144

CHAPTER I

General introduction

1.0 General introduction

1.1 Catalysis in green chemistry

The term *catalysis* (from the Greek *κατα*- “down” and *λυειν* “loosen”) was first introduced by the Swedish chemist Jöns Jacob Berzelius¹ in 1836 in order to rationalize a large number of experimental observations made by chemists in the late 18th and early 19th centuries like the wine and beer fermentation and the decomposition of H₂O₂ by metals, just to mention a few.^{2,3} In a report to the Swedish Academy of Sciences, he proposed the existence of “a new catalytic force acting on the matter” and defined the processes fostered by this force as “catalysis”.⁴

Toward the end of 19th century, Wilhelm Ostwald, with the support of chemical thermodynamics and kinetics, qualified the catalysts as substances able to alter the rate of chemical reactions without appearing in the final products.⁵ Some years later, in 1912, the studies of French chemist Paul Sabatier on the hydrogenation of unsaturated organic compounds using finely divided metals led to the award of Nobel Prize in Chemistry and can be also considered one of the main contributions that gave rise to modern oil hydrogenation and synthetic methanol industries.^{6,7}

During this period, it became quite clear that catalysis was applicable in most chemical processes and that by implementing catalysis in an industrial process might result in extremely beneficial outcomes. Since then, many processes have been developed in response to driving forces like the Chilean embargo on saltpeter as a nitrate source along with the growing European demand for ammonia. Such driving forces motivated Haber and Bosch to develop a process for the fixation of atmospheric nitrogen in ammonia synthesis;⁸ or in the same way the war requirements first, and the automotive market then, have spurred the petrochemical sector, the oil (hydrocarbon) acid cracking process, and hydrocarbon refinery catalysts.^{9,10}

Industrial catalysis has always been closely connected to changes in society. Starting in the 1960s, the massive industrial development has been accompanied by the rise of people's awareness about the environment and the risks derived from pollution, which required the establishment of laws and regulations to control emissions of atmospheric

pollutants, manage correctly recycling activities, and incentivize the use of renewable and alternative feedstocks.¹¹

The complexity determined by this scenario required innovative solutions and new approaches. This led to the foundation of the concept of “Green Chemistry”, which is considered as the “design of chemical products and processes that reduce or eliminate the use and generation of hazardous substances”.¹² In 1998, Paul Anastas and John Warner introduced the Twelve Principles of Green Chemistry to achieve sustainability by harnessing chemical innovations to meet environmental and economic goals simultaneously.^{13,14} The Twelve Principles (**Fig.I.1**) are a guiding framework for the design of new chemical products and processes, applied to all aspects of the process lifecycle from the raw materials used to the efficiency and safety of the transformation, the benignity and biodegradability of products and reagents used.

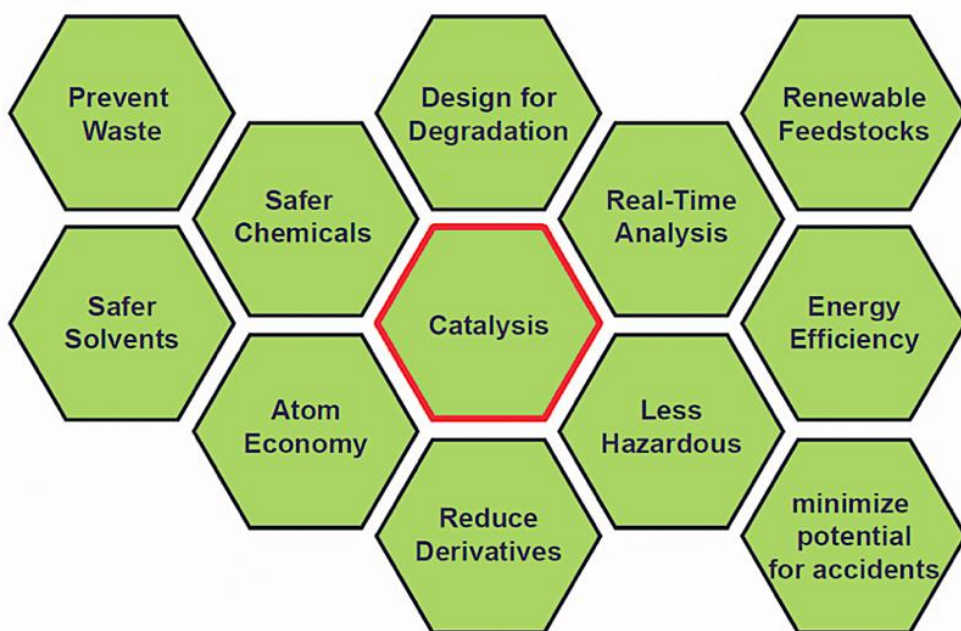


Fig.I.1-Principles of green chemistry.

Said in other words, “Green chemistry” aims at reducing the environmental impact of both chemical products and the processes by which they are produced. In this perspective, catalysis plays a crucial role because it makes possible to operate on several fronts. Having bespoke catalyst allows the designing of eco-friendly processes that eliminate waste at the source through the use of alternative raw materials and it also ensures pollution prevention rather than a mere waste remediation.¹⁵

In Green Chemistry, two parameters, the E-factor¹⁶ and the Atom Efficiency (AE)¹⁷, have been introduced to quantify the eco-sustainability of a transformation. The E-factor indicates the kg of waste per kg of product and AE measures the percentage of the starting material that ends up in products. These two parameters are obviously interconnected. Considering an overview of organic reactions, it is possible to identify some reaction types that have a low E-factor and high AE. Examples of this green general organic reaction type are hydrogenations or C–C couplings catalyzed by transition metals such as Suzuki, Heck, Sonogashira, Buchwald and so on.

Nowadays approximately 85-90% of the products of the chemical industry are made with the aid of catalytic conversions in at least one of the productions steps.^{18,19} The improvement of the quality of chemical products and the steadily decreasing production costs of bulk and fine chemicals can be ascribed to increased knowledge in catalytic systems. Chemical reactions with a long lifetime can be accomplished in minutes or hours and under feasible conditions of pressure and temperature using a suitable catalyst.

The versatility of transition metals as catalysts is due to the availability of *d*-orbitals, filled or empty, that have energy suitable for interaction with a wide variety of functional groups of organic compounds. As an example, it can be recalled the interaction of transition metals with alkenes.²⁰ Simple alkenes are relatively unreactive, being ignored by almost all bases and nucleophiles, requiring a reactive radical or a strong electrophile or oxidizing agent, such as bromine, ozone, or osmium tetroxide. But their reactivity changes when they are coordinated to transition metals and can undergo several organic reactions. Many of the industrially relevant catalytic processes in the fine chemical industry are still based on the second and third row rare late transition metals such as

Pd, Pt, Rh, Ru and Ir.²¹⁻²⁴ Although these metals exhibit very good catalytic performance for advanced organic substrates, the continuous development of their applications are hampered by their high prices caused by the decreasing availability and by their toxicity. Metal residues of these noble metals in pharmaceuticals are subject to strict official regulations in order to minimize their amounts to low ppm level.

Instead, the Earth-abundant first-row transition metals including Mn, Fe, Co, Ni and Cu (“bio metals”) have been comparatively underutilized until the past few years, because of their labile nature compared to their second- and third-row counterparts, complex mechanistic manifolds and less obvious catalytic properties.²⁵

The green and sustainable development of chemicals processes is an essential component of the transition from a linear economy that is exhausting the earth natural resources to a resource-efficient circular economy based also on new design of waste-free processes.

The idea of sustainable development was first introduced some years before the green chemistry concept, in 1987, and it is defined as a *development that meets the needs of the current generation without compromising the ability of future generations to meet their own needs*. Sustainability is dependent on the rates of both resource usage and waste generation.^{26, 27} For this reason, a sustainable process needs to fulfill two conditions:

- Natural resources should be used at rates that do not unacceptably deplete supplies over the long term.
- Residues should be generated at rates no higher than what can be promptly assimilated by the natural environment.

A balance needs to be found between economic and industrial development and environmental impact. Bearing in mind the relevance of sustainability for the long-term development of new catalysts, this research thesis is focused on the use of catalytic nanoparticles based on first row transition metals. Indeed, despite the

prevalence of precious metals in catalysis, there are many problems associated with their extreme use in catalytic processes and toxic effects, as mentioned above. The precious metals are scarce in nature and due to their low abundance and arduous extraction processes they are also very expensive. It is estimated that less than 1% of precious metals are recycled for reuse, in fact they often require special measures that generate a significant amount of waste. Conversely, the first-row transition metals including iron, cobalt, nickel, and copper are among the most abundant metals in the Earth's upper crust, thus being readily accessible and provide some additional advantages such as low cost, global availability, chemical versatility, and minimal safety concerns.

1.2 Chemistry of catalysis

Chemical reactions occur when atoms or molecules collide with each other at an energy level higher than the one needed for the bond cleavage or for the formation events to happen. This energy is known as activation energy (E_a) and is dependent on the temperature and concentration of the reagents.²⁸ Through the Arrhenius equation (eq. 1) is possible to correlate the reaction rate constant (k) with its activation energy as follows:

$$k = Ae^{\left(-\frac{E_a}{RT}\right)}$$

Eq.1

where A is the frequency or pre-exponential factor and $e^{(-E_a/RT)}$ represents the fraction of collisions with enough energy to overcome the activation barrier (i.e. that occur with an energy bigger or equal to the activation energy) at temperature T . At the molecular level, the role of a catalyst is to bind molecules, break their bonds, lets the fragments react, and then release the product, after which the catalyst is available again for the next reaction cycle. In simple terms, the catalytic cycle can be described as shown in **Fig.I.2**.²⁹ The intermediates in the cycle (Cat-R in **Fig.I.2**) are in most cases short-living and difficult to detect.

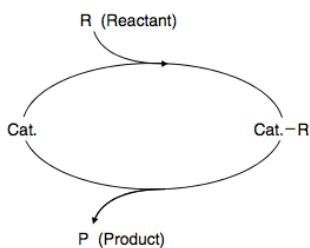


Fig.I.3- Catalytic cycle.

Through an uninterrupted and repeated cycle of elementary steps, the essence of the catalysis phenomenon is to speed up the reaction rate by providing an alternative pathway with smaller activation energy, allowing it to proceed more easily than what would have been in case of an uncatalyzed reaction (**Fig.I.3**).³⁰ The catalyst is not consumed in the reaction, so it is not identified in the final stoichiometric quantity of the reaction. It is important to recall that catalysis is a kinetic phenomenon, therefore it does not alter the thermodynamics of the reaction because it does not affect the energy of the reactants or products

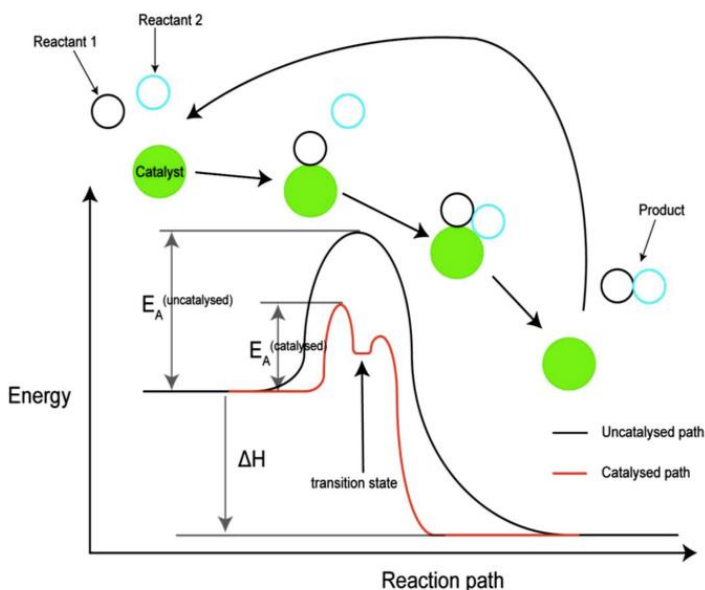


Fig.I.3-This graph compares potential energy diagrams for a single-step reaction in the presence and absence of a catalyst. The effect of the catalyst is to change the reaction mechanism thus lowering the activation energy of the reaction.

In theory, an ideal catalyst is not consumed during the reaction and regenerates indefinitely, but in practice, all catalysts have a finite lifetime. Owing to competing reactions in the reaction environment, the catalyst may undergo chemical changes that affect its action. For these reasons, before moving on to a general classification of catalysis, it is appropriate to evaluate three critical requirements of any catalyst if it is to be exploited for a given chemical process:

- Activity;
- Selectivity;
- Stability (deactivation behavior);

1.2.1 Activity

Activity is a measure of how fast one reaction proceeds in the presence of the catalyst. The reaction rate is calculated as the rate of change of the amount of substance of one reactant A with time relative to the reaction volume or the mass of the catalyst. Activity can be defined in terms of turnover number (TON) and turnover frequency (TOF).³¹ While TON specifies the maximum use that can be made of a catalyst for a special reaction under defined conditions by several molecular reactions or reaction cycles occurring at the reactive center up to the decay of activity, TOF quantifies the turnover number occurring in a certain period of time.

1.2.2 Selectivity

The selectivity of a reaction is the fraction of the starting material that is converted to the desired product. It is expressed by the ratio of the amount of desired product to the reacted quantity of a reaction partner and therefore it provides information about the course of the reaction. Having a selective catalyst available would reduce waste and ensure efficient use of available raw materials. Selectivity, in turn, can be distinguished into chemoselectivity, regioselectivity, diastereoselectivity and enantioselectivity. Chemoselectivity is the preferential outcome of a chemical reaction among a set of possible alternative reactions. It may also refer to the selective reactivity of a particular functional group among another functional group.³²

1.2.3 Stability

The chemical, thermal, and mechanical stability of a catalyst determines its lifetime in industrial reactors. Catalyst stability is influenced by numerous factors, including decomposition, coking, and poisoning. Catalyst deactivation can be followed by measuring activity or selectivity as a function of time.

One of the biggest challenges in catalysis is to create catalysts that exhibit extreme stability, remarkable activity and high selectivity. These factors are the ones on which comparisons between the different kind of catalysts are usually made. Given the large number of different types of catalysts a detailed classification can be quite a challenge. Generally, catalysis can be classified into three broad groups, each of them characterized by its own advantages and limitations: bio-catalysis, homogeneous catalysis, and heterogeneous catalysis. Biocatalysts are typically enzymes, or naturally occurring complex protein molecules, that catalyze reactions with remarkable activity and selectivity under mild conditions, generally at room temperature in an aqueous solution at pH values near 7. Their limitation is that they are sensitive, unstable molecules that are destroyed by extreme reaction conditions. They work well only at physiological pH values in very dilute solutions of the substrate but are very expensive and difficult to obtain in pure form. Homogeneous and heterogeneous catalysts are defined according to the state of aggregation in which they act compared to that of the other reaction components. They will be discussed in more detail in the subsequent section.

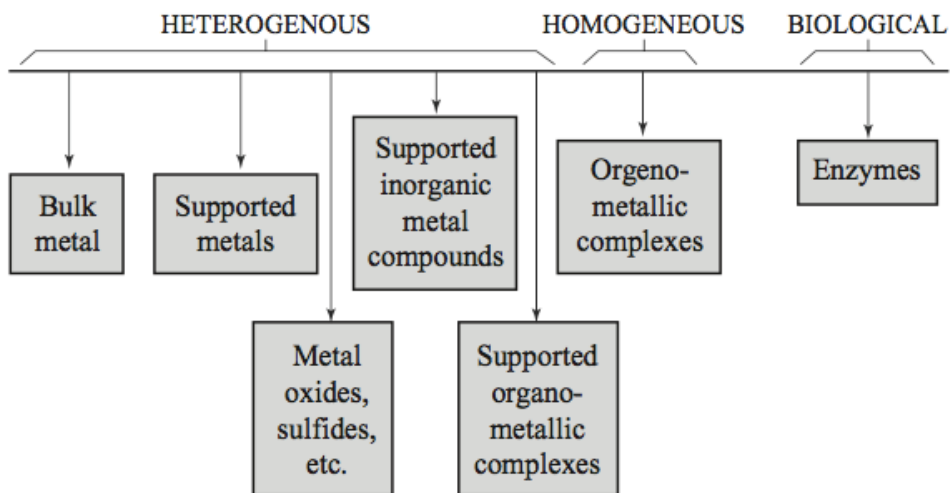


Fig.I.4-General classification of catalyst.

As shown in **fig.I.4**,³³ for heterogeneous catalysts some categories frequently referred to are:

- Pure metals.
- Metal compounds (metal oxides, metal sulfides, salts, etc).
- Supported metals.

1.3 Homogeneous catalysts

A homogenous catalyst is a catalyst that is in the same phase as the substrates for the reaction, frequently the liquid phase.³⁴

The fact of being dispersed in the same medium reaction determines a higher degree of dispersion, so in theory, all sites are available for the reaction and each individual atom can be catalytically active.

Moreover, the high mobility of the molecules in the reaction mixture results in more collisions with substrate molecules. The reactants can approach the catalytically active center from any direction, and a reaction at an active center does not block the neighboring centers. This allows the use of lower catalyst concentrations and milder reaction conditions.

An important class of homogeneous catalysts is that of the coordination complexes consisting of a metal center surrounded by a set of organic ligands. Both the metal and the large variety of ligands determine the properties of the catalyst. In particular, the ligands impart solubility and stability to the metal complex and can be used to tune the selectivity towards the synthesis of a particularly desirable product. By varying the size, shape, and electronic properties of the ligands, the site at which the substrate binds can be constrained in such a way that only one of many possible products can be produced.^{35,36}

Despite all these advantages, the major drawback of homogeneous catalysts is the difficulty of separating the catalyst from the final product.³⁷

Homogeneous catalysis covers only a small portion of the industry. Because is useful only when selectivity to a higher added value product is not possible in another way or there is no alternative process. For example, hydroformylation, the production of aldehydes from alkenes and syngas (hydrogen + carbon monoxide), is carried out on a million-ton scale worldwide. The reaction is carried out only with a homogeneous rhodium catalyst, because too many side reactions occur with heterogeneous catalysis.³⁸

The most common separation methods used are precipitation/filtration of the product, the distillation of the product, destructive catalyst precipitation, extraction/liquid-liquid phase separation. All these procedures are often costly, environmentally unfriendly, and mostly accompanied by common disadvantages like incomplete complex recovery, decomposition of the catalyst, and its deactivation.

1.4 Heterogeneous catalysts

With the heterogeneous catalysts, the catalytic process is considered a surface phenomenon. In fact, phase boundaries are always present between the catalyst and the reactants, and the catalytic reaction occurs at the interface between the reaction mixture and the catalyst surface.^{39,40} The catalytic cycle requires adsorption of reagents first and desorption of products after and for this reason it is affected by diffusion issues.

This type of catalysts is characterized by high thermal stability and increased resistance to oxygen and humidity. However, the main advantage is that being usually a solid material, it is easy to separate from the gas and/or liquid reactants and products of the overall catalytic reaction, allowing easy recyclability for multiple times. Simple and cheap techniques such as filtration and decantation can be used for a successful separation. Nevertheless, each separation method has its own limitations in terms of cost, efficiency, or generation of secondary waste. Due to these problems, in the last years alternative solutions like magnetic separation have emerged as a robust, highly efficient, and rapid separation tool with many other advantages compared to the most used techniques.⁴¹

The heart of a heterogeneous catalyst involves the active sites at the surface of the solid. The latter can reduce the potential energy barrier or the activation energy in the reaction paths by temporarily forming weak chemical bonds with the adsorbing molecules. Either too strong or too weak, the bonding between the active sites and the reacting species could lead to poor catalytic performance. It is possible to recognize two primary functions attributable to active sites, that are promoting the reaction kinetics and controlling the product selectivity. The concept of active sites in heterogeneous catalysis was firstly introduced by Tylor in 1925.⁴² He suggested that only a small fraction of catalyst surface (active sites or centers), which might be composed of an atom, or an ensemble of atoms situated at surface defects such as corners, edges, and other crystalline discontinuities, is catalytically active.⁴³

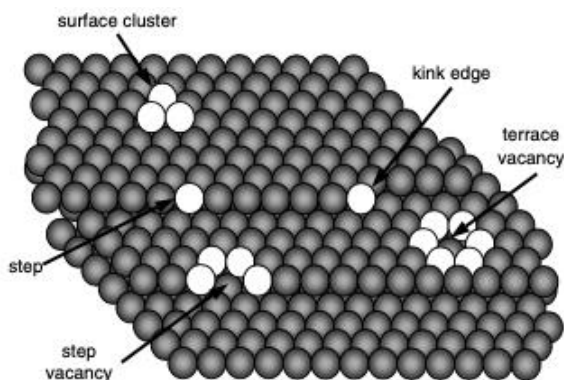


Fig.I.5-Schematic representation of a solid catalyst crystal surface.

Even if the active sites should be all identical, and isolated from each other, solid materials used as catalysts are often amorphous, multicomponent, with surface defects and containing many different types of active sites.

The catalyst is typically a high-surface area material, and it is usually desirable to maximize the number of active sites per reactor volume. This goal is achieved by using particles with sizes in the nanometer length scale. Since catalyst metals, for example, are often expensive materials, it is economically advantageous to employ the catalysts as nanometer-sized particles and support them on the surface of an inert material or metal oxide.⁴⁴

Moreover, heterogeneous catalysts can often be used as fixed beds in reactors for flow chemistry.⁴⁵ In this system the reagents are continuously pumped through the reactor and the products are continuously collected. The separation of the products from the catalyst is built into the process and the catalyst is always kept under the conditions of temperature, pressure, contact with the substrate and products, for which it has been optimized.

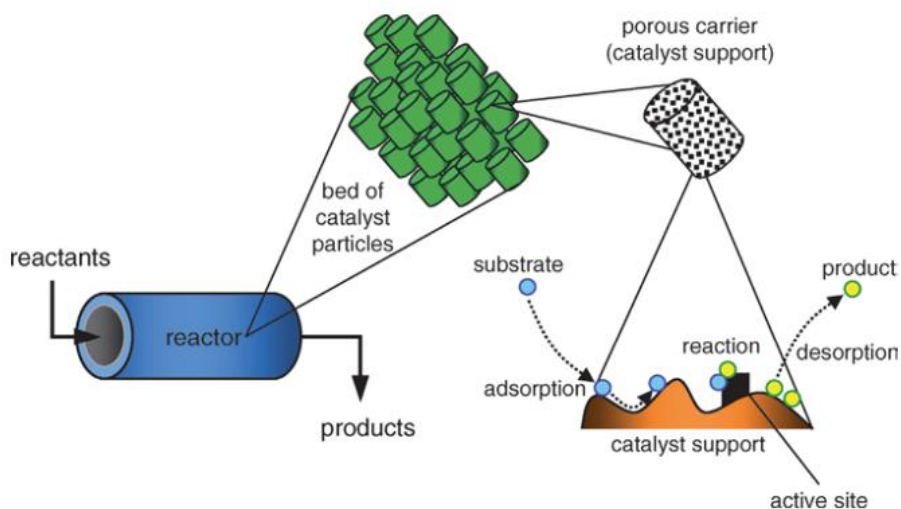


Fig.I.6-Schematic representation of flow reactor system.

Heterogeneous catalysts have a wide application in the petrochemicals and the bulk chemicals industry. In the last two decades heterogeneous catalysis has moved also into the fine-chemicals and pharmaceuticals applications, clean energy applications such as fuel cells, solar energy conversion, and energy storage cycles.⁴⁶

In this research thesis, particular attention will be paid to the study and characterization of supported metals as heterogeneous catalysts.

1.5 Nanoparticles: bridging the gap between homogeneous and heterogeneous catalyst

Some of the properties of catalysts are collected in **Table I.1**, where heterogeneous and homogeneous catalysts have been compared.

	Homogeneous	Heterogeneous
Effectivity		
Active centers	All metal atoms	Only surface atoms
Concentration	Low	High
Selectivity	High	Lower
Diffusion problems	Practically absent	Present (mass-transfer-controlled reaction)
Reaction conditions	Mild (50-200°C)	Severe (often > 250°C)
Applicability	Limited	Wide
Activity loss	Irreversible reaction with products; poisoning	Sintering of metal crystallites; poisoning
Catalyst properties		
Structure	Defined	Undefined
Modification possibilities	High	Low
Thermal stability	Low	High
Catalyst separation	Laborious/Expensive	Easy
Catalyst recycling	Possible	Easy
Cost of catalyst losses	High	Low

Tab.I.1-Comparison between homogeneous and heterogeneous catalyst.

In heterogeneous catalysis, it is possible to underline benefits like the easy removal of catalyst materials and the possible use of high temperatures, despite the absence of a complete understanding of mechanistic aspects that are crucial for parameter improvements. Identifying the reaction intermediates and the mechanism for a heterogeneous catalytic reaction is often problematic because many of these intermediates are difficult to detect using conventional methods (e.g., gas chromatography, mass spectrometry or nmr) as they do not desorb at significant rates from the surface of the catalyst (especially for gas-phase reactions).

On the contrary, homogeneous catalysis is very efficient and selective, although it is affected by the impossibility of removal of the catalyst from the reaction media and its limited thermal stability. Nowadays green chemistry requires that environmentally friendly catalysts must be designed for easy removal from the reaction media and recycling many times with very high efficiency. A combination of both advantages could enable the building of sustainable catalysts able to improve many of the known and used reaction mechanisms. In this framework, the development of nanomaterials represents one of the attempts to overcome the drawbacks of both heterogeneous and homogeneous catalysts.

Nanoparticles (NPs) are materials in which at least one-dimension ranges between 1-100 nm size, that exhibit nanoscopic, size-dependent properties such as superparamagnetism for Fe_3O_4 nanoparticles, visible photoluminescence for CdSe quantum dots, to mention a few.⁴⁷ The nanoscale sizes make huge changes to melting point, fluorescence, electrical conductivity, magnetic permeability, and chemical reactivity. NPs possess unique physical and chemical properties mostly due to their high surface area and nanoscale size. In fact, the small size of the particles leads to increased surface area to volume ratio and as a result the domain where quantum effects predominate is entered. On the other hands, the increasing surface area to volume ratio leads to an increase in the dominance of the surface atoms of the nanoparticle over those in the bulk.

For these reasons, NPs are suitable candidates for various commercial and domestic applications, such imaging, pharmaceutical applications, energy-based research,

optical field, environmental applications, and catalysis.⁴⁸⁻⁵⁰ Thus, the potential applications of nanoparticles are as diverse as the materials and methods from which they are synthesized, indeed it is possible to control the specific morphology, size, and magnetic properties by using different synthetic techniques. Generally, the methods employed for the synthesis of NPs can be grouped into two main classes: bottom-up and top-down approach.⁵¹

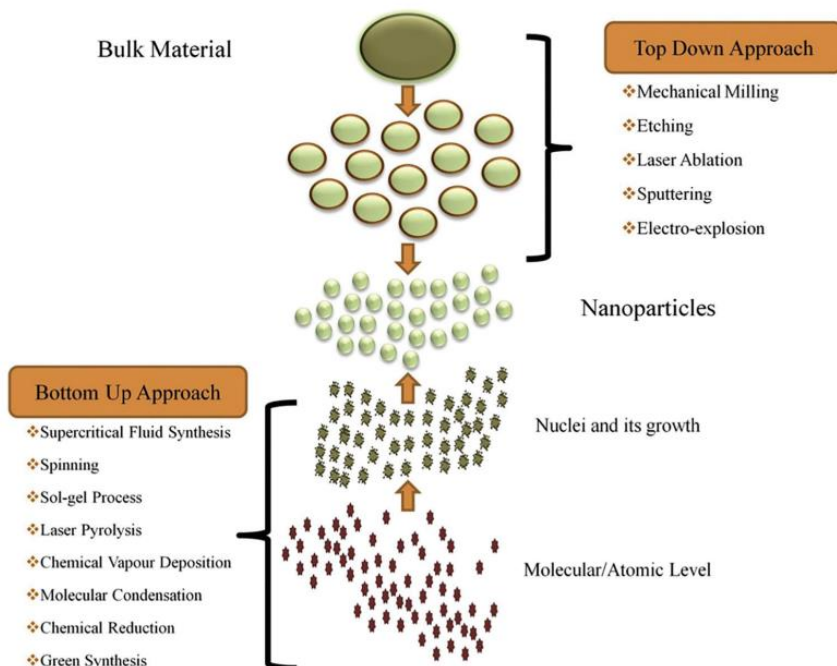


Fig.I.7-The synthesis of nanomaterials via top-down and bottom-up approaches.⁵²

Top-down approach is mostly a physical method and involves the breaking down of the bulk material into nanosized structures or particles. Examples of this method are grinding/milling, CVD, physical vapor deposition (PVD), lithographic techniques and other decomposition techniques. However, this approach is rarely applied due to the physical stress that generates surface defects and contaminants. In the case of mechanical milling is required a lot of energy and hours to complete the process and the size distribution of particles resulting is very broad, and the morphology of the formed particles tends to be quite varied. Hence, nanomaterials synthesized through

this route are most suited for certain application areas, for example, in nanocomposites, where a broad size distribution is not problematic.

Bottom-up approach generates nanomaterials by assembling atoms or molecules via synthetic chemistry, building from the bottom through atom-by-atom or molecule-by-molecule. In this way it is possible to ensure the formation of nanoparticles with less defects, a better control of particle size, homogeneous chemical composition, and improved crystal ordering. Nanomaterials synthesized through this route are suited for optical applications, where it is desirable to have well defined size distribution and uniform shape.

As reported in **Fig.1.7**, example of bottom-up approach are chemical vapor deposition (CVD) that has great significance in the generation of carbon-based nanomaterials, sol-gel process, reverse micelle methods and so on.^{53,54} All of these strategies present advantages and drawbacks, that determinate the resulting properties of materials.

The nanomaterials can be organized into four material-based categories based on their properties, morphologies, shapes, or sizes:

- *Carbon-based nanomaterials.* These nanomaterials containing carbon can be found in several morphologies and phases. They include fullerenes with a defined number of carbon atoms in the structures (for instance C₆₀) that are ellipsoids or spheres, carbon nanotubes (CNTs) that are wire hollow tubes, carbon nanofibers that have the form of nanowires, carbon black, usually in the form of particulate, and graphene composed by a layer of exfoliated graphite.
- *Inorganic-based nanomaterials.* These nanomaterials are mainly made up of metal or metal oxide particles less than 100 nm. They are composed of pure precious metals such as Au or Ag nanoparticles or being in the form of metallic oxides such as TiO₂ and ZnO. This category also includes semiconductors such as silicon and ceramics.
- *Organic-based nanomaterials:* excluding carbon-based or inorganic-based nanomaterials, it is possible to detect nanomaterials and nanostructures composed of organic matter. Dendrimers, micelles, liposomes, and polymer

can be obtained with the utilization of non-covalent (weak) interactions, exploiting the self-assembly properties, or design of molecules.

- *Composite-based nanomaterials*: they are multiphase complex nanostructures with one phase at least on the nanoscale dimension. They can both combine nanoparticles of different compositions and shape together or include nanoparticles within bulk-type materials (e.g., hybrid nanofibers) or more complicated structures (e.g. metal–organic frameworks). The nanocomposites can be any mixture of carbon-based, metal-based, or organic-based nanomaterials and bulk materials of every kind and form (metal, ceramic, or polymer).⁵⁵

1.6 Application of nanomaterials: Nanocatalysis

Nanocatalysis is one of the most important field of utilizations of nanoparticles, which can act as active phase (like metal nanoparticles) or as support materials for various catalytic systems. These systems should be able to combine the positive aspects of both homogenous and heterogeneous catalysts, namely high efficiency and selectivity, stability, and easy recovery/recycling.⁵⁶ Due to their small size, catalytic-active nanoparticles have higher surface area and increased exposed active sites, and thereby improved contact areas with reactants. Moreover, their tunable activity, selectivity and stability can be improved by tailoring the chemical and physical properties of the nanomaterials through various synthetic methods. Several studies focused on the elucidation of the effects of nanoparticle size on the catalytic behavior and more in details about the way in which activity and selectivity are affected by size.⁵⁷ In 1962, M. Boudart, proposed the first definition for structure sensitivity.⁵⁸ He defined that a heterogeneously catalyzed reaction is considered to be structure sensitive if its rate, referred to the number of active sites and, thus, expressed as TOF, depends on the particle size of the active component or a specific crystallographic orientation of the exposed catalyst surface. Generally, three types of particle size-activity relationship can be discerned:⁵⁹ positive size-sensitivity reactions, negative size- sensitivity reactions, and size-insensitive reactions. Positive size-sensitivity reactions are those for which TOF increases with decreasing particle size. The prototypical reactions demonstrating

positive size-sensitivity are methane activation, the Pd-catalyzed hydrogenation of butyne, butadiene, isoprene, aromatic nitro compounds and of acetylene to ethylene. Negative size-sensitivity reactions are those for which TOF decreases with decreasing particle size. The prototypical reactions for this group are dissociation of CO and N₂ molecules, which require in each case step-edge sites and contact with multiple atoms. These sites do not always exist on very small NPs, in which step-edges approximate ad atom sites. Finally, size-insensitive reactions are those wherein there is no significant dependence of turnover frequency on nanoparticle diameter. Benzene hydrogenation over Pt catalysts, acetonitrile hydrogenation over Fe/MgO and benzene hydrogenation over Ni are examples of this type of reactions.^{60,61}

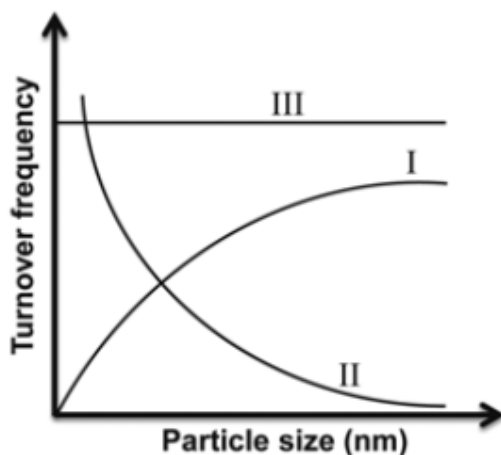


Fig.1.8-Relationships between NP size and turnover frequency for a given combination of reaction and NP catalyst. “I” negative size- sensitivity; “II” positive size-sensitivity; “III” size-insensitivity.⁶²

One of the earliest reported nano catalysis application dates back to 1940 by Nord⁶³ on nitrobenzene reduction and to 1970 by Parravano⁶⁴ on hydrogen-atom transfer between benzene and cyclohexane and oxygen-atom transfer between CO and CO₂ using AuNPs. But the clearest example of the advent of nanomaterials is represented by Au nanoparticles. Gold is usually considered chemically inert but in 1987 Haruta et al.⁶⁵

made the unexpected discovery that gold, when divided to the nanoscale, to just a few hundreds of atoms, can be the most effective catalyst for the oxidation of CO at temperatures as low as 76 °C. Haruta's group explored different procedures to optimize the particle size by controlling the calcination temperature or the presence of support and found that 3 nm-sized Au nanoparticles were most efficient for the oxidation of CO. Gold is indeed active in carbon monoxide oxidation at a much lower temperature ($\leq RT$) than any platinum group metal. This difference in reactivity can be due to the possibility of Pt, Pd, and Rh of easily dissociating molecular oxygen at low temperature and binding strongly both atomic oxygen and CO. Tightly bound adsorbates must overcome sizeable barriers to react, making the reaction rates significant only at rather high temperatures. On the contrary, on gold the reactants are loosely bound, but a higher binding energy of CO on gold nanoparticles than on bulk gold may provide sufficient concentrations of CO on the surface for the reaction of oxidation to occur with negligible energy barriers. Moreover, it has been demonstrated that the reaction takes place at the interface between the gold metal particle and the oxide support, between CO adsorbed on the gold particles and O₂ activated by the oxide support as schematized in figure below.

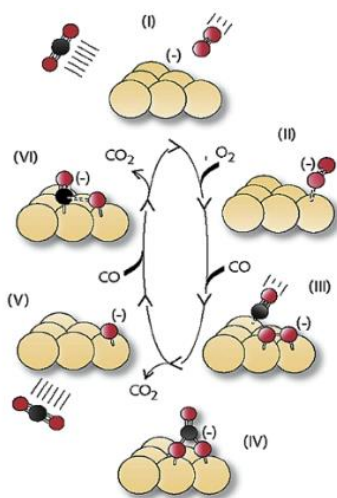


Fig.I.9-Proposed schematic mechanism of the Au catalyzed formation of CO₂ from CO and O₂ in the gas phase (Adapted with the permission from ref.66).

1.7 Metal nanoparticles

Since nano catalysts are made up of nanoparticles or nanomaterials, as a metal or metal oxide active phase or as a support or a combination of both, metal nanoparticles (MNPs) and more in details transition metals nanoparticles have been the object of an ever-increasing interest during recent decades. The main goal is the development of well-defined metal nanoparticles with promising properties to get efficient, versatile catalysts in several relevant reactions.

MNPs-based catalysts are largely employed in everyday life processes, including environmental remediation, processing of raw materials, and energy production.^{67,68} The synthesis of ammonia with iron nanoparticles supported on inorganic oxides like Al_2O_3 , MgO , CaO , K_2O and the hydrocarbon cracking with platinum nanoparticles supported onto alumina/silica⁶⁹ are two examples of application of MNPs-based catalysts in industrial chemistry.

The use of transition metal nanoparticles in catalysis is promising as they mimic metal surface activation and catalysis at the nanoscale and thereby brings high selectivity and efficiency to heterogeneous catalysis. Transition metal NPs are clusters containing from a few tens to several thousand metal atoms, stabilized by ligands, surfactants, polymers or dendrimers protecting their surfaces.⁷⁰ Their sizes vary between the order of one nanometer to several tens or hundreds of nanometers, but the most active are only a few nanometers in diameter. Since the number of surface atoms present in NPs will govern their catalytic reactivity, control of the size of NPs is thus of paramount importance. The methods of preparation of MNPs play a key role in determining the particle morphology (size, shape, agglomeration, and size distribution), composition, magnetic property, surface chemistry, and catalytic applications. There are several protocols reported in the literature for synthesizing MNPs, such as coprecipitation, impregnation, microemulsion technique, sol-gel method, spray and laser pyrolysis, hydrothermal reaction method, microwave irradiation and biological synthesis.

Depending on particular requirements for MNPs, these methods can be operated under optimized conditions (mainly regarding reaction temperature, pH value, concentration, and proportion of starting materials) to synthesize MNPs in different forms. NPs are also well soluble in classic solvents and can often be handled and even characterized as molecular compounds by spectroscopic techniques such as infrared and UV–Vis spectroscopy.⁷¹

Many of the achievements in the field of nano catalysis are due not only to improvements in preparation methodologies, but also to advances in characterization techniques. Determination of the nanoparticle structures and the investigation of their morphology as well as the precise control of the size, enables systematic studies of the influence of composition and structural features of metal nanoparticles on chemical reactivity and selectivity, leading to an increasing understanding of relationships between structure and catalytic activity for the design of more efficient catalysts.

Despite several advantage, due to their high surface area, the dispersions of metal nanoparticles in the reaction environment are unstable because there is a powerful thermodynamic driving force towards particle aggregation and growth. Most nanomaterials start to agglomerate when they encounter each other. The process of agglomeration may be due to physical entanglement, electrostatic interactions, or high surface energy. To overcome this problem, several stabilization strategies have been developed.⁷²

The stabilization of NPs during their synthesis can be electrostatic, steric, electrosteric or by the addition of a stabilizing agent (polymer, surfactant, ligand) as reported in **Fig.I.10**.⁷³ Besides their protecting role, and although they occupy some active sites at the surface of nanoparticles, stabilizers can tune the reactivity of resulting materials by influencing their morphology or/and their surface chemistry. When the nanoparticles are deposited onto a support, the organic ligands can be removed from the nanomaterial by washings with appropriate solvents or by calcination under air at high temperature or under plasma conditions, to obtain “naked” NPs.

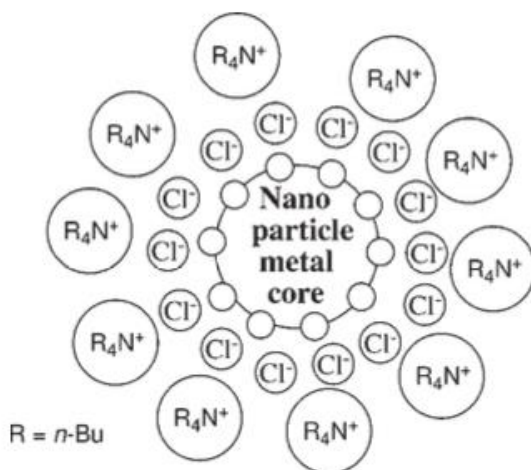


Fig.I.10-Examples of “electrosteric” (that is electrostatic and steric) stabilization of metal nanoparticles obtained by reduction of a metal chloride salt in the presence of a tetra-N-alkylammonium cations.

1.8 The role of support

As mentioned above, the aggregation of naked Earth-abundant transition-metal nanoparticles that generally results from small interparticle distances, high surface energy, van der Waals forces and/or magnetic attraction is virtually unavoidable and causes an obvious decrease in their useful properties. The use of suitable carriers or support materials is one of the best solutions to overcome this drawback.⁷⁴

For many years it was presumed that the support material was simply an inert carrier, a suitable medium to provide physical support for nanocatalysts or metal nanoparticles and ensure optimal performance and minimal cost. Instead, numerous studies have shown that the nature of the support greatly affects the performance of a catalyst.⁷⁵

Among the many factors that have been shown to contribute to the physical and chemical properties of a supported catalyst, one of the most important is the nature of the support material itself. Structural properties such as surface area and porosity can affect the thermal stability of the catalyst. The porosity, in terms of shape and pores

size, plays an important role in increasing the efficiency and stability of catalyst supports, in order to improve the diffusion of substrates. The overall effect of support is that not only stabilize the nanoparticles but it also act in synergy with nanoparticle surfaces to activate substrates in a way comparable to the positive interaction observed between two transition metal atoms in alloys, as reported in details by Corma.⁷⁶ The suitable support should possess a good chemical and mechanical resistance, and a high surface area, in order to favor the dispersion of the active phase, stabilize the latter and control sintering phenomena.

Beyond the stability, the support can strongly affect the selectivity of the catalyst, since the different pathways of a chemical reaction are determined not only by the nature of the active phase but also by the nature of the support, for example, its acidity and redox properties. When a nanoparticle is immobilized onto support its morphology, electronic properties could change due to the energy of adhesion, and transfer effects. These properties change can impact the activity, the selectivity and can affect the lifetime of the catalyst. In the case of metal nanoparticles, the average distance between particles will depend on the metal content, the particle size, and also the surface area of the support.⁷⁷

By the using of different support, it is possible to tune the activity and the selectivity of the reaction. The supports can cooperate with the active phase nanoparticles to promote simultaneous reactions that may favor or disfavor the overall reaction. By keeping in mind these requirements, in the synthesis phase of a new catalyst, the choice of the appropriate support is a topic of main importance. The most used supports are alumina (Al_2O_3),⁷⁸ silica (SiO_2),⁷⁹ titania (TiO_2),⁸⁰ carbon (C)⁸¹ materials and so polymers. Latest, organic polymers are an emerging group of the most extensively employed supports for nanoparticles and mostly metal nanoparticles. They have been widely employed due to their attractive features including availability, enhanced metal nanoparticles stabilization properties and resistance to particle sintering or agglomeration. Poly(*N*-vinyl-2-pyrrolidone) PVP is the most used polymer for nanoparticles stabilization and catalysis, because it fulfills both steric and ligand requirements.⁸² It has been widely used for the stabilization of Pd NPs⁸³ both with

polystyrene- \square -poly(sodium acrylate)⁸⁴ and poly(N,N-dihexylcarbodiimide).⁸⁵ PEG is another very important and useful polymer stabilizer owing to its unique properties including low cost, good solubility both in water and oil, non-toxicity, biocompatibility and ready accessibility. PEG has been extensively applied to the construction of nanocatalysts involving Fe, Cu, Ni and Co.⁸⁶ Astruc and co-workers prepared a tris(triazolyl) fragment-functionalized PEG-2000 ligand and utilized it as stabilizer in syntheses of Fe NPs, Co NPs, Ni NPs, and Cu NPs with very small particle size ranging from 1.3 to 2.1 nm (Fig.I.11).

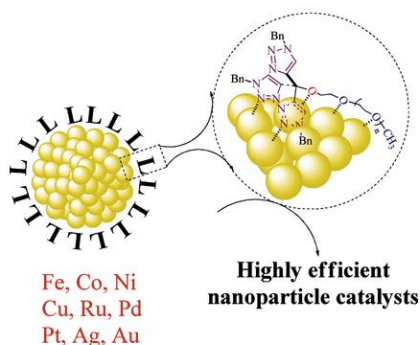


Fig.I.11-Tris(triazolyl)-PEG ligand-stabilized transition metal NPs in 4-nitrophenol reduction and CuAAC reaction. Adapted with permission from ref.88.

1.9 Polymer supported metal nanoparticles

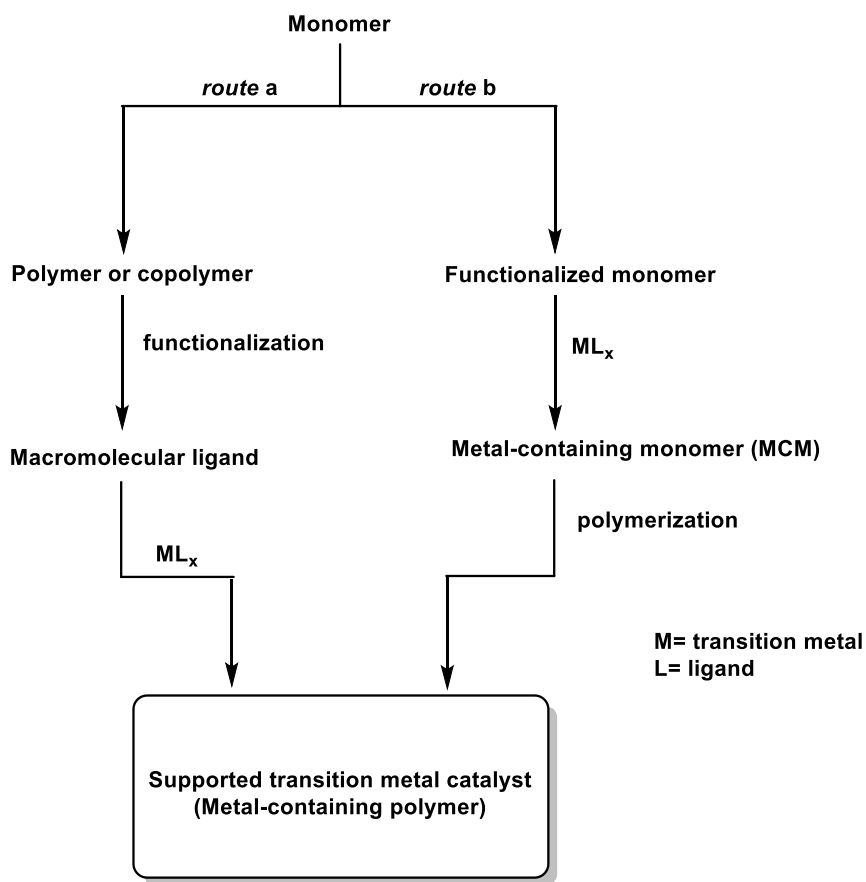
The immobilization of catalysts onto polymeric supports has been extensively investigated in the last years as reported by several studies.^{88,89,90} Polymers are some of the most widely used materials, due to their favorable properties such as high strength, low weight, and low cost. They provide a variety of compositions and properties useful in catalysis. Both insoluble and soluble polymers have been employed as support, the first ones for use in heterogeneous catalysis,⁹¹ the latter ones for carrying out the process in homogeneous phase, with the advantage of being easily separated from the reaction mixture by the addition of a co-solvent or by ultrafiltration.^{92,93,94} An immobilized catalyst onto an insoluble polymer can also be used in continuous flow reactions in a microreactor,⁹⁵ where the catalyst permanently resides

transforming the entering starting materials into the exiting products. Water-soluble polymers are useful as catalyst carriers to perform reactions in aqueous media.⁹⁶

In the case of organic polymers as support, through the choice of a suitable combination of comonomers and crosslinkers, it is possible to control the flexibility of the catalyst as well as to fine-tune its physical properties (polarity, swellability, morphology, etc.).^{97,98,99} The only disadvantages of this approach are sometimes the low thermal capacity and mechanical strength of the obtained heterogeneous catalysts.¹⁰⁰

The first example of an organic polymer supported metal complex was proposed in 1969 by Haag and Whitehurst¹⁰¹ and consisted of sulfonated polystyrene bearing cationic Pt(II) complex. Since then, many polymers have been used for this purpose like styrene, acrylates, acrylamides, natural polymers such as silk,¹⁰² starch,¹⁰³ cellulose¹⁰⁴ and generally all ones suitably functionalized with a moiety capable to bind metals.

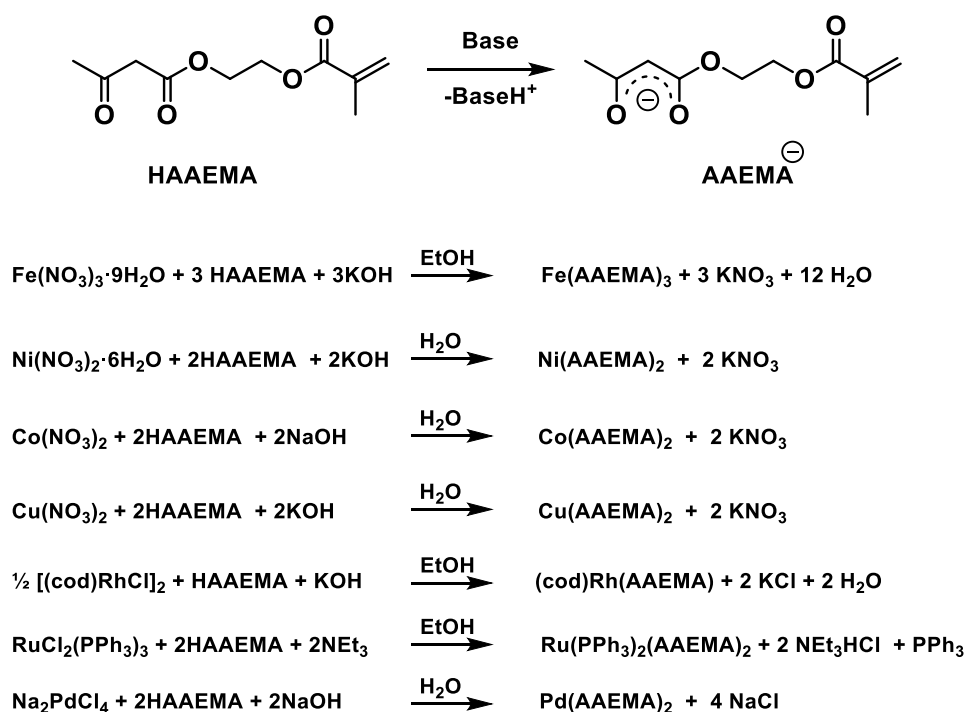
The most commonly used strategies for synthesizing a supported metal complex on organic polymer or resin are essentially those represented in **Scheme I.1**.



Scheme I.1

Route *a* is the “classic” synthesis of a macromolecular ligand followed by the linking of a transition metal as salt or complex.¹⁰⁵ Although the route *b* is less frequently used, it is more interesting both from a synthetic and a catalytic point of view. The route *b* consists of the preparation of a metal containing monomers (MCM), *i.e.* a catalytically active transition metal complex with a ligand having a functionality, which can subsequently be subjected to polymerization with suitable comonomers and crosslinkers for achieving a supported transition metal catalyst as a metal-containing polymer (MCP). Moreover, the use of MCMs offers the advantage of a possible comparison of the activity between the homogeneous and the heterogeneous phase as well as a more uniform distribution of the transition metal in the support with respect to route *a*, and thus a more controllable dispersion of the metal in the polymer matrix.¹⁰⁶

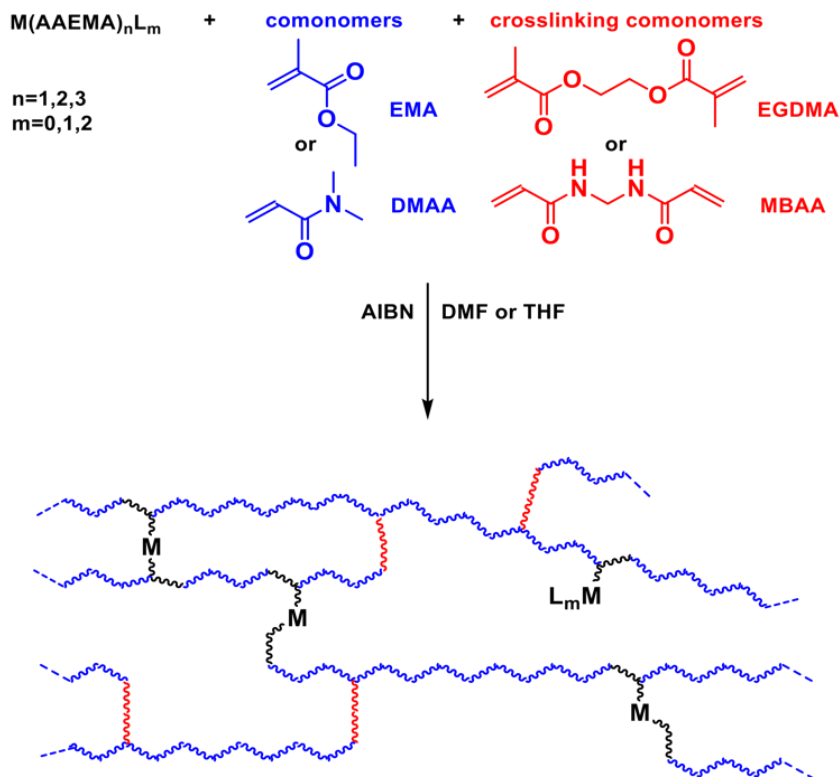
A versatile ligand to prepare MCMs for the obtainment of a wide range of MCPs is 2-(acetoacetoxy)ethyl methacrylate (HAAEMA). HAAEMA is a clear or light-yellow liquid which finds use as versatile functional acrylic monomer¹⁰⁷ for making copolymers to be used in various applications such as, by way of example, dental resins,¹⁰⁸ coatings for glass and metal surfaces,¹⁰⁹ wound sealants,¹¹⁰ waterborne coatings,¹¹¹ thermal nanoimprint lithography,¹¹² and nanoparticles.^{113,114} On the other hand, exploiting the fact that the reactivity of the β -ketoester functionality in HAAEMA towards transition metal salts or complexes resembles that of acetylacetonone, it is possible to prepare several transition metal complexes containing the ligand AAEMA⁻ (**Scheme I.2**).



Scheme I.2

The spectroscopic features of all AAEMA⁻ complexes demonstrate that the β -ketoester moiety is the sole functionality involved in the coordination while the methacrylic tail is indeed left free for other reactions, such as radical polymerizations. Thanks to these characteristics, it was possible to synthesise and employ in catalysis several polymer-supported transition metal catalysts obtained from copolymerization of transition metal-

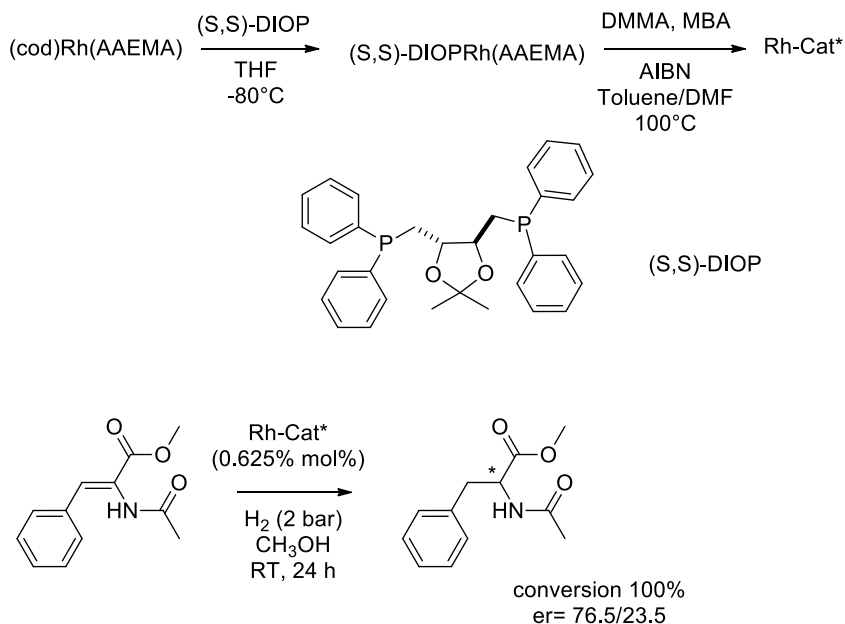
containing AAEMA⁻ with appropriate comonomers and crosslinkers (**Scheme I.3**).¹¹⁵ The resulting MCPs are non-hygroscopic powders which are insoluble in all solvents, but they swelled well in water, acetone, halogenated solvents, dioxane, THF, DMF, and shrink when treated with diethyl ether, ethyl acetate or petroleum ethers. These swellabilities are very valuable in looking for new catalytic systems that could be recoverable and recyclable.



Scheme I.3

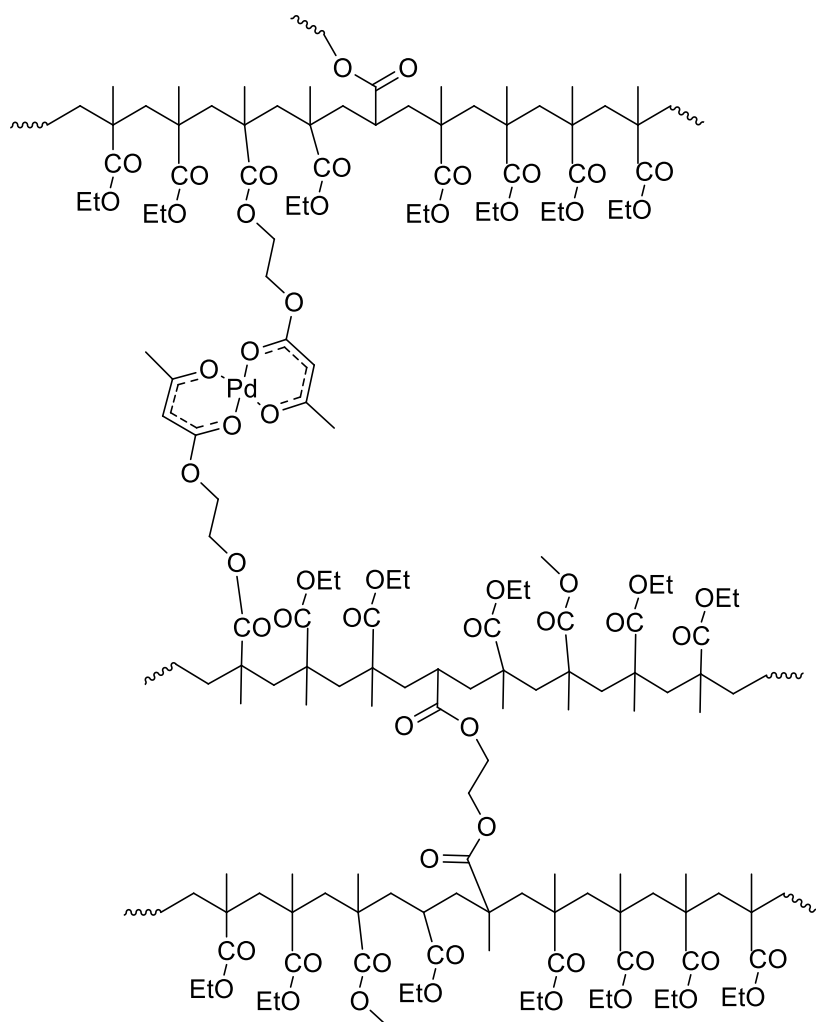
Among the complex reported in scheme I.3, the (cod)Rh(AAEMA) ones was employed with DMAA and MBAA to obtain a Rh-based MCP which catalyzed the hydrogenation of several unsaturated substrates in methanol or CH_2Cl_2 with yields ranging from 64 to >99% under very mild conditions.¹¹⁶ Noteworthy, a chiral version (Rh-cat*) of Rh-cat was synthesised by exchanging the cod ligand in (cod)Rh(AAEMA) with the (*S,S*)-DIOP and copolymerizing the resulting complex [(+)-diopRh(AAEMA)] with DMAA and

MBAA in presence of AIBN in toluene/DMF at 100°C (Scheme). Rh-cat* accelerated the hydrogenation of methyl-(*Z*)- α -N-acetamidocinnamate to N-acetyl-(*S*)-phenylalanine methyl ester with enantiomeric ratio (*er*) up to 76.5/23.5.



Scheme I.4

Concurrent with the development of rhodium catalyst, the supported palladium catalyst (Pd-pol) obtained starting from Pd(AAEMA)₂ as metal containing monomer, assumed great importance. A material with a uniform distribution of the catalytically active sites have been achieved by copolymerization of complex with suitable co-monomer (ethyl methacrylate) and cross-linker (ethylene glycol dimethacrylate) to give a polymer supporting Pd(II) centers, i.e. Pd-pol pre-catalyst (**Scheme I.5**). This latter was then reduced under reaction conditions forming polymer supported Pd NPs immobilized and stabilized by the reticular and macro porous polymeric support.¹¹⁷

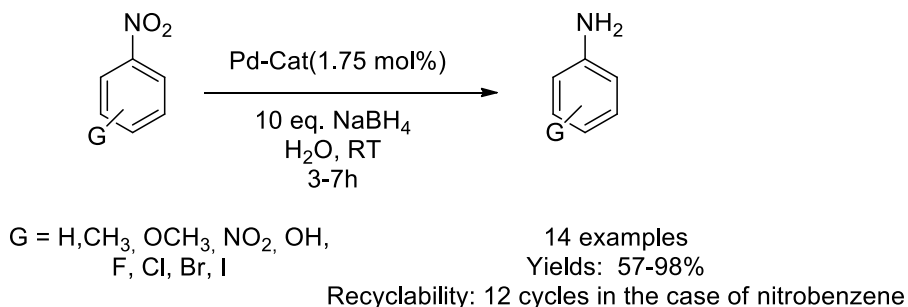


Scheme I.5

Pd-pol swells in water and in many organic solvents, it is microporous and is characterized by a rather low degree of cross-linker. It was employed and found active and recyclable for several palladium catalyzed reactions such as reduction, oxidation, carbon-carbon bond forming reactions as well as esterification and transesterification reactions.¹¹⁸

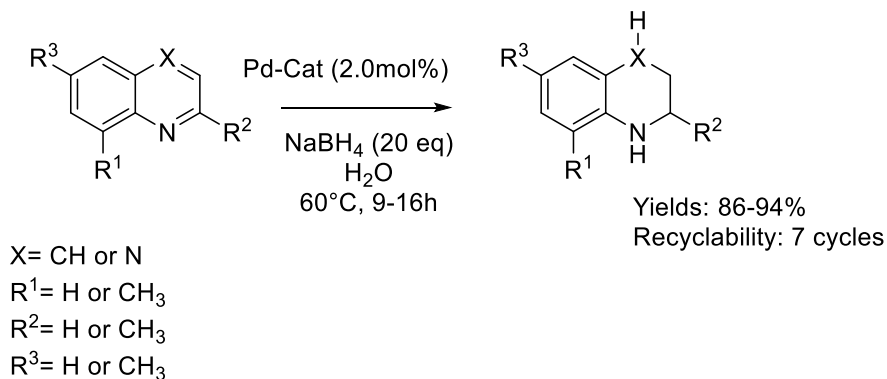
In a greener and eco-friendly framework, Pd-cat was found active in the reduction of nitroarenes to arylamines in the presence of NaBH_4 and water as solvent. As reported

in the scheme I.6 the yields ranging from 57% to 99%. It is worth noting that the system was recyclable at least 12 times without loss of activity and selectivity. In fact, TEM observations showed that the catalytic active species are very small Pd nanocrystallites (mean size diameter ca. 3 nm) formed in the presence of NaBH_4 .¹¹⁹

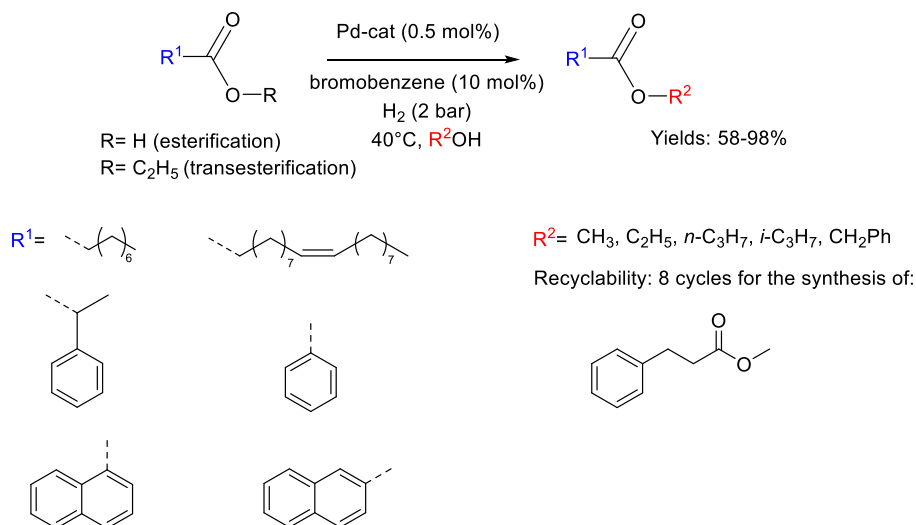


Scheme I.6

Using a loading of 2.0%mol of catalyst, high yields and excellent selectivity were achieved also in the hydrogenation of quinolines in aqueous medium under mild conditions. (Scheme I.7) Always in water was performed the Suzuki cross coupling of arylhalides with arylboronic and the oxidation of alcohols by air. Primary and secondary aromatic alcohols were oxidized to their corresponding carbonyl compounds in excellent yields with a very low Pd loading (0.5 mol%) in a short reaction time. (Scheme I.8)¹²⁰

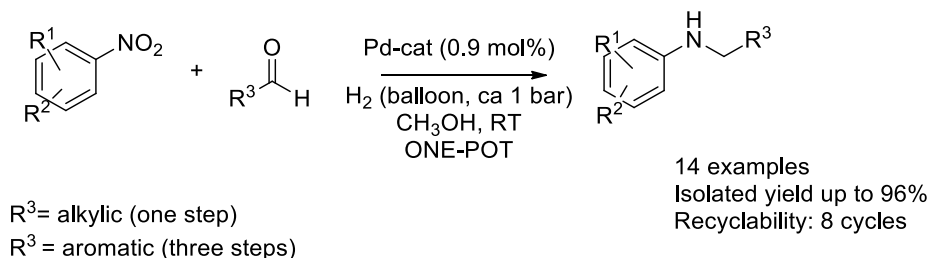


Scheme I.7



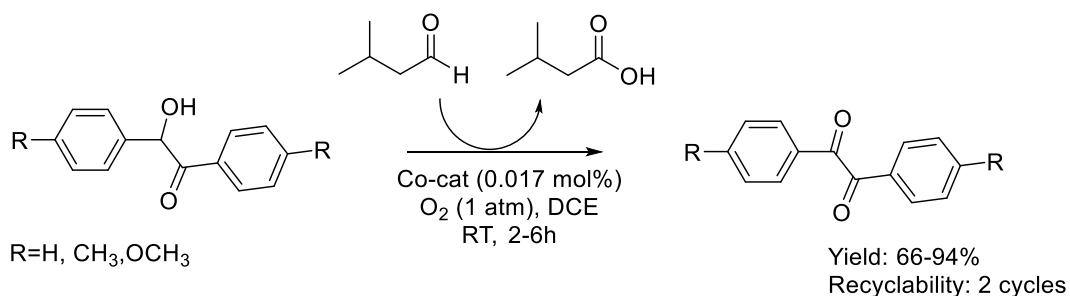
Scheme I.8

Another innovative catalytic application of this system was the one-pot direct amination reaction.¹²¹ The Pd-pol catalyzed reductive amination was successful in one step by using aliphatic aldehydes only. In fact, when benzaldehydes were employed, the one-pot reaction was carried out in three steps to avoid benzyl alcohol formation. The catalytically active species were in situ formed Pd NPs with a narrow size distribution centered at 5 nm in diameter, whose morphology remained almost unchanged during reaction. The catalyst resulted recyclable for at least eight subsequent runs without loss of activity and selectivity. The catalytic reactions were performed under mild conditions (1 atm H₂, room temperature, methanol as the solvent) by using equimolar amounts of nitroarene and aldehyde.

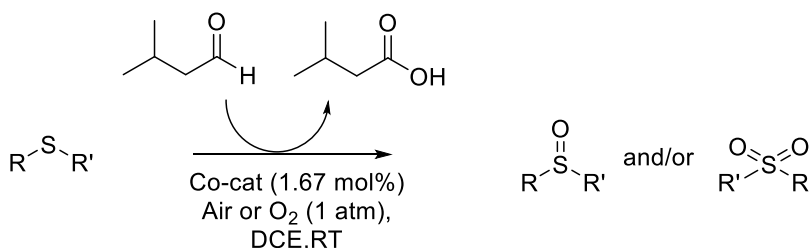


Scheme I.9

Cobalt based catalyst (Co-cat) was obtained as pink solid by copolymerizing the complex $\text{Co}(\text{AAEMA})_2$ with DMAA as comonomer, and MBAA as crosslinker in DMF at 50°C for 24 h (**Scheme I.2**).¹²² In the aerobic epoxidation of olefins under “Mukaiyama’s conditions”, the Co-cat was active, selective, and recyclable for the epoxidation of norbornene, cholesteryl acetate, and cyclohexene but a severe metal leaching was observed in the epoxidation of linear alkenes. However, this cobalt-based catalyst demonstrated to be suitable catalyst in the oxidation reactions. In fact, under “Mukaiyama’s conditions”, the catalyst acted for the heterogeneous aerobic oxidation of hydroxyketones to diketones, for the oxidation of disubstituted sulfides to sulfoxides and/or sulfones and for the oxidation of benzylic and secondary alcohols as reported in Scheme I.10 and I.11.¹²³



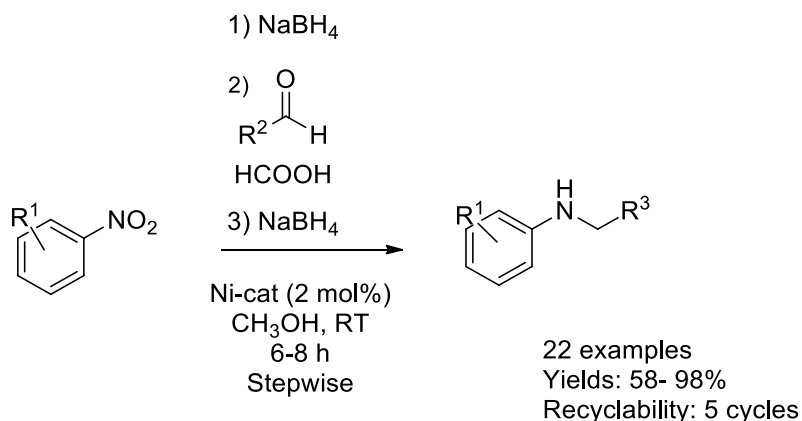
Scheme I.10



Scheme I.11

On the basis of the good results achieved with Pd-pol, the strategy of synthesis followed for Pd-pol was transferred for the synthesis of Ni-pol, wherein the noble metal Pd was replaced by nickel. The polymer has been prepared by co-polymerizing the $\text{Ni}(\text{AAEMA})_2$

complex with *N,N*-dimethylacrylamide and *N,N*-methylenebisacrylamide¹²⁴ and then submitting it to calcination at 300 °C under nitrogen, obtaining a Ni-containing organic polymer (Ni-pol) with a homogeneous distribution of cubic nanocrystals of Ni average cross section value of 35 nm. Ni-pol was tested in the stepwise amination reaction of various benzaldehydes with different nitroarenes in methanol at room temperature, using NaBH₄ as the reductant (Scheme I.12). The addition of few drops of formic acid was necessary in the condensation step to promote the formation of the imine intermediate. Twenty-two secondary amines have been synthesized with Ni-pol catalytic system, some of them containing halogen substituents (no hydrodehalogenation occurred) or reducible group (-CN). Ni-pol was recovered at the end of reaction and used for five subsequent runs without loss.



Scheme I.12

1.10 Aim of this work

The development of sustainable reactions for industrial application, i.e., cost-effective, and environmentally friendly, is one of the major current challenges. The most employed catalytic systems are still largely dominated by noble metal, which determines environmental issues that can no longer be ignored.

As reported above, the recent advances of transition metal nanoparticles as catalyst can be combined with the properties of polymeric support in order to development new active and selective systems. In this framework, with the aim to replacing noble metals, this work provides a sustainable alternative tool by developing or upgrading catalytic systems based on earth abundant transition metals. According to previous studies, the polymerizable ligand AAEMA it has been chosen to prepare different supported metal catalysts by polymerization with suitable comonomers and crosslinkers.

The chapters of this thesis have been divided according to the transition metal used (Co, Ni,) in the metal containing monomer (MCM).

The first part of the thesis was centered on the revisiting of the metal-containing monomer Co(AAEMA)₂ and the development of its copolymer, evaluating its activity as catalyst in the reduction of nitroarenes to the corresponding anilines.

The second part of the thesis deals with the optimization of the synthetic procedure for nickel-based catalysts supported on different matrices. The morphology and the influence of a range of factors on the catalytic performance were investigated to obtain highly selective catalysts for the reduction of several structurally different nitroarenes towards the corresponding azoxyarenes.

CHAPTER II

Polymer supported cobalt nanoparticles as efficient and recyclable catalyst for the reduction of nitroarenes to anilines

2.0 Polymer supported cobalt nanoparticles as efficient and recyclable catalyst for the reduction of nitroarenes to anilines

2.1 Cobalt Chemistry and major catalytic application

Cobalt (Co) is the first and lightest element among the transition metals of group 9 (heavier congeners are rhodium (Rh) and iridium (Ir), and is also the most abundant element of the group (Co:Rh:Ir = c. $10^4 : 5 : 1$) in the geosphere.¹²⁵

The name “Cobalt” derived from the German word “Kobold” meaning goblin and it was given by the miners due to the fact that during the extraction of ores, they were exposed to poisonous fumes released from the rock and they held goblin responsible for this phenomenon, underground sprites of local folklore. Even though the reason for these vapors is to be found in the arsenic, contained in the ores, when chemists extracted cobalt from these minerals, they kept this name.¹²⁶

The cobalt has been isolated for the first time in 1735 by the Swedish chemist Georg Brand, who also recognized its elemental character. It is an essential trace element for humans and animals in the form of vitamin B12 (cobalamin) with an important role in the regeneration of erythrocytes. Cobalamines¹²⁷ are organometallic compounds with cobalt–carbon bonds, possessing cobalt in the oxidation states +1 to +3 and provide the only known cobalt-containing natural products. Moreover, ⁶⁰Co radioactive isotope is widely used in medicine for radiotherapy and medical supply.

Cobalt is a d⁹-metal, and its complexes are available in a large range of oxidation states, ranging from –1 to +3, allowing simple change of oxidation states in catalytic reactions as well as the possibility to prepare compounds in the respective oxidation states.

In general, the largest number of catalytic processes include a catalyst generation step, in which, Co(II) salts are introduced, together with an appropriate ligand and a reducing agent or other additives to lower the oxidation state, from which the active species enters the catalytic cycle.

One of the first appearances of cobalt in catalysis dates to 1938 in the oxo-process (hydroformylation reaction) performed by Otto Roelen at Ruhrchemie in Oberhausen.¹²⁸ Nowadays, cobalt has become one of the most promising metals used in catalytic

reactions, with important applications in the efficient and selective synthesis of natural products, pharmaceuticals, and new materials as schematized in **Fig. II.1**.¹²⁹

Cobalt complex has been widely employed as catalyst in a large range of homogeneous reactions such as hydrogenations,¹³⁰ hydrofunctionalizations,¹³¹ cycloaddition reactions,¹³² C-H functionalizations,¹³³ radical processes,¹³⁴ cross-coupling reactions,¹³⁵ biomimetic reactions,¹³⁶ and reactions that generally involve with multiple bonds containing molecules.¹³⁷

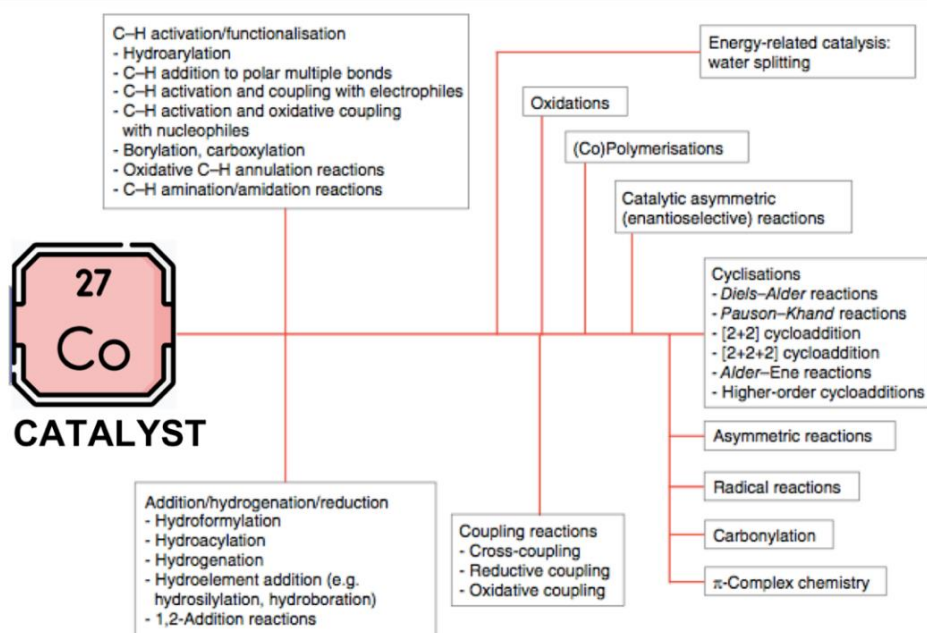


Fig. II.1 Cobalt-catalysed reactions for synthetic purposes. Figure adapted from ref.126.

However, in the last decades very good results have been obtained also in its application in the field of heterogeneous catalysis.¹³⁸ Cobalt complexes have been already used as heterogeneous catalyst in the famous Fischer–Tropsch industrial process to convert carbon monoxide into liquid fuels.¹³⁹ While modern applications in heterogeneous catalysis are often related to the conversion of small molecules in steam-reforming¹⁴⁰ or partial oxidation processes (ethanol, methane) towards the formation of syngas,¹⁴¹ together with other applications for the allocation of clean energy and environmental remediation.¹⁴² A highly current topic is, therefore, the use of

cobalt in heterogeneously catalyzed photoelectrochemical oxidation of water,¹⁴³ electrochemical water splitting¹⁴⁴ or the reduction of CO₂ on cobalt-containing surfaces.¹⁴⁵

Over recent years, cobalt complexes and mostly cobalt-based nanomaterials have seen a significant increase of their application in modern and challenging reactions, to replace the expensive group homologs, rhodium, and iridium. Many efforts are directed to developed innovative cobalt complexes with different dimension, ligand, structures, supports and properties to expand the application of cobalt in a greater number of reactions.¹⁴⁶

Aiming to replace noble metals with earth abundant first-row transition metals,¹⁴⁷ and continuing our studies on metal-containing polymers to be used as heterogenous catalysts,¹¹⁵ we revisited the synthesis of the metal-containing monomer **Co(AAEMA)₂** (**Fig. II.2**) and its copolymer evaluating this time its activity as catalyst, under sustainable conditions, in hydrogenation reactions such as the reduction of nitroarenes to corresponding anilines.

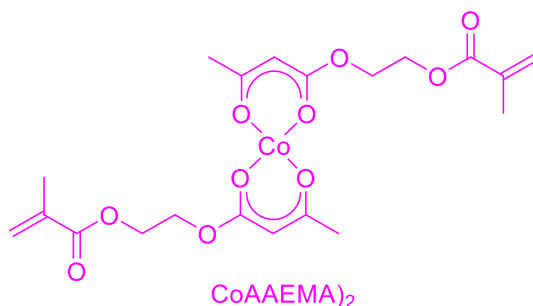
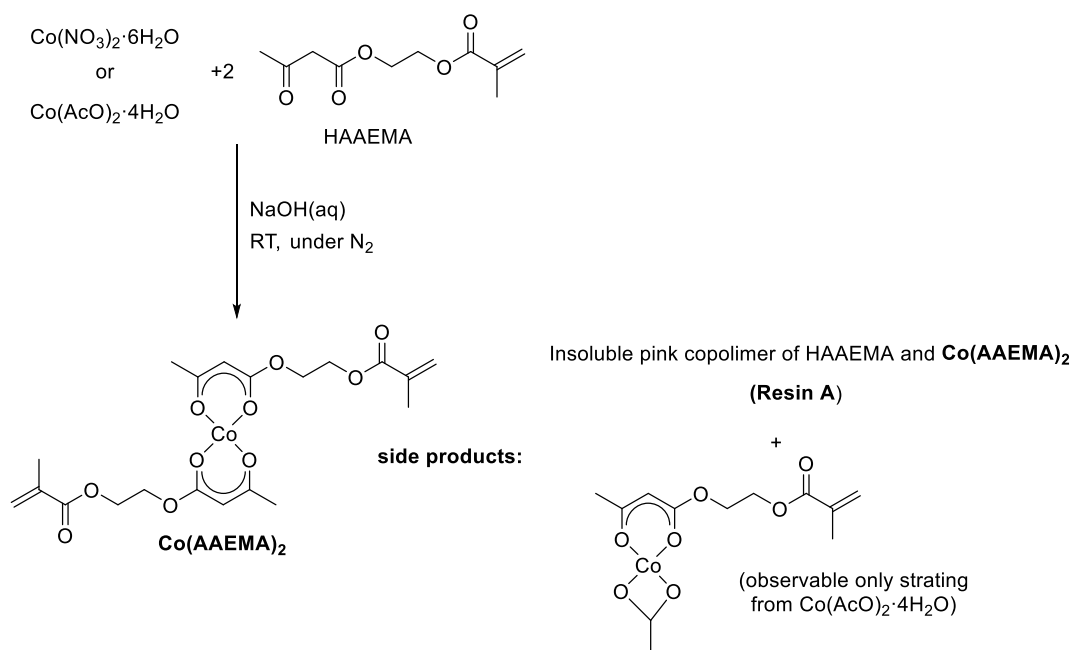


Fig. II.2 **Co(AAEMA)₂**: a cobalt-containing monomer.

2.2 Synthesis and characterization of cobalt (II)- containing monomer: Co(AAEMA)₂

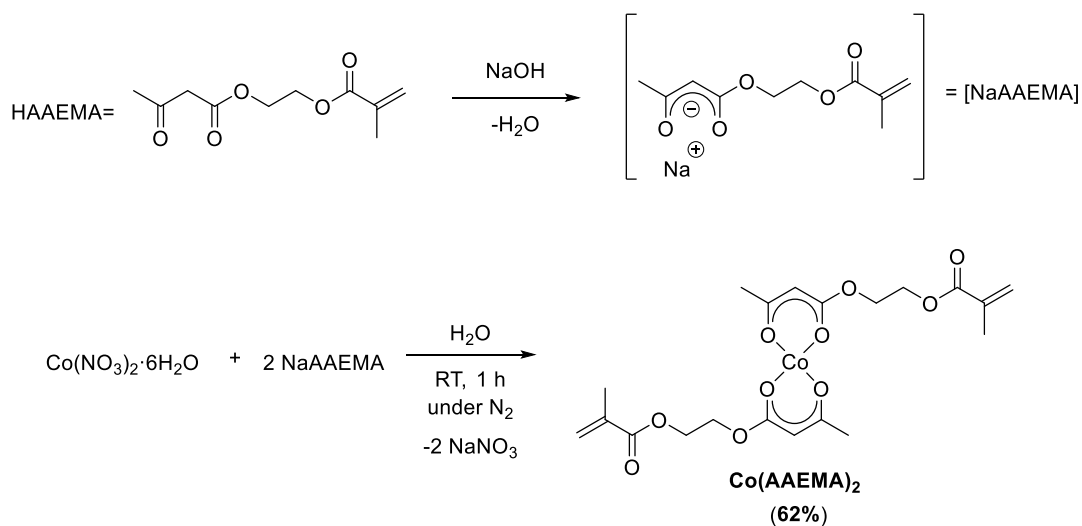
The cobalt-containing monomer **Co(AAEMA)₂** was already synthesized in our group but with low to moderate yields and some drawbacks in its purification (**Scheme II.1**).



Scheme II.1

Inspired from the synthesis of metal β -diketone complexes such as $\text{Co}(\text{acac})_2$,^{148,149} adding HAAEMA to an aqueous solution of $\text{Co}(\text{NO}_3)_2 \cdot 6\text{H}_2\text{O}$ or $\text{Co}(\text{AcO})_2 \cdot 4\text{H}_2\text{O}$ formed an emulsion to which a solution of NaOH was added dropwise causing the precipitation of $\text{Co}(\text{AAEMA})_2$. However, its reprecipitation revealed the presence of a relevant amount of an insoluble residue (**Resin A**) which was separated by filtration. The **Resin A** turned out to be the homopolymer of HAAEMA crosslinked by $\text{Co}(\text{AAEMA})_2$. Moreover, starting reaction from $\text{Co}(\text{AcO})_2 \cdot 4\text{H}_2\text{O}$ demonstrated that $\text{Co}(\text{AAEMA})_2$ was contaminated from the heteroleptic complex $\text{Co}(\text{AAEMA})(\text{AcO})$.

In this study, we were able to revisit and improve the synthesis of $\text{Co}(\text{AAEMA})_2$ in terms of reaction yield as well as its purity. In particular, after several attempts, we found that adding slowly and within an hour a solution of NaAAEMA (obtained by dissolving in water equimolar amounts of NaOH and HAAEMA) to an aqueous solution of $\text{Co}(\text{NO}_3)_2 \cdot 6\text{H}_2\text{O}$ (**Scheme II.2**) led to the formation of pure $\text{Co}(\text{AAEMA})_2$ as a violet-pink precipitate achieving better yield (62%) and preventing the concomitant formation of the **Resin A**.



Schema II.2 An improved synthesis of **Co(AAEMA)₂**.

It is well-known that Co(II) salts or complexes are paramagnetic. Therefore, they cannot be observed either on ¹H NMR or on ⁵⁹Co NMR (⁵⁹Co is a spin 7/2 nucleus and is therefore quadrupolar). As a result, the signal width increases with asymmetry of the environment. ⁵⁹Co NMR is only observable for Co(III), Co(I) and some clusters that are formally Co(0) or Co(-I). Nevertheless, we were able to characterize **Co(AAEMA)₂** by HRMS (ESI), UV-vis, and FTIR (ATR) techniques as well as elemental analyses. In particular, the identity of **Co(AAEMA)₂** was unequivocally ascertained thanks to its ESI spectrum (**Fig. II.3**) that shows an exact mass with a mean error between observed and calculated isotopic patterns of -3.3 ppm. Moreover, the whole mass spectrum rules out an oligomeric structure for **Co(AAEMA)₂** in which each β-ketoesterato ligand bridges two or more cobalt atoms as is generally found in β-diketonate anion complexes.¹⁵⁰

FTIR (ATR) spectrum of **Co(AAEMA)₂** (**Fig. II.4**) shows the expected strong combination bands of the β-ketoesterato ring at 1628 and 1515 cm⁻¹, when it is coordinated, along with the β-ketoesterato ring out of plane bending at 772 cm⁻¹. Moreover, the presence of a strong 1713 cm⁻¹ absorption, ascribable to the uncoordinated methacrylate carbonyl stretching, rules out a possible coordination of the methacrylic moiety of AAEMA⁻ to cobalt. On the other hand, the presence of some water molecules in the coordination sphere cannot be excluded.

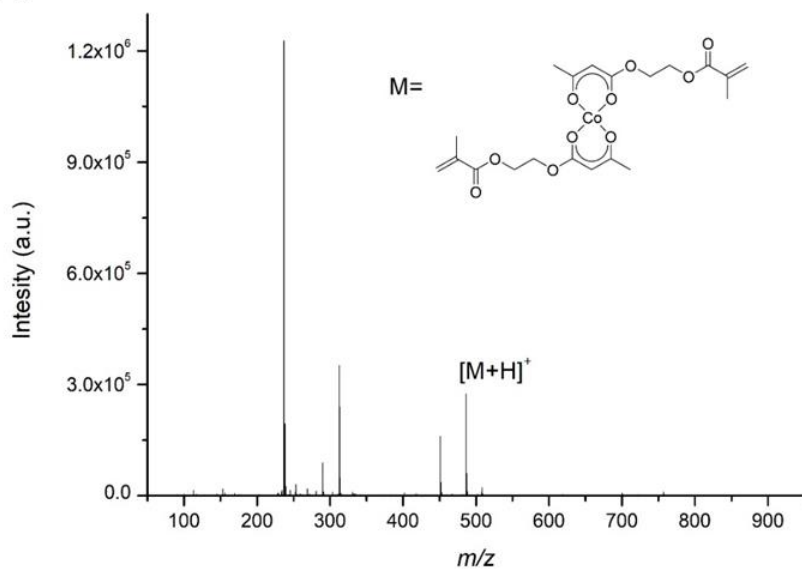
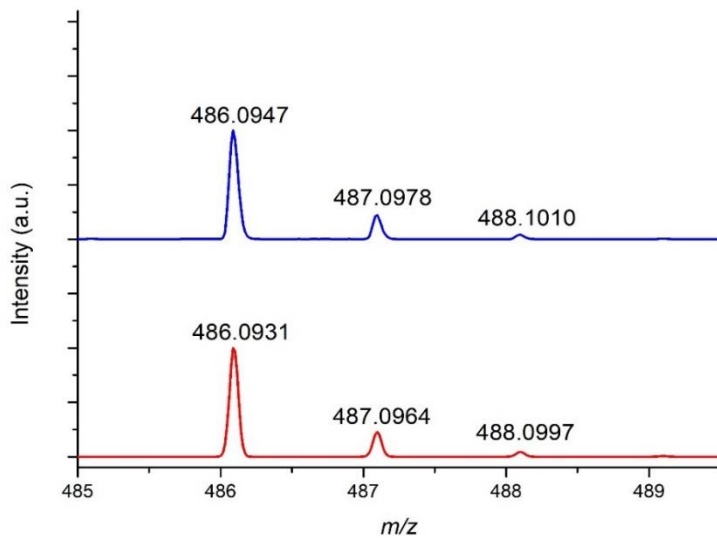
A**B**

Fig. II.3 A: Experimental HRMS (ESI+) of **Co(AAEMA)₂** in CH₃OH. **B:** Experimental (blue top trace) and calculated (red bottom trace) isotopic patterns of [**Co(AAEMA)₂**+H]⁺ (exact mass = 486.0931 da, C₂₀H₂₇O₁₀Co). The mean error between observed and calculated isotopic patterns is -3.3 ppm.

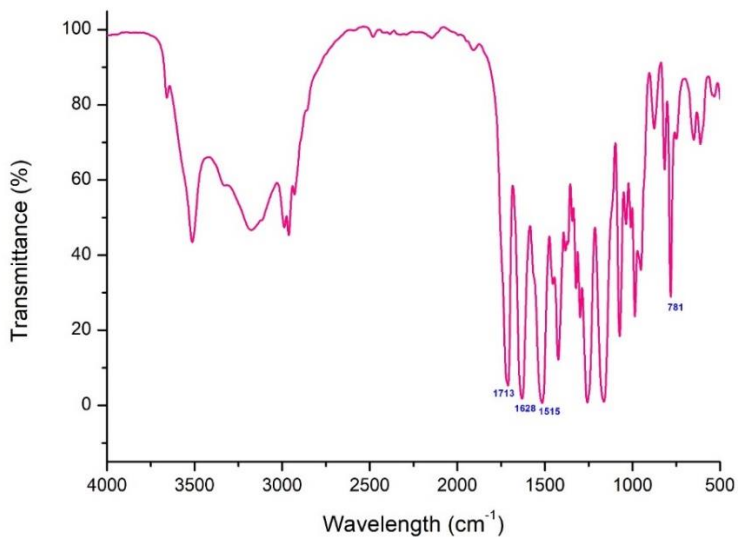


Fig. II.4 FTIR (ATR) spectrum of **Co(AAEMA)₂**.

Co(AAEMA)₂ UV-vis spectrum is also in agreement with the chromophore of a bis- β -ketoesterate Co(II) complexes. For instance, in **Fig. II.5** an UV-vis spectrum of **Co(AAEMA)₂** in dichloromethane solution is depicted exhibiting the maximum absorption at $\lambda = 273 \text{ nm}$ ($\epsilon = 17300 \text{ L mol}^{-1} \text{ cm}^{-1}$).

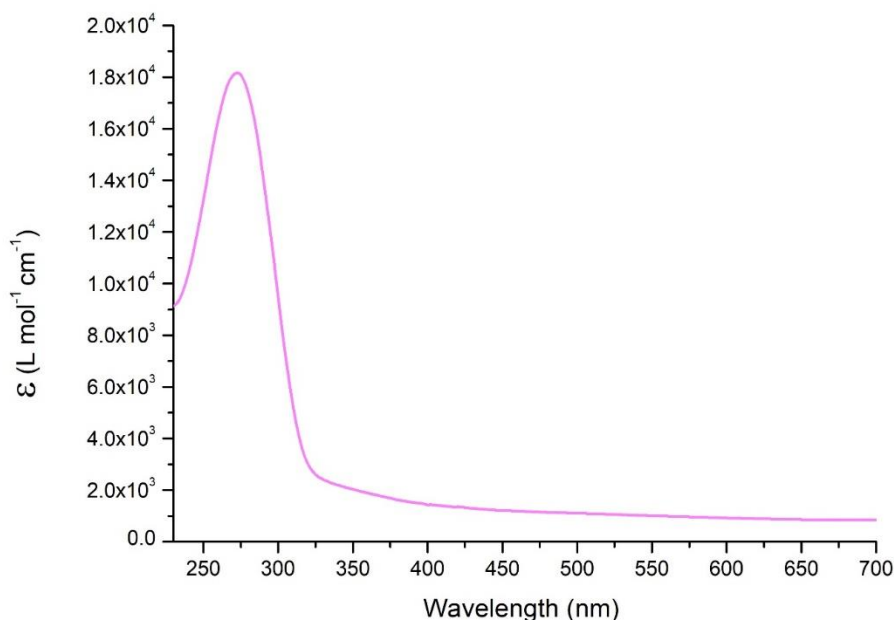
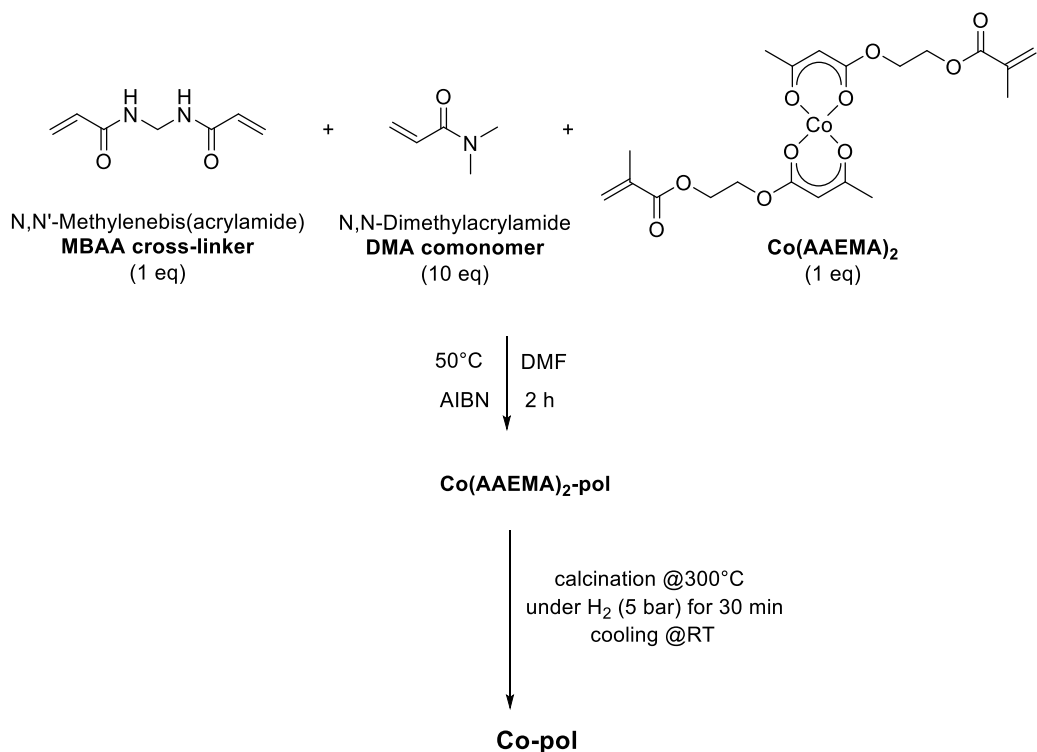


Fig. II.5 UV-vis spectrum of a dichloromethane solution **Co(AAEMA)₂** (1.57×10^{-5} M).

Finally, combustion analysis (for C and H) and graphite furnace atomic absorption spectroscopy (GFAAS) for cobalt content confirms a good purity for **Co(AAEMA)₂** without excluding again the presence of some water molecules in the coordination sphere.

2.3 Synthesis and characterization of a cobalt-containing polymer from Co(AAEMA)₂: Co(AAEMA)₂-pol and Co-pol

Having in our hands pure **Co(AAEMA)₂**, we found it very prone to thermal radical copolymerization reaction. The best reaction condition for copolymerization were found when 1 equiv of **Co(AAEMA)₂** was treated with 10 equiv N,N'-dimethylacrylamide (DMAA) as comonomer, 1 equiv of N,N'-methylenebisacrylamide (MBAA) as cross-linker in presence of a very small amount of α, α' -azaisobutyronitrile (AIBN) as radical initiator in dimethylformamide (DMF) at 50°C (**Scheme II.3**).



Scheme II.3 Synthesis of resin **Co(AAEMA)₂-pol** and **Co-pol**.

Within 2 h, the precipitation of resin blocked the reaction stirring, and the reaction was then blocked. After work-up, **Co(AAEMA)₂-pol** was obtained in 56% yield as a non-hygroscopic pink-violet resin, which is insoluble in all solvents but swells well in water, acetone, halogenated solvents, and dioxane, and shrinks when treated with diethyl ether, ethyl acetate or petroleum ethers. The comparison of IR of the copolymer **Co(AAEMA)₂-pol** with those of the precursor complex **Co(AAEMA)₂** indicates that the polymerization preserves the cobalt(II) chemical environment (**Fig. II.6**). In fact, **Co(AAEMA)₂-pol** IR spectra showed the features of the coordinated β -ketoesterate moiety (1513 and 1631 cm^{-1}) at roughly the same wavenumbers of the corresponding complex **Co(AAEMA)₂** (1515 and 1628 cm^{-1} , see above par. 2.2), thus substantiating that the metalloorganic units in both soluble and supported materials are very similar. Eventually, elemental analysis gave a 4.25%_w of cobalt content in **Co(AAEMA)₂-pol**.

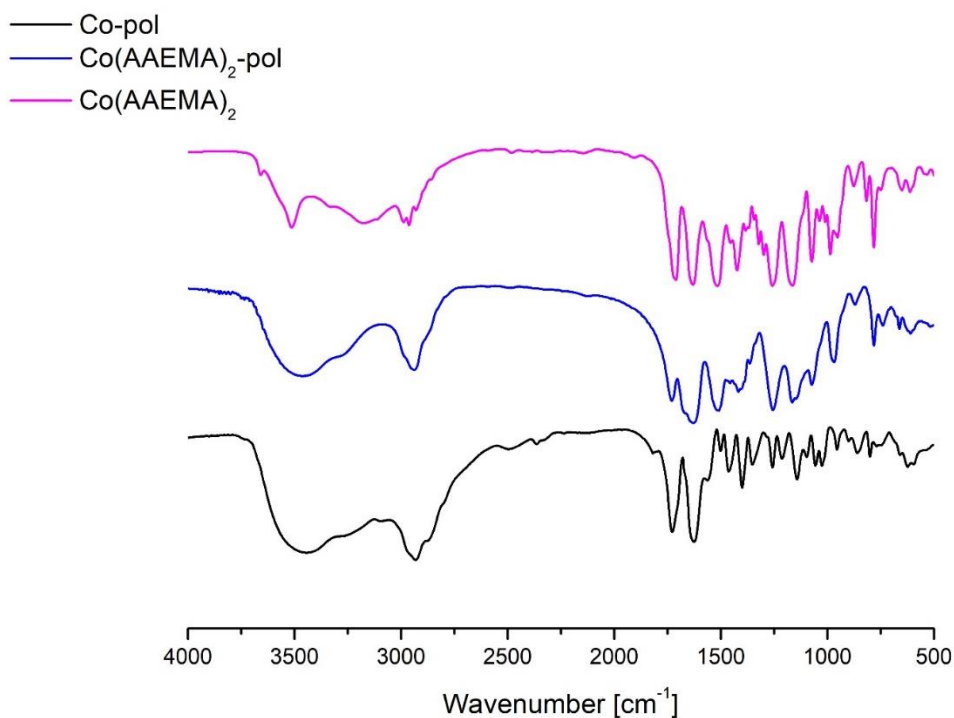


Fig. II.6 Comparison of FTIR (ATR) of **Co(AAEMA)₂**, **Co(AAEMA)₂-pol**, and **Co-pol**.

Co(AAEMA)₂-pol is similar to another metal-containing polymer synthesized in our laboratory: **Ni(AAEMA)₂-pol**, which was found, under very mild reaction conditions, a very active, selective, recoverable and reusable catalyst for the reduction of several functionalized nitroarenes to corresponding aromatic amines in aqueous medium, and for the one-pot stepwise reductive amination of arylaldehydes with nitroarenes.¹⁵¹ However, to achieve these remarkable results, before catalysis, **Ni(AAEMA)₂-pol** was subjected to calcination at 300°C under N₂. Indeed, investigation on surface morphology by Transmission Electron Microscopy (TEM) demonstrated that such thermal annealing led to embedding in polymeric matrix Ni(0) nanoparticles in the average cross section value of 35 nm with a quite narrow (25-45 nm) and monomodal distribution. In fact, calcination under hydrogen or nitrogen atmosphere of a catalyst is a well-known technique¹⁵² used for preparing metallic nanoparticles anchored to an insoluble support by thermal reduction of supported metal ions. Depending on the calcination temperature, the thermal treatment also modifies the insoluble matrix (which

may lose water, crystallization solvent molecules and/or carbon-based moieties), thus enhancing or depressing the ability of the support in stabilizing and retaining the so formed metal nanoparticles.

In this framework, we also decided to carry out the calcination of **Co(AAEMA)₂-pol** by studying in advance its thermal behavior by thermal gravimetric analyses (TGA). TGA trace of **Co(AAEMA)₂-pol** (**Fig. II.7**) suggested us to set the calcination temperature at 300°C, because over 300°C the loss in weight of the polymeric material exceeded 5% of the initial mass, due to a plausible structural modification of the support. Next, by annealing **Co(AAEMA)₂-pol** under hydrogen atmosphere (5 Bar) for 30 min at 300°C and reporting it to room temperature under the same atmosphere (see above **Scheme II.3**), we obtained a black resin named as **Co-pol** containing 5.17%_w of cobalt.

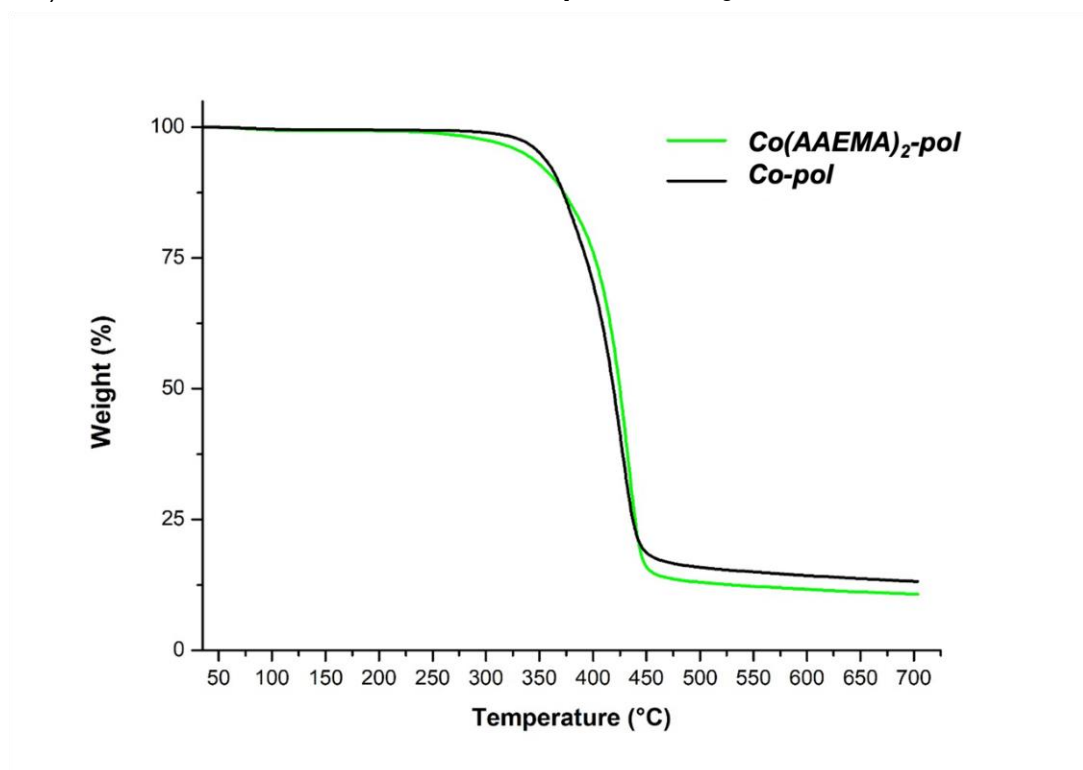


Fig. II.7 TGA of **Co(AAEMA)₂-pol** and **Co-pol**.

2.3.1 TEM analysis

Transmission electron microscopy (TEM) has become a powerful and versatile tool for the study of material structures, particularly nanomaterials. Using electrons as a source is advantageous because they interact strongly with matter. In order to elucidate morphological and structural features of our catalysts, we carried out TEM analysis of pristine Co(AAEMA)₂-pol and Co-pol after calcination.

In **Fig. II.8(a-b)** TEM images of Co-(AAEMA)₂-pol at different magnifications are reported. The figures show the porous structure of the polymer and that no cobalt particle formation has occurred before the calcination.¹⁵³

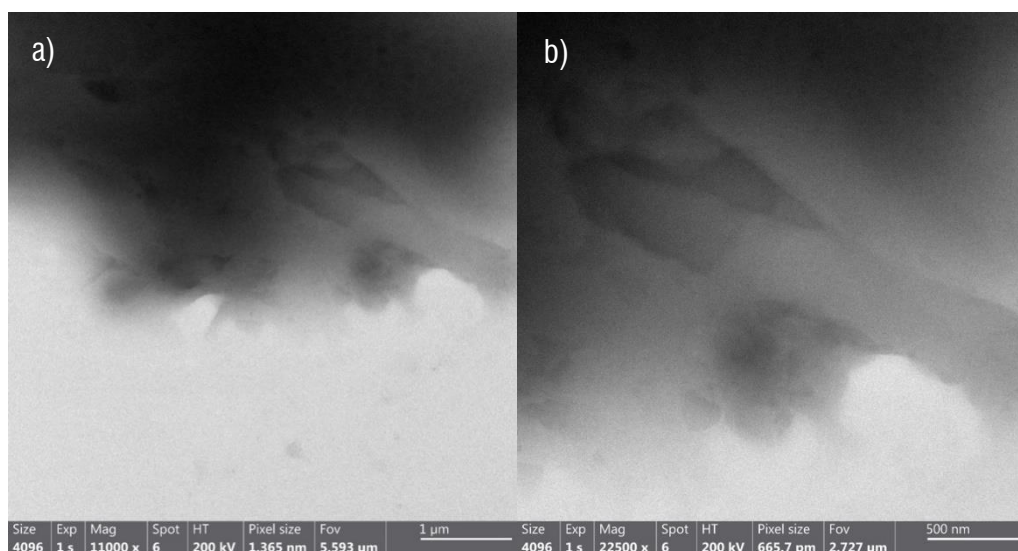
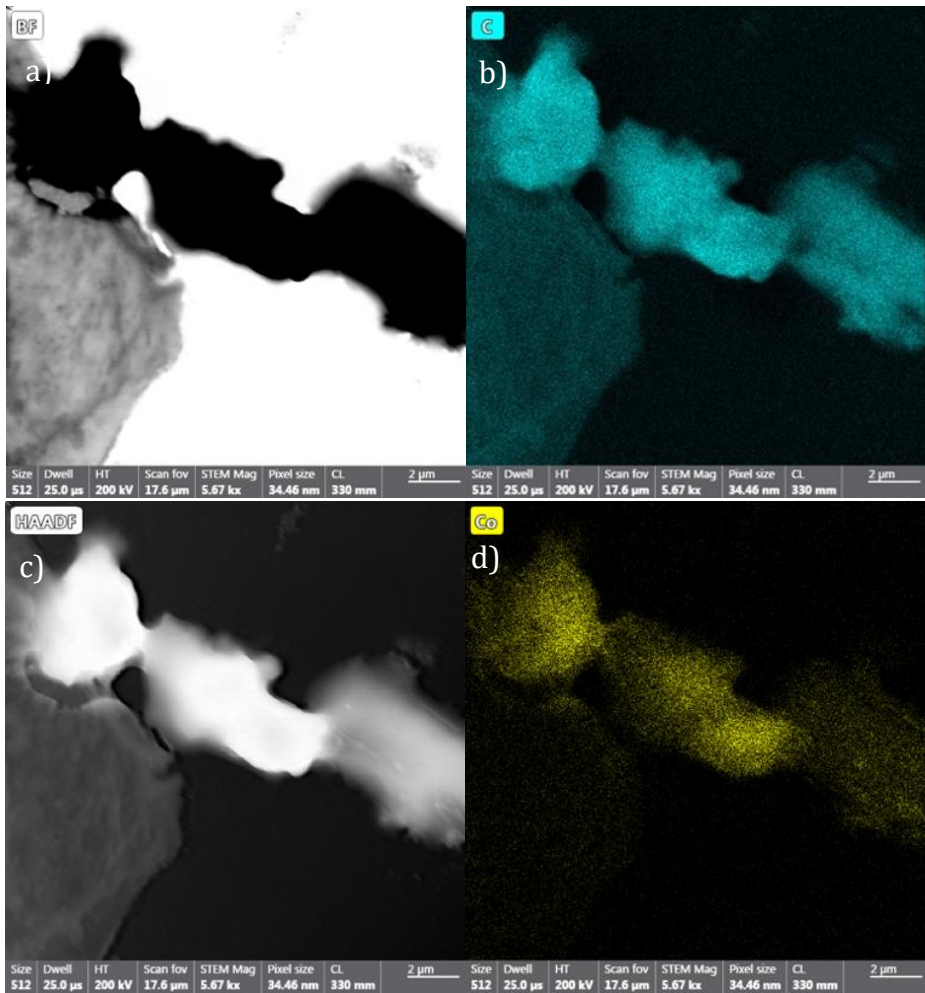


Fig.II.8 a-b: TEM image of Co(AAEMA)₂-pol at different magnification before the calcination.

TEM analysis offers a wide range of complimentary information which are available as a result of different operation modes and imaging techniques, like bright-field (BF), high angle annular dark field (HAADF) detector, dark-field (DF) or selective area electron diffraction (SAED). The elemental identity of the materials was determined by means of Energy Dispersive Spectroscopy (EDS). In **Fig.II.9(a-f)** STEM images of Co(AAEMA)₂-

pol and the corresponding C, O, N and Co EDS mapping are reported, clearly indicating a uniform distribution of Co, C, O and N on the sample.



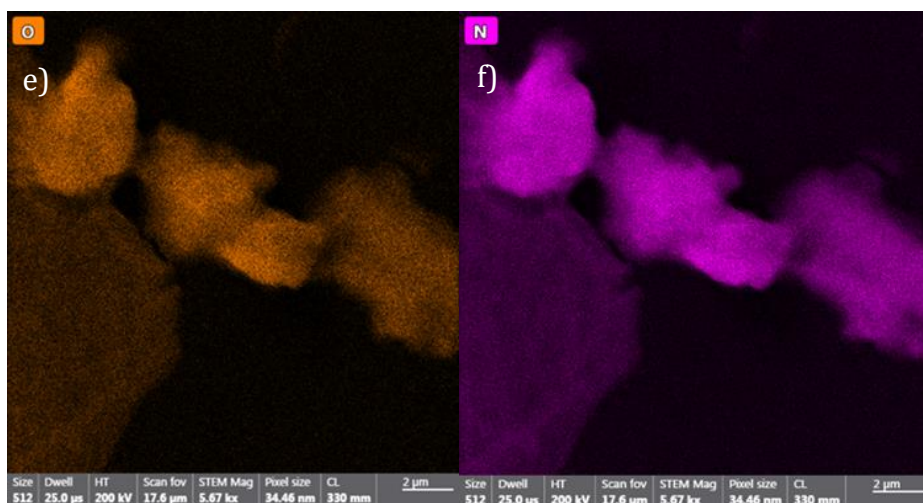


Fig.II.9 a-f: STEM-EDS images of Co(AAEMA)₂-pol of different element maps.

In **Fig. II.10(a-c)** TEM images of Co-pol after calcination at different magnifications are reported, showing the formation of uniformly distributed metal nanoparticles with very low sizes (less than 10 nm).

Notably, EDS mappings (**Fig. II.11 a-e**) of Co-pol reveal that Co distribution goes together with O distribution, suggesting the presence of Co₃O₄ nanoparticles, besides Co nanoparticles onto the supporting matrix. A similar composition was already observed in many Co-based heterogeneous catalysts synthesized by Beller and co-workers, that even proposed a core-shell nanostructure Co@Co₃O₄ for their nanocomposites.^{154,155} In fact, cobalt oxide nanoparticles have been found catalytically active in reduction reaction, although the highest catalytic activity has been attributed to Co-N_x species, due to electron transfer capability of nitrogen centers. In this framework, Co-pol is an example of N-doped catalyst due to use of acrylamide comonomer and cross-linker during preparation, and the presence of nitrogen onto the organic support is confirmed by EDS images reported in Fig. II.11.

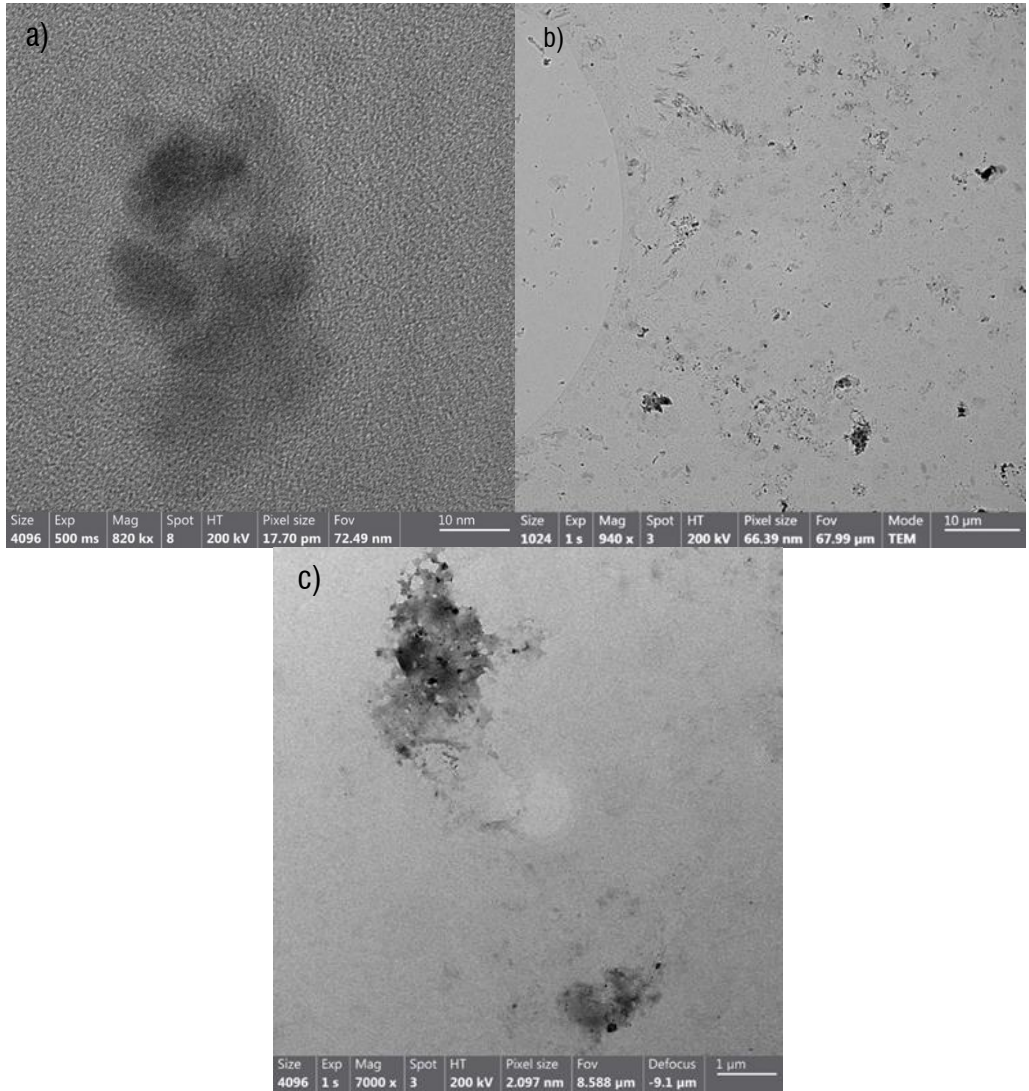


Fig.II.10 a-c : TEM images of Co-polt at different magnification.

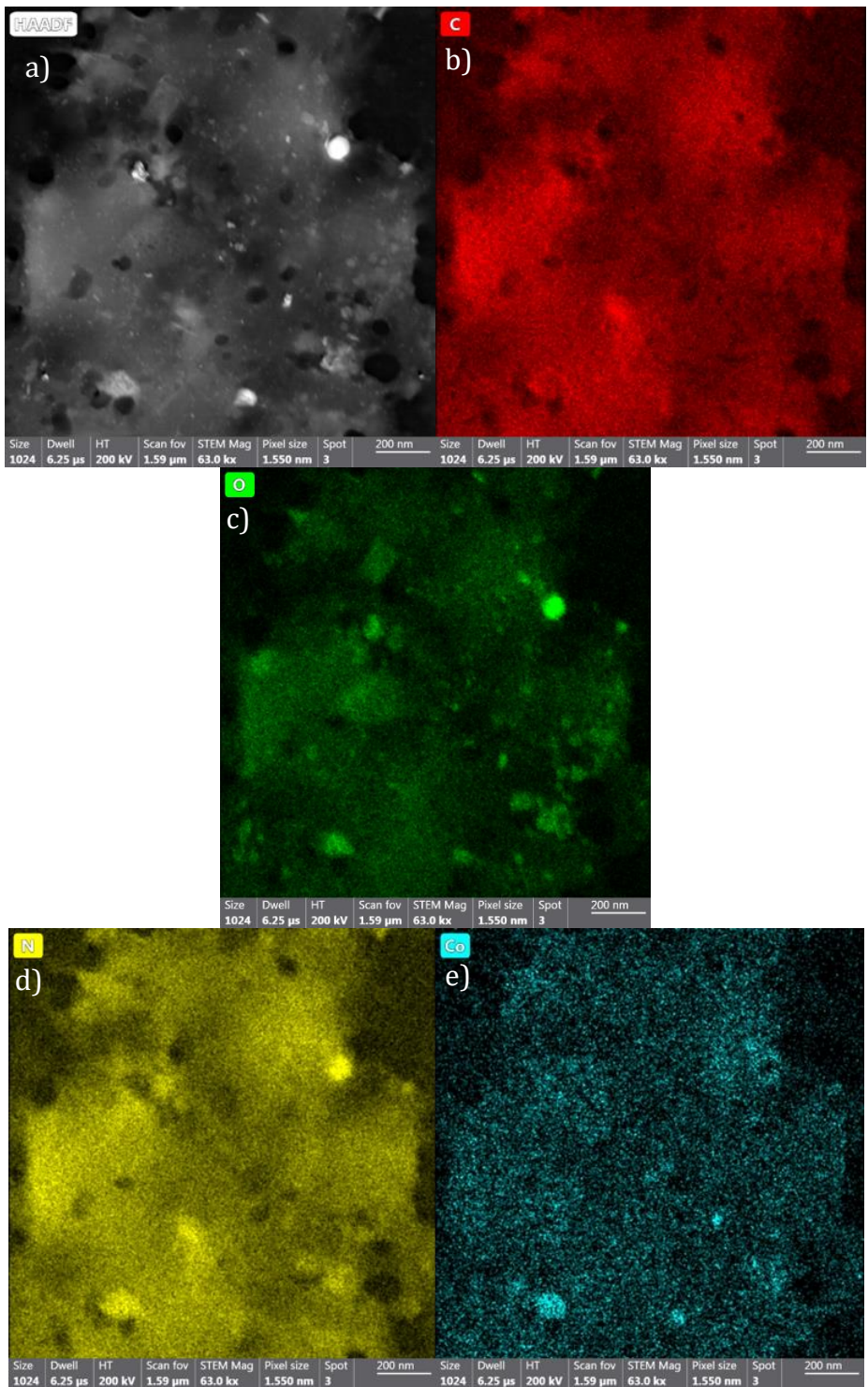


Fig. II.11 a-e: STEM-EDS images of Co-pol of different elemental maps.

2.4 Catalytic activity of Co-pol in the reduction of nitroarenes to anilines

2.4.1 Overview on the reduction of nitroarenes to corresponding anilines

Aniline and its derivatives represent one of the most important building blocks in the organic chemical industry due to its versatility and wide usage for the synthesis of dyes, agrochemicals, pharmaceuticals, polymers, and other fine chemicals.¹⁵⁶ Aniline was isolated for the first time in 1826 as the product of the dry distillation of indigo by German chemist Otto Unverdorben. In 1839 under the name of Zinin's reaction, the first preparation of aniline was performed by reduction of nitrobenzene using sodium sulfides as stoichiometric reductants.¹⁵⁷ The greatest shortcoming of this method is the toxicity and bad smell of reducing agents.¹⁵⁸ Some years later, in 1854, the French chemist Pierre J. A. Béchamp developed the use of metallic iron in acidic media as a reducing agent for the production of aniline starting from nitrobenzene, but this method has problems with the management of large amounts of residues iron oxide and apparatus corrosion. A considerable problem is also the separation of residues iron oxides from amine residua. Steam or vacuum distillation can be used for this purpose but increasing the production cost.¹⁵⁹ For many years this was the most used industrial process along with others using different stoichiometric reducing agents such as Zn, Sn, Al, and sulfur compounds.¹⁶⁰ However, this kind of process is economically unviable and does not fulfill the principles of sustainable chemistry due to the large quantities of waste produced.

During the last decades, a lot of efforts has been put by chemical companies for the studies and development of an active catalytic system that could operate in mild and ecofriendly conditions suitable for the industrial production of anilines. These systems are often heterogeneous, differing in the active metal (copper, palladium, or palladium-platinum), in the support (carbon or inorganic oxides) but also on the reaction conditions (temperature, pressure) and the reactor configuration (gas or liquid phase reactions). Harsh conditions in terms of high temperature (up to 300°C) and high pressure (up to 3MPa) are required to do so, nevertheless, these procedures are not

able to avoid the formation of noxious azo and azo derivatives, which lower the yield into anilines.^{161,162}

Noble-metal catalysts (Au, Ag, Pt, Pd, Rh, and Ru), as well as a commercial catalyst like Ni-Raney, have been deeply investigated for the catalytic hydrogenation of nitro groups and although the hydrogenation of simple substituted nitro compounds does not pose significant selectivity problems, the situation is more challenging for substrates carrying reducible functional groups. Probably their high activity implies significant selectivity problems due to the possible action in the presence of other reducible substituents, such as ketones, aldehydes, alkenes or alkynes. Therefore, a suitable catalyst should be able to selectively reduce nitro compounds containing other functionalities.

To avoid these issues, these catalysts must be modified by alloying or poisoning with other metal oxides or molecules that improve the selectivity (but on the other hand decrease activity), like in the case of Siegrist, Blaser and co-workers that achieved the selective reduction of substituted nitroarenes using commercially available platinum catalysts modified by special additives.¹⁶³

In 2005 J. Qui and co-workers demonstrated that the activity of Ag-based catalyst for the selective hydrogenation of a range of chloronitrobenzenes is highly effective and selective. In contrast to silver, no precedent for nitro group reduction exists for gold. However, several cases of gold-catalyzed hydrogenation of C=C and C=O groups have been published.¹⁶⁴ While, in 2006 Corma et al. described an innovative system based on Au NPs supported on TiO₂ as an efficient, active, and selective catalyst in the presence of a large number of functional groups that avoided the accumulation of hydroxylamines and their potential exothermic decomposition. In particular, they achieved high chemoselectivities for the hydrogenation of 4-nitrostyrene, 4-nitrobenzaldehyde, 4-nitrobenzotrile, and 1-nitrocyclohexene. The success of this system has been attributed to the control of the coordination of metal surface atoms and the selecting of appropriate support, in particular by the preferential adsorption of the nitro group rather than other moieties at the interface between the support and the active NPs.¹⁶⁵

Despite these good results achieved with noble metals, the limited availability of these metals in nature, their high cost, and the problems connected with their environmental

impact still remain a big issue which push researchers to develop more economical and eco-friendly alternatives. In this scenario, catalytic reductions based on transition 3d-metals, such as Fe, Cu, Ni and Co that are among the most abundant metals in the Earth's upper crust, thus being readily accessible and meet these requirements.

In particular way, merging suitable modified supports and transition metals centers for heterogeneous systems have become one of the most investigated routes for the design of new active, selective and cheap catalytic materials.

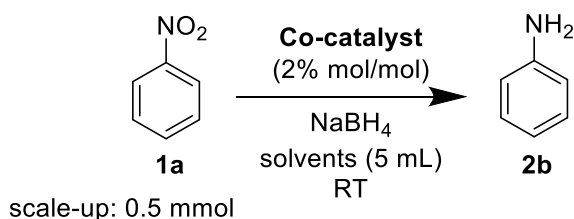
Among the transition metals, cobalt catalysts have rarely been used until 2005, when Raja *et al.* reported one of the first applications of Co-NPs in the hydrogenation of nitroarenes. They performed a Co-based catalyst derived from colloidal precursors and supported on commercially available mesoporous silica, that showed high reactivity, selectivity, and easy separation even if their recyclability was incomplete.¹⁶⁶ In 2013, the group of Beller described a novel heterogeneous Co-catalyst prepared by loading Vulcan XC72R carbon powder with Co(II)/N-ligand complex, which was subjected to pyrolysis at 800 °C under Ar achieving an ordered nitrogen-doped carbon layers along with core-shell nanoparticles. The synergistic and complementary combination of both the Co-based NPs and the nitrogen-doped carbon seems to be crucial for the peculiar reactivity of this class of materials.¹⁵⁴

After this seminal work, a lot of report have been followed this approach to synthesize heterogeneous cobalt-based catalysts for the reduction of nitro compounds to the corresponding amines.¹⁶⁷

In this framework, we believe that our catalysts and especially **Co-pol** can be included in this kind of catalysts.

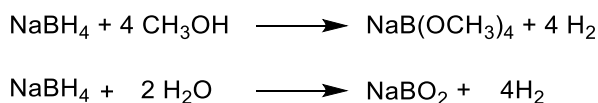
2.4.2 Optimal reaction conditions for the reduction of nitroarenes to anilines mediated by Co-containing polymers

To evaluate the catalytic activity of both **Co(AAEMA)₂-pol** and **Co-pol**, at room temperature the reduction of nitrobenzene (**1a**) to afford aniline (**2a**) was chosen as the paradigmatic reaction (**Scheme 2.5**). The reaction was carried out with 2.0% mol/mol ratio of cobalt with respect to **1a** and in the presence of different amount of NaBH₄ as mild reducing agent.



Scheme II.4

The choice of using NaBH_4 as a reducing agent has dictated by the fact that it is well-known to have broad applications in organic and inorganic synthesis for its ready availability, moderate cost, and ease of handling with respect to other reducing reagents.¹⁶⁸ Under aqueous or protic solvent conditions, NaBH_4 is very slowly hydrolyzed to give H_2 , but transition metal catalysts can further accelerate these reactions (**Scheme II.5**).



Scheme II.5

In **Table II.1** the main results in the reduction of **1a** to **2a** mediated by **Co(AAEMA)₂-pol** or **Co-pol** are summarized.

Table II.1. Preliminary tests to achieve the best reaction conditions

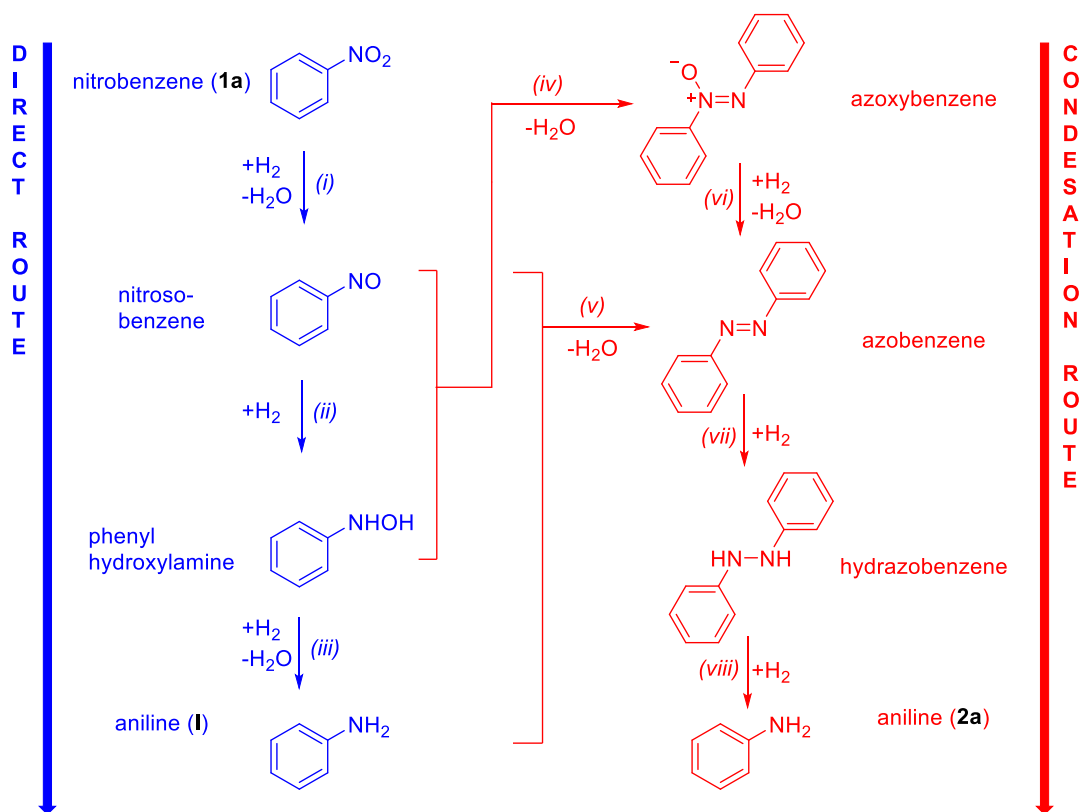
Entry ^a	Co-Catalyst	Solvent	$\text{NaBH}_4/1\text{a}$ ratio	Conversion (%) ^b	Time (h)	Yields (%) ^b
1	none	CH_3OH	4	--	--	--
2	Co(AAEMA)₂- pol	CH_3OH	4	35	3	23
3	Co-pol	CH_3OH	4	50	3	45
4	Co-pol	CH_3OH	10	60	9	52

5	Co(AAEMA)₂-pol	H ₂ O/Et ₂ O	4	45	3	27
6	Co-pol	H ₂ O/Et ₂ O	4	66	3	60
7	Co(AAEMA)₂-pol	H ₂ O/Et ₂ O	20	60	9	48
8	Co-pol	H ₂ O/Et ₂ O	20	85	6	75
9	Co-pol	H ₂ O/Et ₂ O	30	100	12	90

^a Reaction conditions: 0.5 mmol of nitrobenzene, 11.4 mg of Co-pol (Co%_w = 5.17) or 13,48 mg of Co(AAEMA)₂-pol (Co%_w = 4.15), solvent (5 mL, CH₃OH or H₂O/Et₂O, v/v = 1/1) and given amounts of NaBH₄ were stirred at room temperature under nitrogen.

^b Conversions and yield were determined by GLC with the internal standard (biphenyl) method.

First, based on our previous expertise,¹⁶⁹ we fixed as the initial NaBH₄/**1a** molar ratio a value of 4 and chose as solvent the methanol that it is very good solvent both for substrate (**1a**) and product (**2a**) as well as ensures an excellent hydrogen production through methanolysis of NaBH₄.¹⁷⁰ It is noteworthy that a blank experiment (i.e. without catalysts) did not give any conversion of **1a** (Entry 1, **Table 2.1**). Next, we tested the catalytic activity of **Co(AAEMA)₂-pol** on benchmark reaction (Entry 2, **Table 2.1**), the reaction stopped after 3 h to 35% conversion of **1a** giving also poor selectivity in product **2a** (23% yield). With **Co-pol** catalyst (Entry 3, **Table 2.1**), within the same time (3 h) a slight improvement was achieved: 50% conversion of **1a** and 45% yield in product **2a**. The difference between conversion of **1a** and yield in **2a** has to be found in the reduction mechanism of nitroarenes (**Scheme II.6**).



Scheme II.6 Accepted Haber's mechanism for the hydrogenation of nitrobenzene (**1a**) to aniline (**2a**)

Already more than 100 years ago, the famous German chemist and Nobel laureate Fritz Haber¹⁷¹ proposed a reaction pathway for the reduction of nitrobenzene (**1a**) according to which the “direct” route (three steps in blue, **Scheme II.6**) reduction of **1a** molecule competes with a “condensation/reduction” route implying larger molecules (steps in red, **Scheme II.6**). Nowadays, the Haber's idea has been substantially demonstrated and this mechanism has been generally accepted.¹⁷² In our study, thanks to GCMS studies, we observed that **Co(AAEMA)₂-pol** and **Co-pol** catalysts followed both routes. Indeed, GCMS analysis showed together substrate (**1a**) and product (**2a**) the species: nitroso-benzene, azobenzene, and azoxybenzene.

By increasing the $\text{NaBH}_4/\mathbf{1a}$ molar ratio up to 5 in the catalysis with **Co(AAEMA)₂-pol** had no effect on reaction conversion, whereas with **Co-pol** it was possible to push conversion up to 60% in 9 hours (Entry 4, **Table II.1**). Thus, we decided to stop the

use of CH₃OH as solvent and switch towards other solvents. We found very useful a mixture of water/diethyl ether (1/1 = vol/vol) because water ensures through hydrolysis of NaBH₄ a more constant but slower hydrogen production and the biphasic reaction medium on one side facilitates the access of the water insoluble substrate to the catalytically active sites and on the other side renders more workable the acrylamide-based catalyst, becoming the latter too jelly employing neat water. In addition, the polymeric support seems to better retain the Cobalt centers by swelling (in water) and shrinking (in diethyl ether) at the same time. Thus, the hydrophobic property of diethyl ether might potentially help to prevent catalyst deactivation.

Next, by employing water/diethyl ether mixture as solvent and NaBH₄/**1a** molar ratio of 4, the catalytic activity of **Co(AAEMA)₂-pol** on title reaction (Entry 5, **Table II.1**) only a slight improvement in conversion and yield were obtained within the same time (3 h) with respect to methanol. However, the same reaction conditions were more beneficial for **Co-pol** catalyst (Entry 6, **Table II.1**): a 66% conversion of **1a** and 60% of **2a** yield were achieved within 3 h. Again, increasing the NaBH₄/**1a** molar ratio (up to 10) in the catalysis with **Co(AAEMA)₂-pol** had poor effect on reaction conversion and yield (Entry 7, **Table II.1**). Furthermore, during this reaction, we observed that both **Co(AAEMA)₂-pol** and solution reaction turned from pink to green and then into grey, presumably due to different oxidation state of metal centers. In fact, elemental analysis by GFAAS on **Co(AAEMA)₂-pol** recovered at the end of reaction showed a severe cobalt leaching in solution and, thus, we stopped to study its catalytic activity.

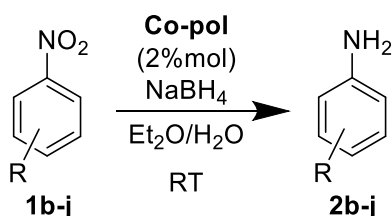
On the other hand, using water/diethyl ether mixture as solvent and NaBH₄/**1a** molar ratio of 10 with **Co-pol** catalyst it was possible to push **1a** conversion up to 85% in 6 h (Entry 8, **Table II.1**) reaching a 75% yield in **2a**. Conversely to **Co(AAEMA)₂-pol**, **Co-pol** maintained its appearance during the reaction and did not show cobalt leaching as demonstrated by analysis GFAAS. Finally, with catalyst **Co-pol** in the H₂O/Et₂O solvent mixture, raising NaBH₄/**1a** molar ratio up to 30 the complete conversion of **1a** substrate was obtained within 12 h (entry 9, **Table II.1**) achieving an excellent yield (90%) into **2a**, despite the fact that a larger use of NaBH₄, increasing the pH value,¹⁷³ could potentially favor the formation of azo-derivatives.¹⁷⁴ The reaction conditions of Entry 9 of **Table 2.1** were chosen as the optimal ones to study both the substrate scope and

the recyclability of **Co-pol** catalyst in the reduction of nitroarenes towards the corresponding anilines.

2.4.3 Scope and general applicability of Co-pol catalytic system

With the optimized reaction conditions in our hand, we passed to explore the scope and general applicability of the present catalytic system in the reduction with various substituted nitroarenes (**1b-j**). Results obtained are reported in **Table II.2**.

Table II.2 Reduction of various nitroarenes catalyzed by **Co-pol**



Entry ^a	Substrate	Product	Time (h) ^b	Yields (%) ^c
1	2-Nitrotoluene (1b)	2-Toluidine (2b)	12	90
2	3-Nitrotoluene (1c)	3-Toluidine (2c)	14	88
3	4-Nitrotoluene (1d)	4-Toluidine (2d)	14	90
4	3-nitroanisole (1e)	3-anisidine (2e)	12	81
5	4-nitroanisole (1f)	4-anisidine (2f)	12	85
6	4-fluoronitrobenzene (1g)	4-fluoroaniline (2g)	12	78
7	4-chloronitrobenzene (1h)	4-chloroaniline (2h)	12	74
8	4-bromonitrobenzene (1i)	4-bromoaniline (2i)	12	72
9	4-iodonitrobenzene (1j)	4-iodoaniline (2j)	24	74

^a Reaction conditions: 0.5 mmol of nitrobenzene, 11.4 mg of Co-pol (Co%_w = 5.17), 5 mL of H₂O/Et₂O (v/v = 1/1) and 15 mmol of NaBH₄ were stirred at room temperature under nitrogen for the appropriate amount of time.

^b time at 100% of substrate conversion.

^c Yield determined by GLC with the internal standard (biphenyl) method.

The **Co-pol** catalytic system was found to be very efficient regardless of the presence of electron-withdrawing and electron-donating substituents in the aromatic ring. Nitroarenes possessing electron-donating groups such as 2-, 3- and 4-nitrotoluene (**1b-d**) afforded excellent yields (88-90%) into the corresponding toluidine (**2b-d**) in 12-14 h (entries 1, 2 and 3, **Table II.2**). The result achieved with substrate **1b** (entry 1, **Table 2.2**) suggests that the catalytic system is also devoid of steric hindrances. Also 3- and 4-nitroanisole (**1e-f**) were converted almost quantitatively into the corresponding anisidine (**2e-f**) in 12 h (entries 4 and 5, **Table II.2**).

Next, the selectivity of the catalyst was also tested in the reduction of different halonitrobenzenes (**1g-j**). In fact, the selective hydrogenation of halonitrobenzenes catalyzed by transition metals is regarded as a high atom efficiency and environmentally friendly process for the synthesis of haloanilines, which are important fine chemicals, widely used in the production of pharmaceuticals, dyes, herbicides, pesticides. However, up to now, the major challenge is avoiding the undesired hydrodehalogenation reaction, which is a side-reaction favored by the electron withdrawing effect of the nitro group in para and/or ortho positions (with respect to the halogen), that enhances the rate of the Ar-X (Cl, Br, I) oxidative addition to the metal center. Also, the product of the reaction (haloaniline) undergo dehalogenation due to the activation of carbon-halogen bond by the electron-donating amino group that makes much higher the negative charge on halogen atom than in the corresponding nitro compounds.¹⁷⁵

In this context, with our delight, we also found that **Co-pol** resulted active and selective in the reduction of halonitrobenzenes (entries 6-9, **Table II.2**), even in the case of challenging bromo- and iodo-nitrobenzene (entries 8 and 9, **Table II.2**). In all case, the selectivity of halonitrobenzenes towards the corresponding halogenated anilines was higher than 70% and only 4-iodonitrobenzene (**1j**) required a long reaction time (24h) to be converted into the corresponding iodoaniline (**2j**) (entry 9, **Table II.2**).

2.4.4 Recyclability of Co-pol

The hydrogenation of nitrobenzene (**1a**) to aniline (**2a**) was also chosen as a test reaction to demonstrate reusability of **Co-pol** in the reduction of nitroarenes under optimized conditions. To handle and study with a greater quantity of **Co-pol** the reaction scale-up was raised up to 1.5 mol of **1a** (Fig. II.12).

Co-pol catalyst showed a slight decrease (71 % yield in **2a**) in the catalytic activity already in the second run and a significant decline (47 % yield in **2a**) in the third run (see red legend in Fig. II.12). However, leaching experiments demonstrated that only 0.1% of the total amount of Co leached out during catalysis. For other cobalt catalysts supported on polymeric matrix,¹⁷⁶ this effect of catalyst deactivation without Co leaching has been already found. The main reason for the deactivation is the formation of stable Co oxides on polymeric matrix. However, in these cases, the catalytic activity could easily be regained through a new calcination of catalyst.

To our delight, reactivating **Co-pol** by calcination under H₂ at 300°C for 30 min after any reaction runs, its recyclability was maintained up to five times without any substantial decrease in catalytic activity (see blue legend in Fig. II.12) and with only a slight increase in the Co particle size (Fig. II.13).

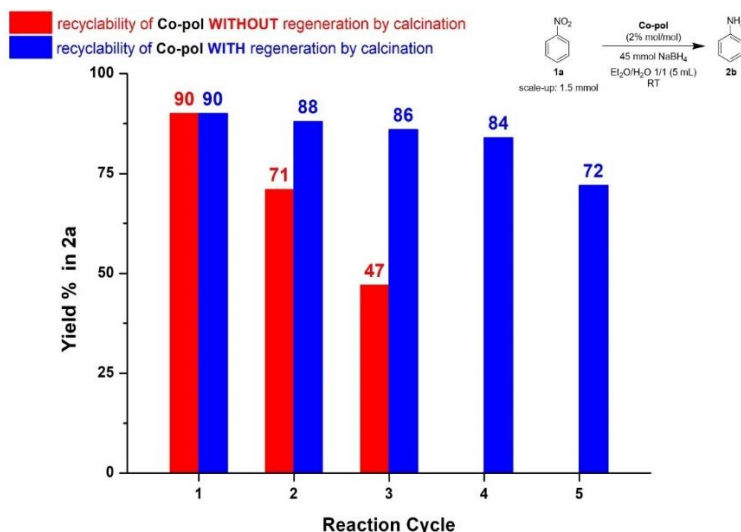


Fig II.12 Recyclability of **Co-pol** in the reduction of **1a** to **2a** under optimized reaction conditions.

Last but not least, to verify whether the observed catalysis was truly heterogeneous or not, the reduction of nitrobenzene was again taken as the model reaction. The mixture was filtered after 6 h reaction (43% conversion of the substrate) and added of 15 mmol NaBH₄. Further stirring of the filtrate under the above reaction conditions did not increase the conversion of nitrobenzene. The filtrate was analyzed by GFAAS showing negligible cobalt amount. In addition, **Co-pol** recovered from the filtration was mineralized and analyzed by GFAAS showing the same cobalt content (within the experimental error) of the fresh catalyst. The same cobalt amount was also found in the catalyst recovered at the end of the fifth cycle. All these results rule out any possible contribution of homogeneous catalysis by leached cobalt species, suggesting that the catalysis was truly heterogeneous.

2.4.5 Analysis of Co-pol recovered after reduction

Fig. II.13 and **II.14** show Co-pol morphology recovered after the first and the fifth reaction run respectively. Cobalt nanoparticles retain their morphology, they are fully embedded and uniformly distributed in the amorphous polymeric matrix. However, on passing from the Co-pol before use (**Fig. II.10c**) to first and fifth run the cobalt particle sizes became slightly larger probably due to aggregation phenomena.

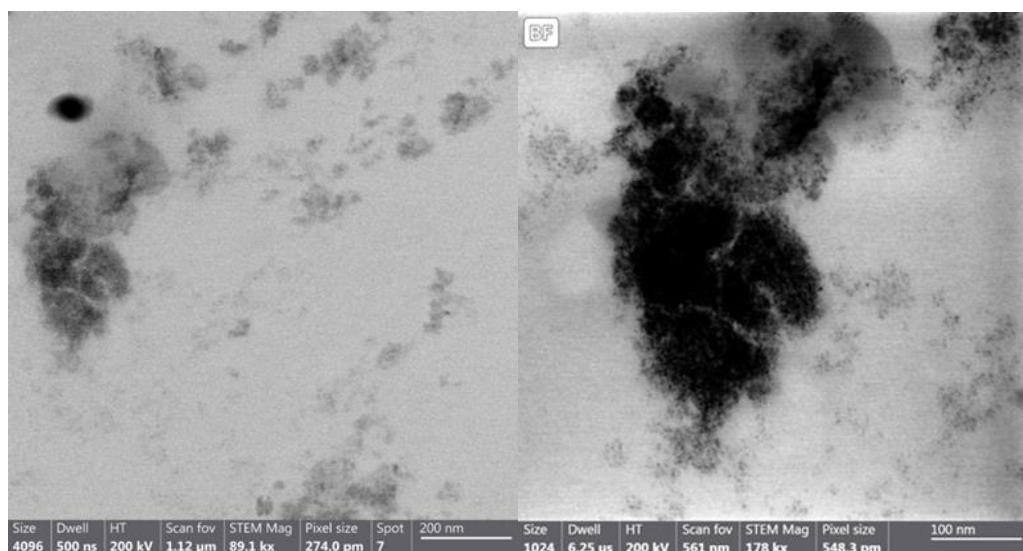


Fig. II.13 Co-pol recovered after the first run of reaction.

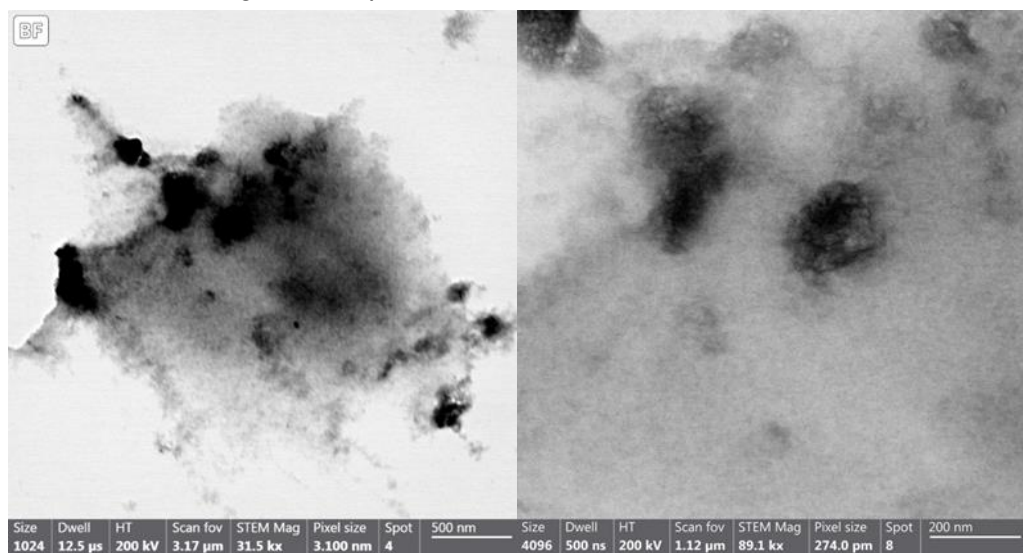


Fig. II.14 Co-pol recovered after the fifth run of reaction.

2.5 Conclusions

In conclusion, the synthesis of the cobalt-containing monomer **Co(AAEMA)₂** was revisited and by far improved. Thanks to the easy radical polymerization of **Co(AAEMA)₂** with appropriate comonomer and crosslinker the cobalt-containing polymer **Co(AAEMA)₂-pol** was achieved. Subsequent calcination of **Co(AAEMA)₂-pol** under H₂ gave a polymer supported cobalt catalyst **Co-pol**, that efficiently promoted the reduction of aromatic nitroarenes in aqueous medium at room temperature in the presence of a safe and mild reduction agent such as NaBH₄. No other additives were needed for the reaction yielding sustainable the whole process. This heterogeneous catalytic system was especially selective towards haloaniline in the reduction of halonitrobenzene. The catalyst could be easily recovered at the end of the reaction and recycled for at least fifth times maintaining good selectivities and yields provided that **Co-pol** was regenerated after each cycle by thermal annealing at 300°C

CHAPTER III

Nickel based catalyst

3.0 Nickel based catalyst

3.1 Chemistry of nickel and major catalytic application

Nickel (Ni) is the first element among group 10 of transition metals, it is the fifth-most common element on earth and occurs extensively in the earth's crust and core. Nickel, along with iron, is also a common element in meteorites and can be found in small quantities in plants, animals, and seawater.

The origin of its name, as for cobalt, is related to legends about miners. In the 16th century, miners who used to work in the neighborhood of Annaberg in Sachsen tried to recover copper from a reddish ore. However, they never made it because this source contained only nickel and arsenic. Due to this failure, they ended blaming demons for it. In fact, nickel derives from German "Kupfernichel" meaning literally copper demon.¹⁷⁷ Many years later, nickel was first identified and isolated by the Swedish chemist Axel Cronstedt in 1751 and then, in 1888 Ludwig Mond found an easy way of extracting it. He discovered an unusual reactivity patterns of nickel by noticing that elemental nickel and CO reacted at room temperature to form $\text{Ni}(\text{CO})_4$, an extremely toxic, low-boiling liquid, which could be used to purify the metal (Mond process).¹⁷⁸ Shortly thereafter, Sabatier performed the first hydrogenation of ethylene using nickel, for which he was awarded the 1912 Nobel Prize in Chemistry.¹⁷⁹

From this moment on, it has been used in large amounts due to its attractive qualities like strong corrosion resistance, high temperatures resistance and durability. Moreover, these properties can be transferred to other metals owing to the nickel attitude to form alloys. Today, for example, the widely used stainless steel is a nickel containing alloy.¹⁸⁰ Nickel can have different oxidation state (0, +1, +2, +3, +4), but the most common compounds possess the +2 oxidation state.

It has been recognized as one of the most interesting transition metals for homogeneous catalysis. In the last decades, thanks to recently developed of new ligands, new reaction conditions and new method to control the reactivity, the application of these catalysts has been expanded to a variety of bond-forming reactions.¹⁸¹ Additionally, the development of a new generation of analytical equipment and rapid progress in computational studies and characterization techniques has

provided outstanding systematic tools for improving also the using in heterogeneous catalysis.

Therefore, fine tuning of the ligands has been the key to the design of homogeneous nickel catalysts, while understanding the role of the nanoscale environment helped the development of solid nickel catalysts. As result, Ni complexes have been synthesized and used as catalysts in a variety of reaction including reduction and C–C, C–O, C–N and S–S coupling reactions, hydrogen generation, oxidation of CO, alcohols, CO₂ reforming, alkene hydrosilylation with tertiary silanes, synthesis of primary amines from alcohols and ammonia, epoxidation and so on.¹⁸²⁻¹⁸⁷ (Fig.III.1)

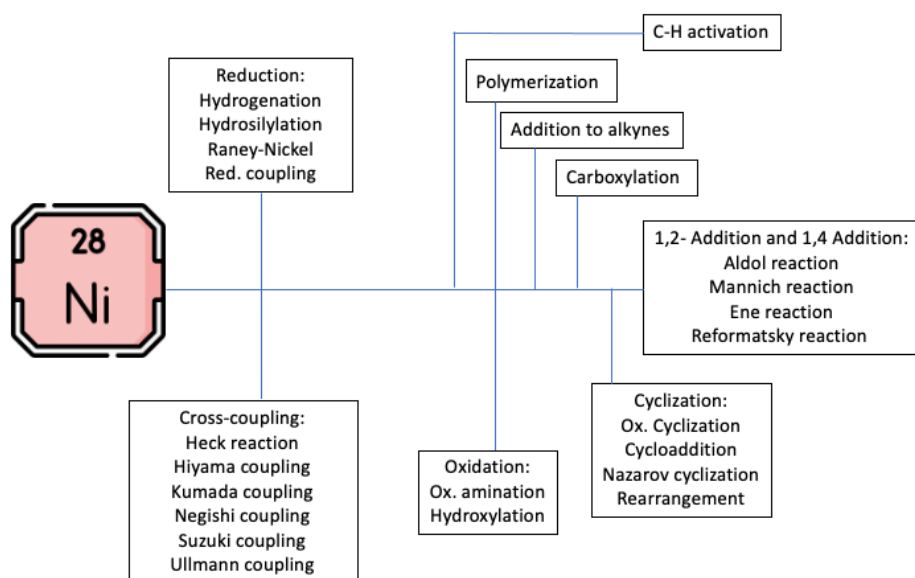
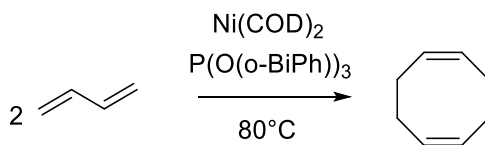
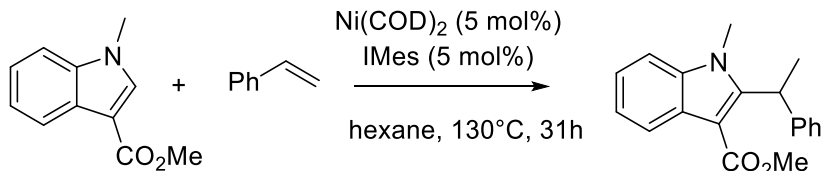


Fig.III.1 Nickel-catalysed reactions.¹⁸⁸

Ni complexes have gained attention in the coupling reactions through the early work of Wilke on the cyclooligomerization of butadiene (scheme III.1).¹⁸⁹ The property of Ni(cod)₂ to coordinate olefins with subsequent electron transfer was used also in the catalytic hydrovinylation of indole derivatives with different vinylarenes (scheme III.2).¹⁹⁰

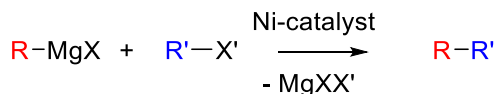


Scheme III.1



Scheme III.2

Ni^0 complexes were among the first catalysts employed in selective cross-coupling. In fact, in 1972 the groups of Kumada (scheme III.3)¹⁹¹ and Corriu¹⁹² reported independently the successful C-C bond formation between aryl chlorides and Grignard reagents.



X, X' = Cl, Br, I, OTf

Scheme III.3

Nevertheless, in the last 20 years C-C cross-coupling reactions have been dominated by palladium catalysts underlined also in 2010 by the Nobel prize awarded to R. Heck, E. Nigishi and A. Suzuki.¹⁹³

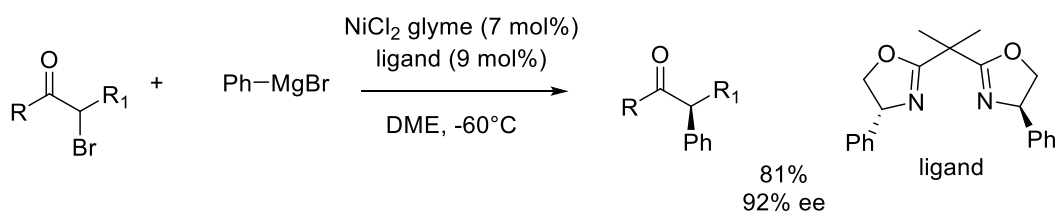
Nowadays, the increased awareness about nickel properties has allowed to replace palladium not only for lowering the reaction cost but mostly for broadening the substrate scope due to its different reactivity.

Nickel is a relatively electropositive late transition metal. The oxidative addition, which results in loss of electron density around nickel and oxidation, for example from Ni(0) to Ni(II), tends to occur quite readily (in the same time reductive elimination is more difficult).

For this reason, it is possible employed cross-coupling electrophiles that would be considerably less reactive under palladium catalysis, such as phenol derivatives,¹⁹⁴ aromatic nitriles¹⁹⁵ or even aryl fluorides.¹⁹⁶

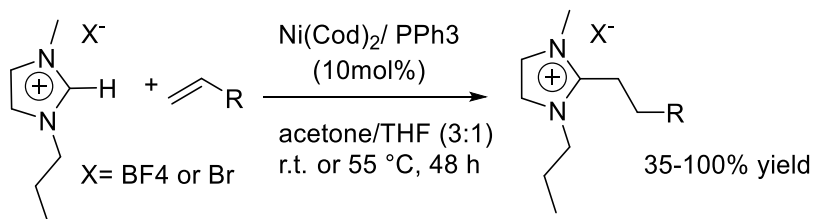
Moreover, the easy accessibility to several oxidation states allows single electron pathways and different modes of reactivity and radical mechanisms can be achieved. In 2003 the Fu group's reported the system Ni(cod)₂/s-Bu-Pybox that allows the first room-temperature Negishi reactions of an array of functionalized primary and secondary alkyl bromides and iodides.¹⁹⁷

Following the studies in sp₃-sp₃ bond forming reaction, some years later, Fu and coworkers described an asymmetric version of the Kumada reaction for the enantioselective cross-couplings of racemic secondary benzylic halides (scheme III.4).

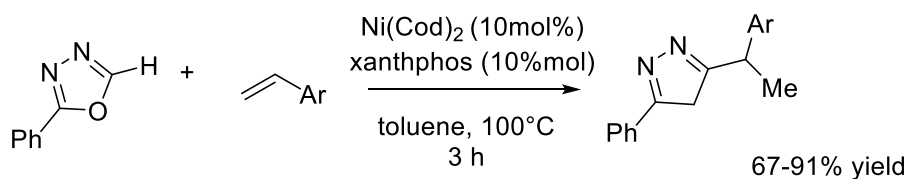


Scheme III.4

Another important application of Ni-catalyst is represented by the C-H aromatic activation. The first Ni-mediated aromatic C-H bond activation was reported by Kleiman and Dubeck in 1963, who observed that by heating di-cyclopentadienyl nickel with diazobenzene was afforded a purple-blue colored organo-nickel species.¹⁹⁸ However, this kind of reaction remain undeveloped until the pioneering work about C-H functionalization carried out by Cavell in 2004. In this work has been described the coupling of imidazolium salts with alkenes achieved by using a Ni(cod)₂/PPh₃ catalyst system (scheme III.5).¹⁹⁹ In 2009, Miura reported the addition reaction, Ni(0)-catalyzed, of 1,3,4-oxadiazoles to styrene derivatives via C-H bond cleavage as reported in scheme (scheme III.6).²⁰⁰



Scheme III.5



Scheme III.6

In 2010, Hirano and Miura reported the Ni(II)-catalyzed the direct CH alkylation of electron-deficient benzothiazole with unactivated alkyl bromides and chlorides and the arylation of azoles with arylboronic acids by using air as an oxidant.²⁰¹

Some years later, Itami demonstrated the cross coupling of azoles with aryl halides and aryl triflates by using respectively $\text{Ni(OAc)}_2/\text{bipy}$ or $\text{Ni(OAc)}_2/\text{dppf}$ catalysts in the presence of LiOtBu .²⁰² Thiazole, benzothiazole, oxazole, benzoxazole, and benzimidazole are applicable as heteroarene coupling partners.

Among the reaction catalyzed by nickel nanocatalyst, the reduction is the most investigated reaction. Ni-nanoparticles supported on different materials ranging from silica to polymers, have been found active in the catalytic reductions of substituted benzenes, styrene, p-nitrophenol, furfural, nitroarenes, carbonyl compounds and nitrile and so on.²⁰²⁻²⁰⁶

Among the reduction processes, the reduction of nitro compounds has been the subject of intense research since industrially important chemicals can be obtained starting from them. Namely, anilines or azoxy- compounds that can be synthesized by tuning the reaction conditions.

Ni and Ni-based nanocatalysts shown promising properties that making them not only an inexpensive substitute for palladium, but rather a valid alternative that allows to implement catalyst applications. Based on the considerations made so far, this chapter is focused on synthesis and deeper studies of the activity and selectivity achieved with different supported Ni(AEMA)_2 catalysts towards the reduction of nitroarenes.

3.2 Influence on catalytic activity of different morphologies

Noble metal nanocatalysts have been usually employed in several organic reactions, due to their high versatility.²⁰⁷ In the last years, many studies have been devoted to replacing expensive noble metals with earth abundant metals in catalysis, in a conservative vision of the natural resources. In this scenario, Ni NPs supported onto insoluble matrices (inorganic oxides or polymers) have been successfully used as active and recyclable catalysts for reduction reactions of unsaturated substrates.²⁰⁸ On the basis of previous works, an innovative synthetic route for polymer-supported catalyst is based on the preliminary preparation of a metal containing monomer, followed by its co-polymerization with suitable co-monomers, in order to obtain an insoluble material containing a well dispersed distribution of metal centers.¹⁵³ A technique to convert the supported complexes into metal NPs, stabilized by the insoluble matrix, is calcination, which is usually carried out under inert atmosphere or reductive conditions (dihydrogen flow). Calcination temperature is chosen depending on both the nature of support and metal catalyst. It is widely recognized that the morphology of the obtained nanoparticles greatly affects the activity and selectivity of the final catalyst.²⁰⁹ There are several strategies to control the morphology of the obtained nanoparticles (use of additives, choice of solvent, selection of the reductant, etc.).²¹⁰

In particular, herein, synthetic protocols already performed¹⁵¹ will be slightly modified by changing calcination procedure. In fact, the calcination procedure of the same polymer supported Ni(II) complex leads to different materials, depending on how the cooling step (under dihydrogen or under air) takes place after the heating run. These variations will be studied focusing on the characterization and morphology of the obtained catalysts, to evaluate the effective correlation between morphology and final catalytic activity.

To our delight, if the cooling phase occurs under air, the obtained material supports uncommon urchin-like Ni NPs, whose activity and selectivity in catalyzing the nitrobenzene reduction are different from those shown by the catalyst obtained by dihydrogen cooling step.

3.2.1 Synthesis and characterization of Ni(II) complex: Ni(AAEMA)₂

The synthesis of metal containing monomer was performed by following the same procedure already reported in literature.¹⁵¹ To a solution of KOH in ethanol, 2-(acetoacetoxy) ethyl methacrylate (HAAEMA) was added and left under stirring at room temperature for 5 min. The resulting solution was added to a solution of Ni(NO₃)₂·6H₂O in ethanol, causing the sudden precipitation of Ni(AAEMA)₂ as a pale green solid. After 1h stirring, the solid was filtrated and washed with water, ethanol, and pentane, and dried overnight under vacuum. Ni(AAEMA)₂ was carefully characterized through HRESI-MS, IR, UV-vis and elemental analyses. In particular, the identity of Ni(AAEMA)₂ was unequivocally ascertained thanks to its ESI spectrum (Fig. III.2 and Fig. III.3) that shows an exact mass with a mean error between observed and calculated isotopic patterns of -1.3 ppm. The formation of Nickel complex was also confirmed by UV-vis spectrum (Fig. III.4).

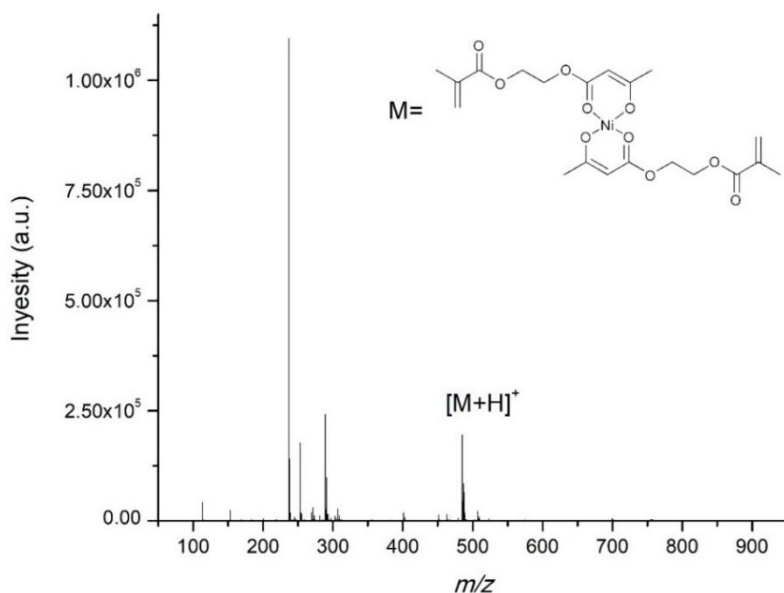


Fig. III.2 Experimental HRMS (ESI+) of Ni(AAEMA)₂ in CH₃OH.

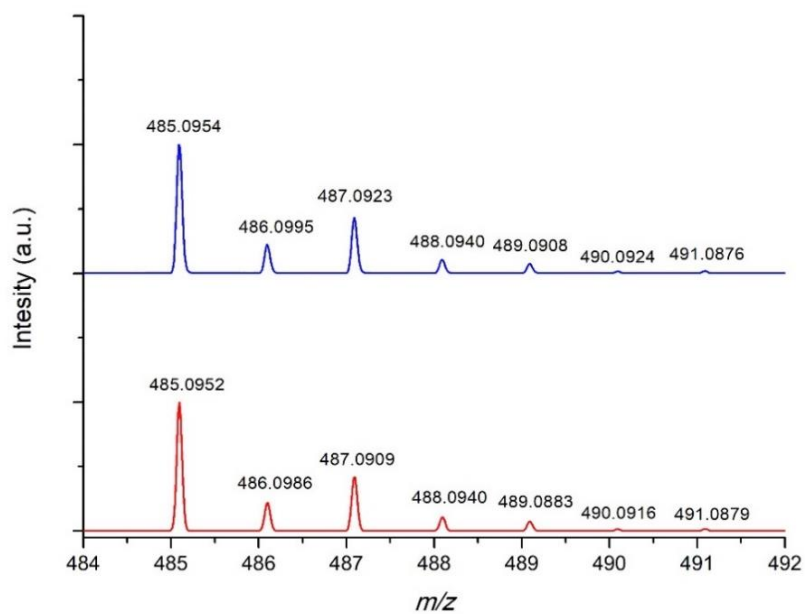


Fig.III.3 Experimental (top) and calculated (bottom) isotopic patterns of $[\text{Ni}(\text{AEMA})_2+\text{H}]^+$ (exact mass = 485.0952 da). The mean error between observed and calculated isotopic patterns is -1.3 ppm.

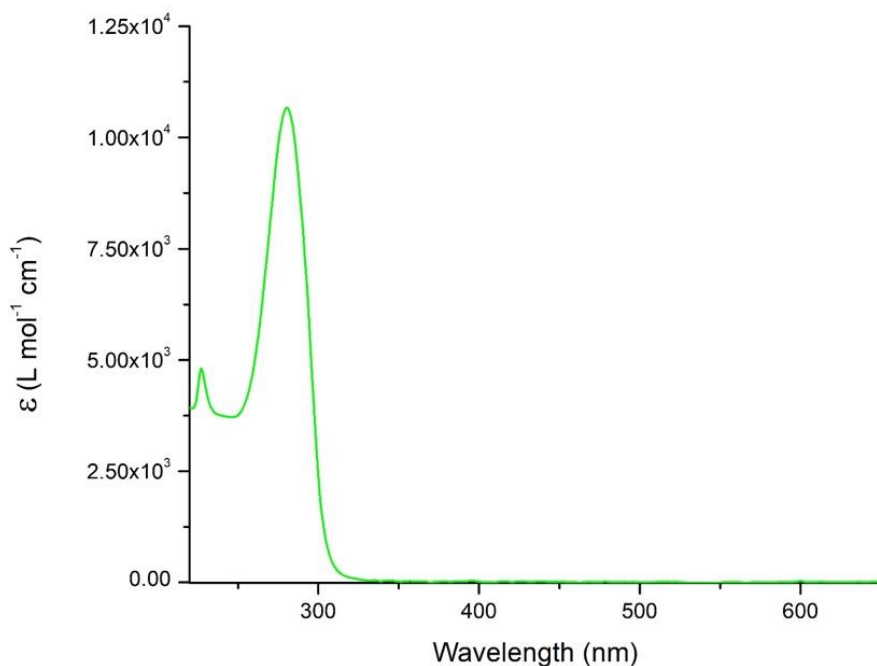
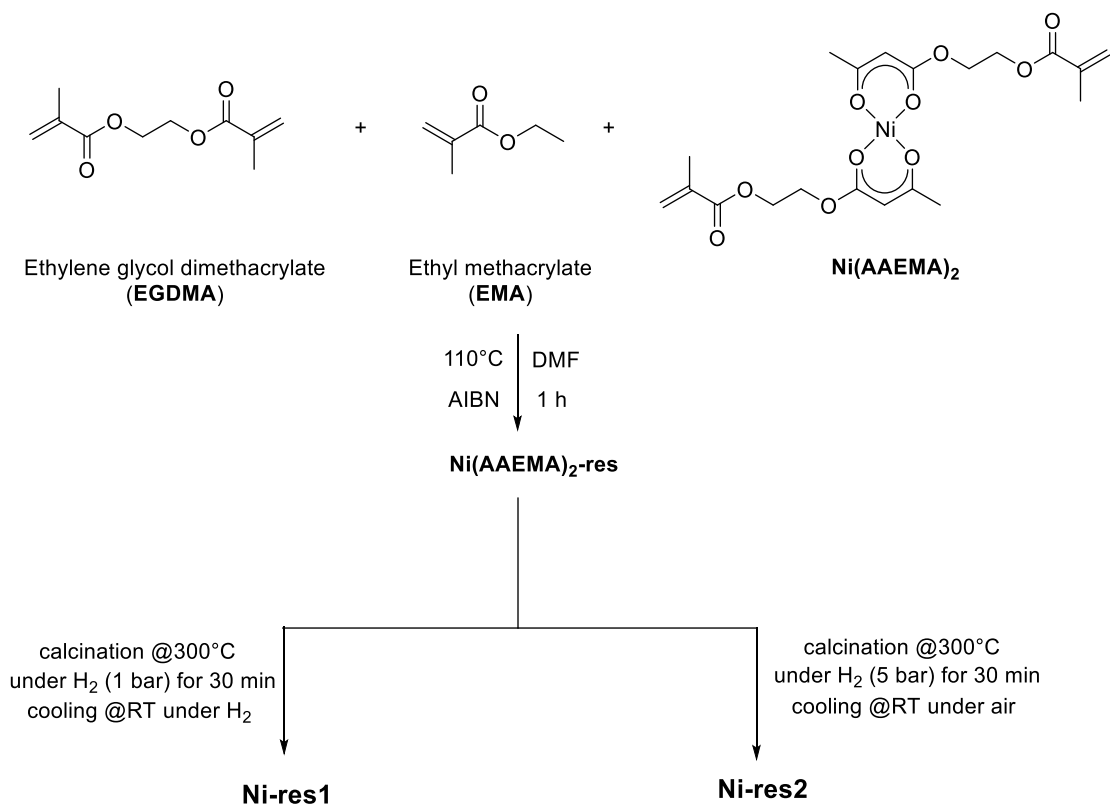


Fig.III.4 UV-vis spectrum of 6.9×10^{-5} M **Ni(AAEMA)₂** in dichloromethane solution.

3.2.2 Synthesis of Ni-res1 and Ni-res2

The methacrylic polymer supported **Ni(AAEMA)₂-res** was synthesized according to the literature, similarly to its Pd(II) analogous.¹¹⁷ **Ni(AAEMA)₂-res** was recovered as a pale green powder by copolymerizing the complex **Ni(AAEMA)₂** with ethyl methacrylate (EMA) as comonomer, ethylene glycol dimethacrylate (EGDMA) as crosslinker and azaisobutyronitrile (AIBN) in DMF at 110°C for 1h under stirring. After adequate washing to remove excess solvents, the green polymer **Ni(AAEMA)₂-res** obtained was then calcined under dihydrogen at 300°C and cooled at room temperature following two different pathways under dihydrogen or air, in order to obtain **Ni-res1** and **Ni-res2**, respectively.



Scheme III.7

3.2.3 Characterization of Ni-res1 and Ni-res2: TEM analysis in STEM mode

To get insights into its unexpected catalytic activity, **Ni-res2** was subjected to TEM analyses in STEM mode. STEM pictures (**Figure III.5**) show that Ni NPs formed, and the latter are homogeneously distributed throughout the polymeric matrix and are embedded in it. The Ni NPs dimension ranges from 75 to 400 nm in diameter (**Figure III.5 c**), having most of them a size comprised between 150 and 250 nm. The most interesting point stands in their very unusual morphology. In fact, they have an urchin-like shape. All these morphological features are held responsible for their unexpected catalytic activity and selectivity. EDS analyses excluded the presence of nickel oxide in both catalysts, confirming that the oxidation state value of Ni in all the observed NPs is zero for **Ni-res1** and **Ni-res2**.

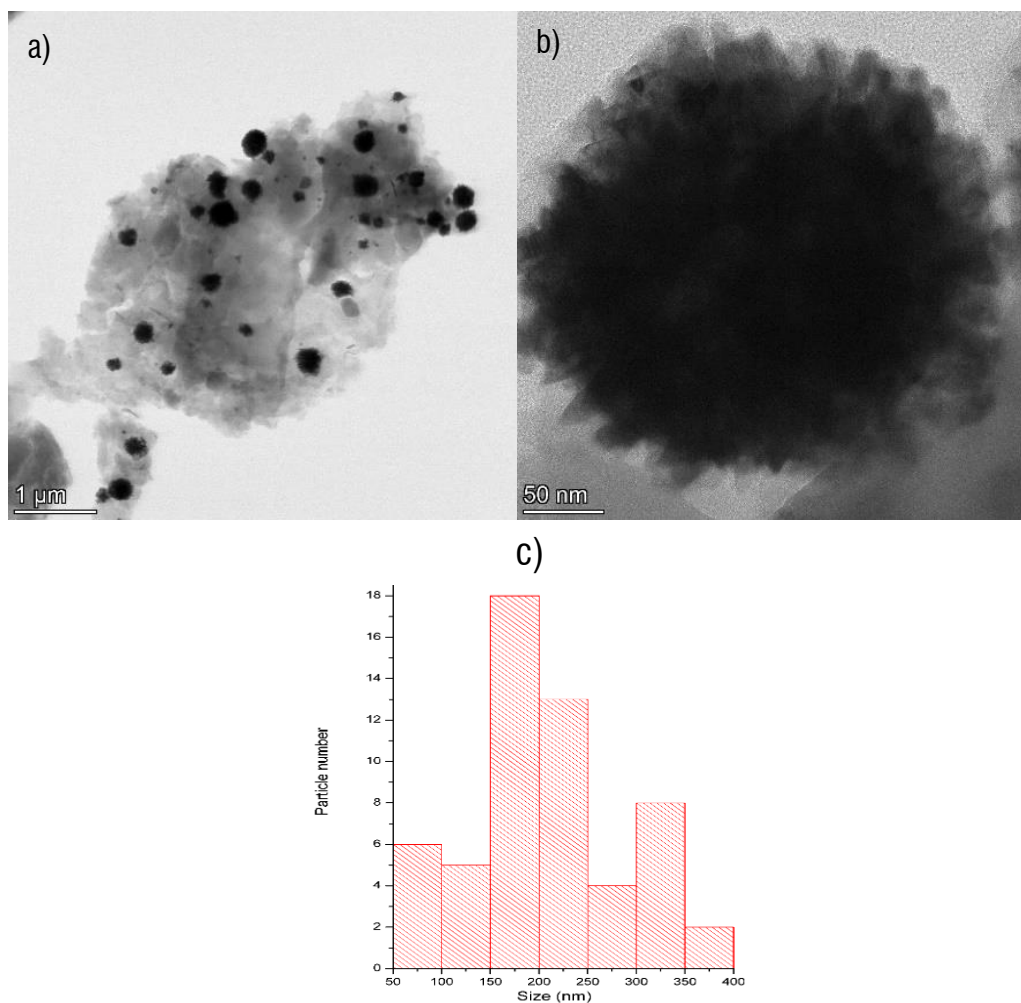


Fig. III.5 a) Low magnification SEM image of **Ni-res2**. b) High magnification SEM image of **Ni-res2**. c) size distribution of Ni particles in **Ni-res2**.

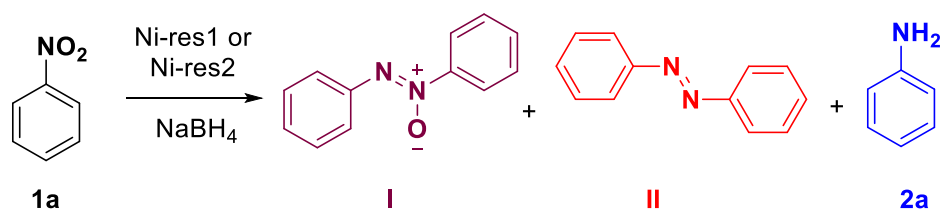
3.2.4 Catalytic activity of Ni-res1 and Ni-res2

To evaluate the influence of different synthetic protocols on the catalytic activity of **Ni-res1** and **Ni-res2** we tested the transfer hydrogenation of nitrobenzene in methanol using NaBH_4 as the reducing agent.

In this framework, 0.50 mmol of nitrobenzene, the catalyst (**Ni-res1** or **Ni-res2**, 0.010 mmol of Ni) and 1.7 mmol of sodium borohydride were stirred under nitrogen at room temperature in 5 mL of methanol for the appropriate amount of time, using a three-necked flask equipped by a gas bubbler to discharge the hydrogen excess produced during reaction. The progress of the reaction was monitored by GLC. Chromatographic yields were assessed by using biphenyl as the internal standard.

As shown in the **Table III.1**, **Ni-res1** was active for the nitrobenzene reduction and selective towards the formation of aniline. In fact, the substrate conversion was quantitative after 3 hours and the major product recovered was aniline (III, Entry 1, **Table III.1**). The activity and selectivity of **Ni-res1** resembled the ones already observed for the analogous acrylamide polymer-supported Ni catalyst.¹⁵¹

On the contrary, the reaction catalyzed by **Ni-res2** (Entries 2 ÷ 4, **Table III.1**) proceeded slower than the one reported in Entry 1. It took 9 h to reach 82% conversion of the substrate (entry 4) and the selectivity was always directed towards azoxybenzene (I).



Entry ^{a)}	Catalyst	Time [h]	Conv. [%]	Selectivity [%]		
				I	II	2a
1	Ni-res1	3	>99	24	1	75
2	Ni-res2	3	33	>99	-	-

3	Ni-res2	6	64	>99	-	-
4	Ni-res2	9	82	96	4	-

Table III.1 Catalytic tests for the reduction of nitrobenzene: ^{a)} Reaction conditions: nitrobenzene (0.50 mmol); NaBH₄ (1.7 mmol), Ni-catalyst (0.010 mmol of Ni), methanol (5 ml), room temperature.

Considering that the proposed mechanism for the reduction of nitroarenes can be direct or indirect (see **Scheme II.6** in previous chapter), the presence of azo- and azoxy- compounds (**Table III.1**) in the reaction mixture catalyzed by **Ni-res1** or **Ni-res2** strongly suggests that the here-reported Ni catalysts follow the condensation route. However, the results reported in **Table III.1** indicate that, **Ni-res1** can almost totally convert the substrate into the final product (aniline), while **Ni-res2** is less active, although always selective to azoxybenzene.

3.2.5 Concluding remarks on Ni-res1 and Ni-res2

A new methacrylic polymer supported Ni(II) complex was synthesized as precursor of Ni(0) NPs obtained from calcination under dihydrogen. Depending on the cooling step of the calcination procedure, two different materials were obtained: **Ni-res1** (cooling under hydrogen) and **Ni-res2** (cooling under air). **Ni-res1** and **Ni-Res2** showed a different catalytic activity and selectivity in the nitrobenzene reduction, due to the different morphologies of the Ni NPs supported onto them. TEM analyses showed an uncommon urchin-like shape for Ni NPs of Ni-res2 catalyst.

Based on this result we decided to evaluate the effect of the matrix and therefore, we extended our studies to the synthesis of an acrylamide-based resin as a support for nickel nanoparticles.

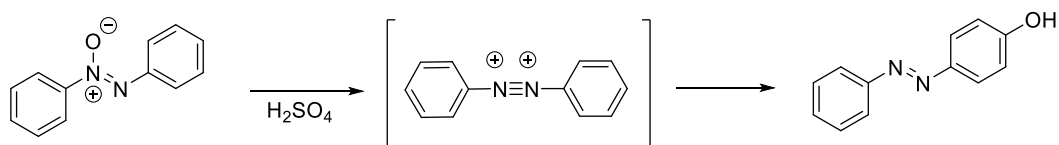
3.3 Efficient and selective reduction of nitroarenes towards azoxyarenes catalysed by Ni nanoparticles supported on an acrylamide-based resin

3.3.1 Importance of azoxyarenes

Azoxyarenes have gained considerable attention both from academic and industrial research. These compounds, members of the 1,3-dipole family, are characterized by conjugated system with polar functionality that make them suitable for versatile applications as dyes and pigments, reducing agents, analytical reagents, food additives, chemical stabilisers, polymer inhibitors, and liquid crystal displays.²¹¹⁻²¹⁴

Thanks to their physical and chemical properties, they are used in polymer materials and due to their retinoidal activities they are also studied by medicinal chemist.²¹⁵

In addition, azoxy compounds are employed as precursors for Wallach rearrangement (**Scheme III.8**),²¹⁶ which offers a straightforward path for the synthesis of azo compounds with one aromatic ring substituted with a hydroxyl group in para-position in concentrated aqueous sulfuric acid media.

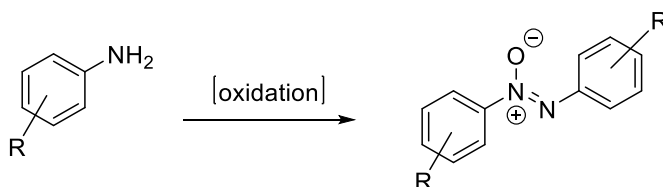


Scheme III.8

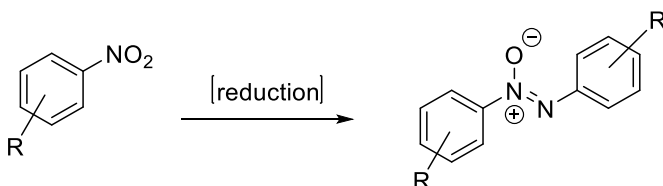
Traditional industrial preparations of azoxyarenes are achieved by diazotisation but the process is costly and environmentally unfriendly, due to the formation of unstable intermediates and harsh conditions (strict temperature control and use of corrosive acids). Alternative synthetic approaches for azoxyarenes are either the oxidation of amines or the reduction of nitro compounds (**Scheme III.9**) to generate the aforementioned species in situ from condensations.

Generally accepted protocols for the selective synthesis of azoxyarenes

1) Selective (stoichiometric or catalytic) oxidation of anilines



2) Selective (stoichiometric or catalytic) reduction of nitrobenzenes



Scheme III.9

Due to the possible formation of different by-products, the challenge in these methods lies in controlling the selectivity to a desired product. Moreover, mild reaction conditions (low temperature and atmospheric pressure) and use of green solvents and oxidants or reductants are preferable.

Among the oxidation methods, several attempts were made using stoichiometric oxidants such as peracetic acid, MnO₂,²¹⁷ Pd (OAc)₂,²¹⁸ and Hg(OAc)₂,²¹⁹ but the employment of these systems involves environmental issues and low yield.

Molybdenum and vanadium-compounds catalyze aniline oxidation in presence of tert-butyl hydrogen peroxide (TBHP).²²⁰ Nevertheless, also in this case, the use of TBHP suffers from disposal problem.

For this reason, numerous transition-metal based homogeneous and heterogeneous catalysts have been studied by using the greener H₂O₂ as the oxidant. Hydrogen peroxide in presence of rhenium, tungsten or molybdenum catalysts also gives nitrosoarenes with good yields.²²¹ Homogeneous catalysts such as tetrasteryl tetra titanate²²² or ruthenium chloride,²²³ have been found to be active and selective in the oxidation of aromatic amines into azoxy compounds. Recently, the reaction could be achieved also with 2,2,2-trifluoroacetophenone as organo-catalyst using hydrogen

peroxide as the oxidant.²²⁴ But in the field of homogeneous catalysts, the recyclability of the catalysts and the product separation from the reaction mixtures become the main drawbacks. To overcome this issue, various heterogeneous catalysts have been tested. In 2008, Corma's group reported gold nanoparticles supported on titanium dioxide (TiO_2) and nanoparticulated cerium dioxide (CeO_2) catalytic systems to aerobic oxidation of aromatic anilines and obtained the corresponding azo compounds with good yield.²²⁵ In 2016, Camargo and co-workers used Ag/Au nano shells and Au nanoparticles as catalysts for the synthesis of azobenzene in liquid phase.²²⁶ In 2014, spinel CuCr_2O_4 nanocatalyst was found to be suitable for oxidation of aniline to azoxybenzene at 70°C with 78% aniline conversion and 92% azoxybenzene selectivity.²²⁷

Furthermore, microporous and mesoporous titanium silicate (TS-1) and mesoporous silica containing cobalt oxide (CoO-SiO_2) using H_2O_2 as oxidant have been employed for the oxidation of aromatic amines into azoxybenzene derivatives.²²⁸

Although all these heterogeneous catalytic systems are active in the selective oxidation of amines to azoxy derivatives, some issues linked to heterogeneous catalysis still unsolved, namely the use of expensive transition metals that may be prone to leaching, inefficient recyclability, high loading of catalyst require and diffusion limitations.

Many procedures have been reported for the reduction of nitroarenes into anilines. Besides nitroarenes are the organic pollutants of industrial and agricultural wastewater and from a sustainable point of view their transformation into high value products and new chemicals has notably economic importance. But very few studies are available for the only production of one of the possible reductive products, due to different possible pathways in the condensation route that competing. To achieve high yields of such intermediates (azoxy-) and avoid further conversion (to azo-) have been development various strategies, such as using additives, modifying catalyst properties, changing reaction conditions, or using photoreactions.²²⁹

Nanomaterials based on Pt, Pd, Ru, Rh, Au, Ag, Cu, Ni, Co^{230,231} are often preferred for this purpose. Liu et al. reported supported Au nanoparticles on meso- CeO_2 and 2-propanol/water combination as reducing agent of nitrobenzene to azoxybenzene at $30\text{-}60^\circ\text{C}$.²³² In 2017 Au-NPs supported on hydrotalcite (HT) was studied for selective

reduction of nitro to azoxy compounds in an argon atmosphere at 40 °C using isopropyl alcohol and KOH as base.²³³

More recently, Vaccaro et al. investigated Au@Zirconium-Phosphonate NPs for selective production of azoxy compounds using NaBH₄ as reducing agent in ethanolic medium at 30 °C. Notably, that in this work it has been possible to control and to switch the selectivity of system by using EtOH_{96%} or EtOH_{abs} respectively as solvent.²³⁴ In 2016, Song and Han reported a visible-light driven reduction of nitrosobenzene to form azoxybenzene using glucose as the external reduction that in the same time was converted into arabinose.²³⁵ Recently, Sakai et al. described a highly selective method to obtain three coupling compounds by using trivalent indium salt and hydrosilane as hydrogen source.²³⁶

Metallic catalysts based on Ir and Rh are largely recognized as catalyst with moderate reduction abilities that could be used to avoid the formation of aniline. In this regard, in 2016 Zhang and coworkers reported the synthesis of monometallic nanosheets Ir-Ns, Rh-Ns and bimetallic Ir-Rh-Ns ones that showing high selectivity in the formation of azoxybenzene under alkaline conditions at room temperature.²³⁷

However, due to economic and environmental requirements, it is important to emphasize the progress achieved with first-row transition metals, especially with Nickel. In 2016, Suib's group synthesized urchin-like Ni/Graphene nanocomposites for the selective reduction of nitrobenzene using hydrazine hydrate as reducing agent at room temperature and atmospheric pressure.²³⁸ Hou et al. prepared a ceria-supported Ni–Ni^{δ+} nanocluster catalyst for the formation of metastable azoxy intermediate at 80°C in EtOH under argon atmosphere. In this work it is possible to underline the correlation between active site and support. In fact, due to the strong electronic metal–support interactions, ceria prevents the complete reduction of NiO to the Ni metal. The latter could be more active in the reduction and allowing the further conversion of azoxy to aniline.²³⁹ In 2018, Corma and coworkers described a bifunctional catalyst system (Ni@C-CeO₂) for the base-free chemoselective reduction of nitrobenzene.²⁴⁰

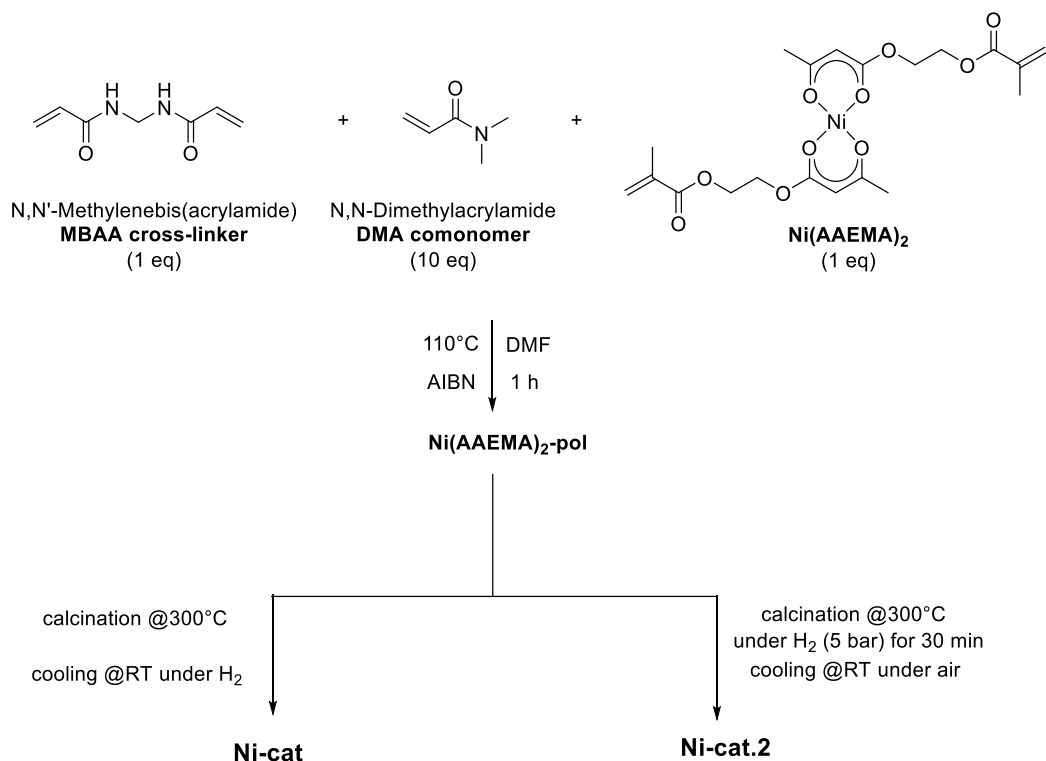
In this framework and encouraged by the results obtained with the catalysts **Ni-res1** and **Ni-res2**, we decided to synthesize new Ni-based catalysts supported on an acrylamide-resin for selective reduction of nitroarenes towards azoxyarenes

3.3.2 Synthesis of Ni-cat and Ni-cat1

In the previous work on the catalysts **Ni-res1** and **Ni-res2** we have proven that morphologically different catalysts can be obtained by modifying just the last step of the catalyst preparation. Since both the morphology of the polymer and the nature of support determine the final application of the material, herein we have reported the synthesis of new catalysts obtained by changing the matrix employed.

To evaluate the validity of the procedure and compare the influence of different matrix on the resulting catalytic performance, we have prepared precursor Nicke-containing polymer **Ni(AAEMA)₂-pol** by copolymerizing Ni(AAEMA)₂ with *N,N*-dimethylacrylamide and *N,N'*-methylenebisacrylamide in presence of AIBN. Eventually, by

submitting **Ni(AAEMA)₂-pol** to calcination at 300°C under H₂ followed by natural cooling under H₂ or respectively under air at room temperature **Ni-cat** and **Ni-cat.2** were obtained respectively (**Scheme III.10**).



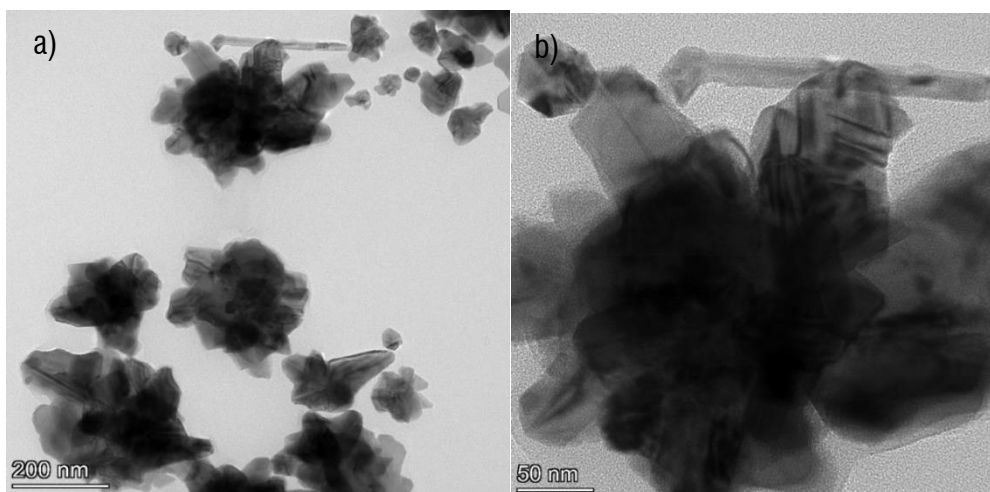
Scheme III.10

3.3.3 Characterization of Ni-cat and Ni-cat.2

Electron microscopy techniques such as SEM, STEM and TEM have opened up new possibilities to investigate the micro- and nano-scale features of the synthesized catalysts with complex molecular structures via morphological and chemical characterization. These techniques can be used in the *ex situ* approach when the catalyst is processed by calcination as well as separated from the solution, allowing a vast array of synthetic parameters to be varied without concern for the delicacies of the microscope equipment. In this respect, careful catalyst separation from the reaction media might be an important requirement in order to prevent contamination, deformation and particles release. Thus, electron microscopy gives a more direct approach for determining distribution, growth, and dissolution rates of metal NPs onto the catalyst surface than the indirect reaction conversion rate or yield.

3.3.3.1 Ni-cat

STEM images and the corresponding size distribution of **Ni-cat** are reported in **Fig. III.6** and **Fig. III.7**, respectively. At low magnification a bimodal distribution of nickel nanoparticles can be observed: the first distribution represents the most nanoparticles with a particle size ranging from 25 to 75 nm; while the second distribution is related to the few aggregates of the nanoparticles with particle size centered at *ca.* 250 nm. At high magnification all particles showed almost the same structure consisting of a round irregular polyhedral embedded in a smooth nanostructure of the polymeric matrix. Interestingly **Fig. III.6 d)** the presence of polymeric layer of *ca.* 40 nm that "decorates" the nanoparticles, or their aggregates are clearly observed.



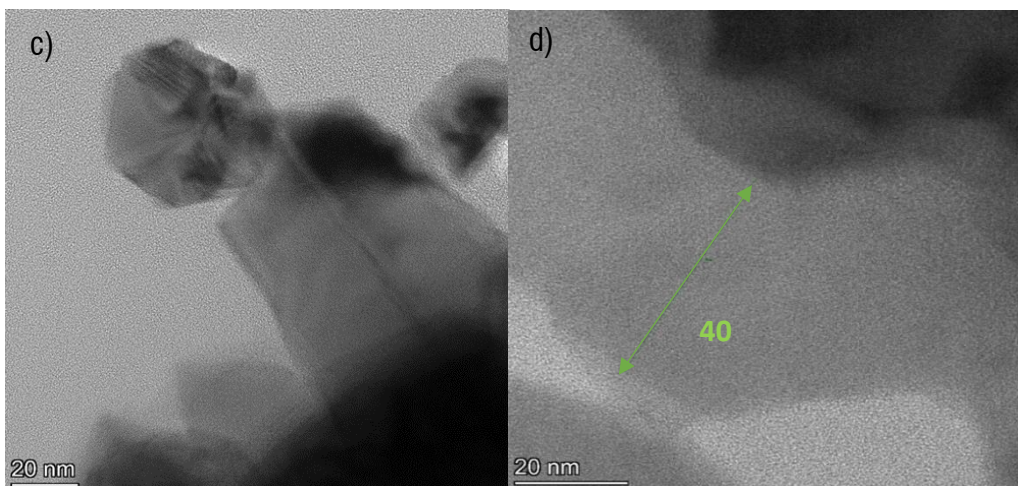


Fig.III.6 a-c) STEM images of three different magnification of Ni-cat; (d) enlargement of a selected area of (c).

Selected area (electron) diffraction (abbreviated as SAD or SAED), is a crystallographic experimental technique that can be performed inside a transmission electron microscope (TEM). SAED image of **Ni-cat** reported in **Fig. III.7 b)** apparently consists of spots arranged in a ring pattern due to the crystalline nature of the nanoparticles.

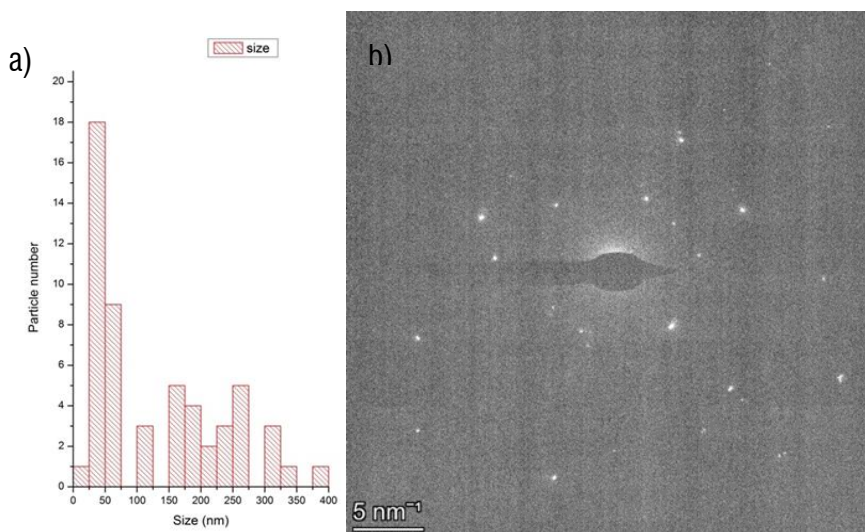


Fig. III.7 a) Size distribution of **Ni-cat** b) SAED pattern of **Ni-cat**.

The elemental identity of the nanoparticles was also determined by means of Energy Dispersive Spectroscopy (EDS). In **Fig.III.8** and **Fig.III.9**, the EDS analysis performed on the HAADF STEM image of **Ni-cat** is reported. This analysis show that the nanoparticles are composed mostly by metallic nickel with a low content of oxygen with deriving environmental contamination. The layer which decorates the nickel nanoparticles, or their aggregates are composed by C, N and O confirming the acrylamidic nature of the matrix.

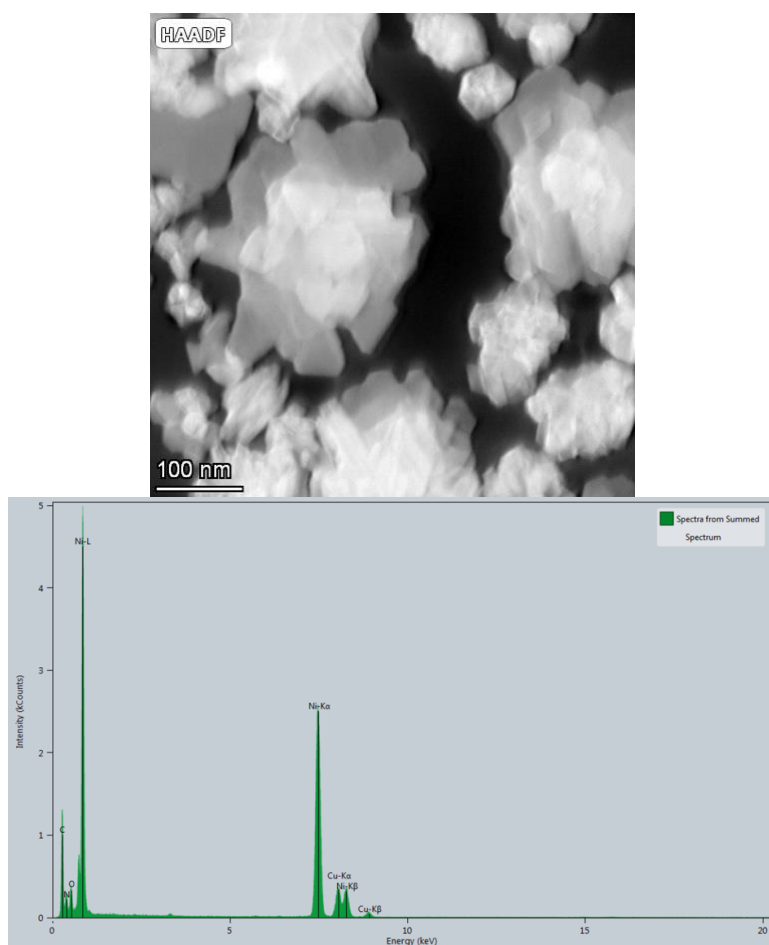


Fig.III.8 EDS spectrum of **Ni-cat**.

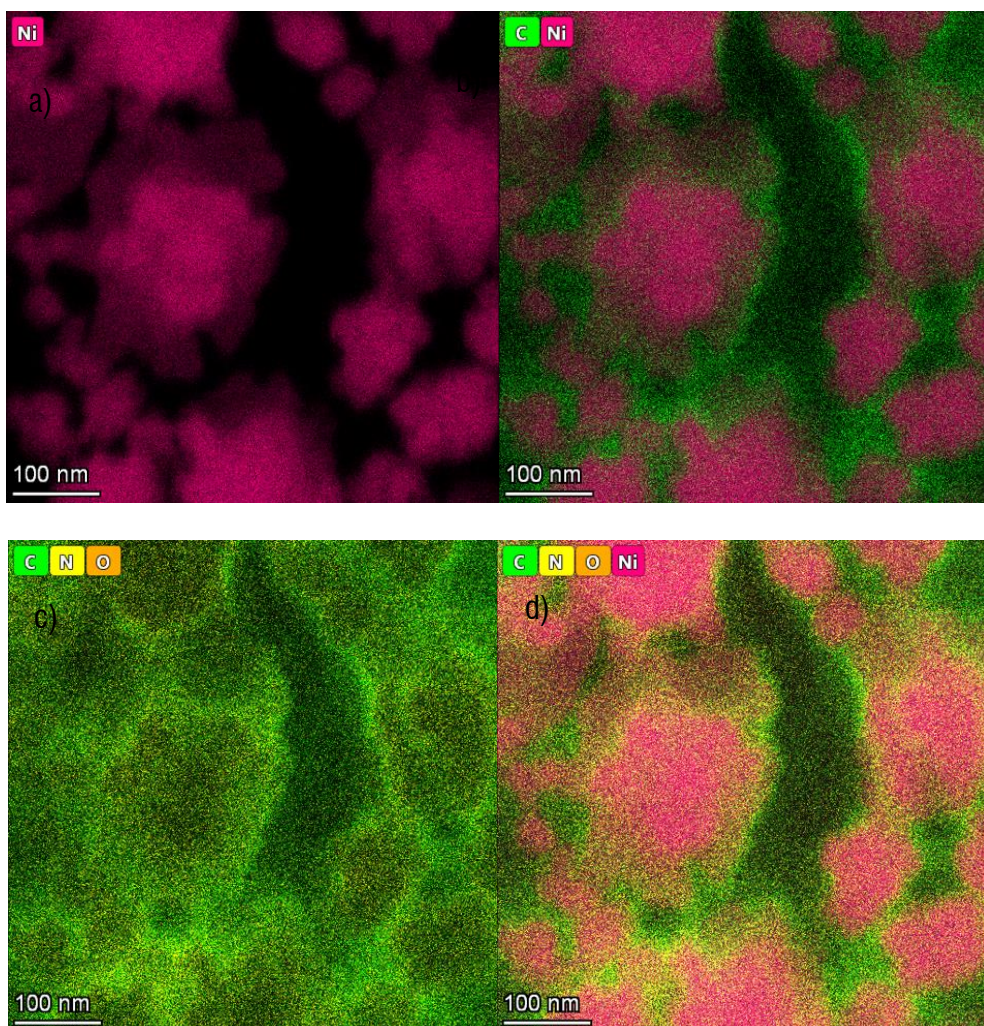


Fig.III.9 STEM-EDS images of Ni-cat. a) Ni-mapping b-d) Elemental combining maps.

3.3.3.2 Ni-cat2

STEM images at different magnification of the **Ni-cat2** sample and the corresponding size distribution are reported in **Fig.III.10**. At low magnification, the catalyst shows a uniform distribution of round irregular particles ranging from 200 to 400 nm. At high magnification these particles are observed as urchin-like shaped aggregates embedded into polymeric matrix.

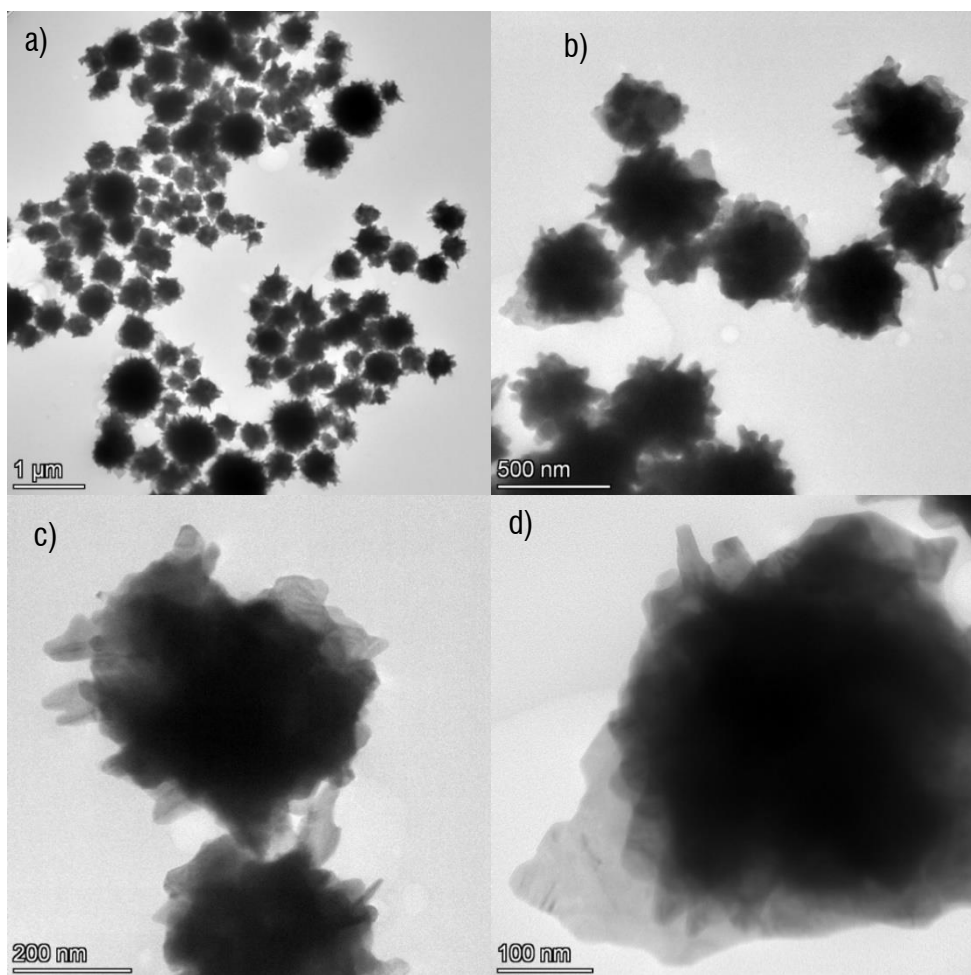


Fig.III.10 a-d) STEM images of different magnification of Ni-cat2.

In **Fig.III.11** SAED image of the **Ni-cat2** are shown. SAED pattern shows not ordered spots, confirming the multi-crystalline nature of the nanostructured urchin-like shaped aggregates. In particular, the interplanar spacing of 0.21 nm is ascribable to Ni {1 1 1} plane, indicating the crystallinity nature for these Ni NPs and the absence of NiO plane.²⁴¹

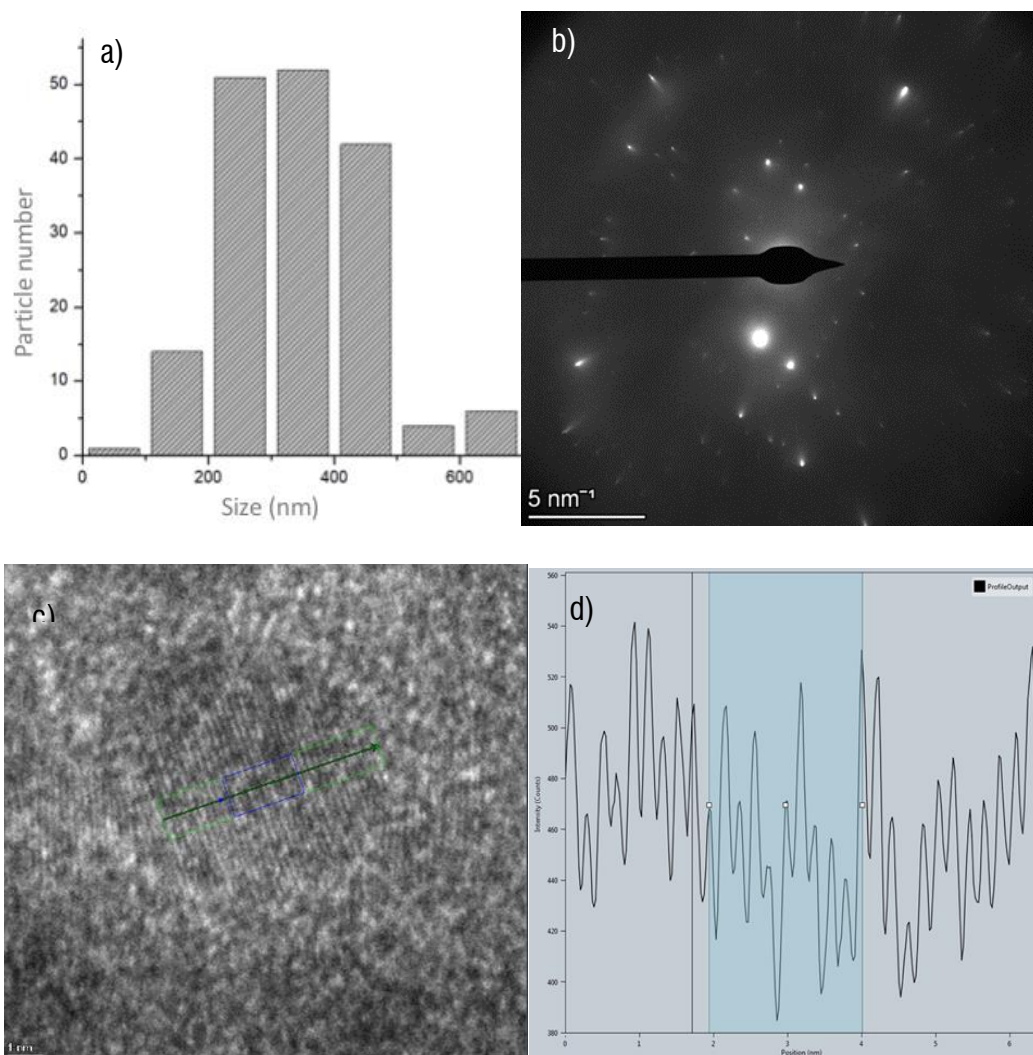


Fig. III.11 a) Size distribution of **Ni-cat2**. b) SAED pattern of **Ni-cat2**. c) Enlargement of a selected area of Fig. III. 10c d) Distance profile corresponding to green line drawn on image c).

In **Fig.III.12** a comparison between BF and HAADF STEM images of **Ni-cat2** is reported. HAADF STEM image permits to enhance the topography and the transparency of a sample composed by a polymeric composite, giving a different point of observation respect to a BF image causing a brightness inversion. In fact, the edges of urchin-like particles are brighter than those observed in BF images that are dark, due to the small thickness of these particles' sites. In the HAADF STEM image the urchin-like aggregates are slightly dark confirming that they are embedded in the polymeric matrix.

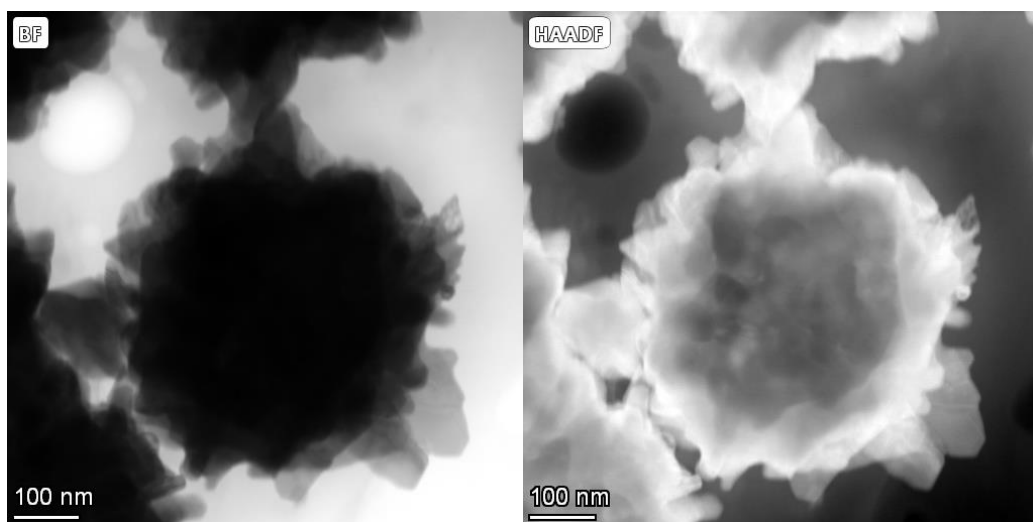
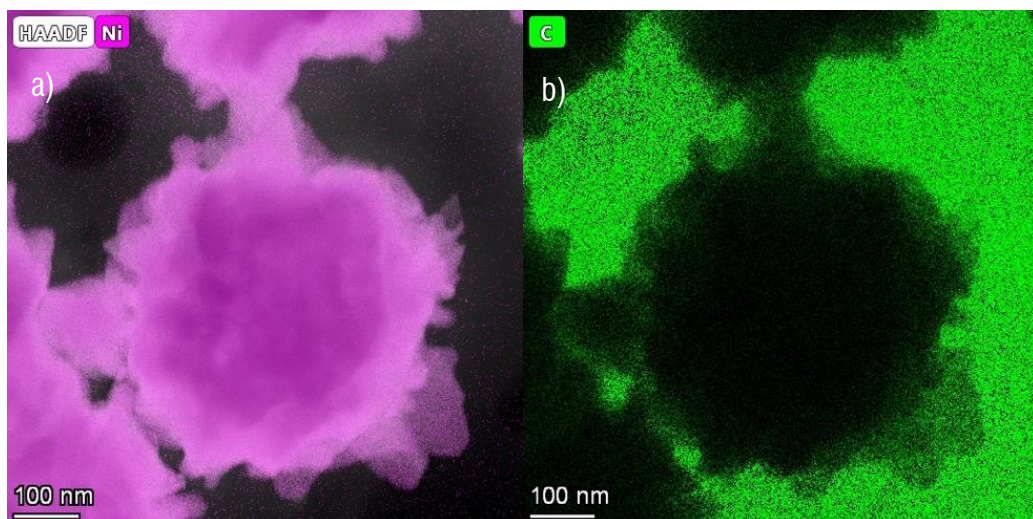


Fig.III.12 BF and HAADF STEM images of **Ni-cat2**.

In **Fig.III.13** the EDS analysis performed on the HAADF STEM image of **Ni-cat2** showed the elemental identity of the obtained nickel nanostructure, while in **Fig.III.14** EDS analysis carried out on two different area demonstrated that the first area (Area #1) is the urchin-like aggregate composed mostly by metallic nickel, and the second area (Area #2) is ascribable to C, N and O of an acrylamidic resin.



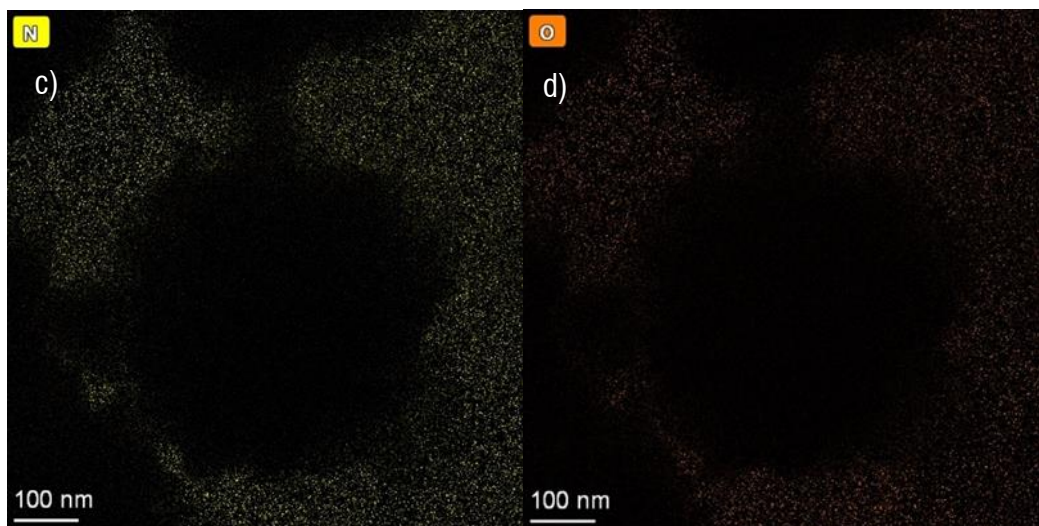


Fig.III.13 STEM-EDS images of Ni-cat2. a-d) Elemental mapping.

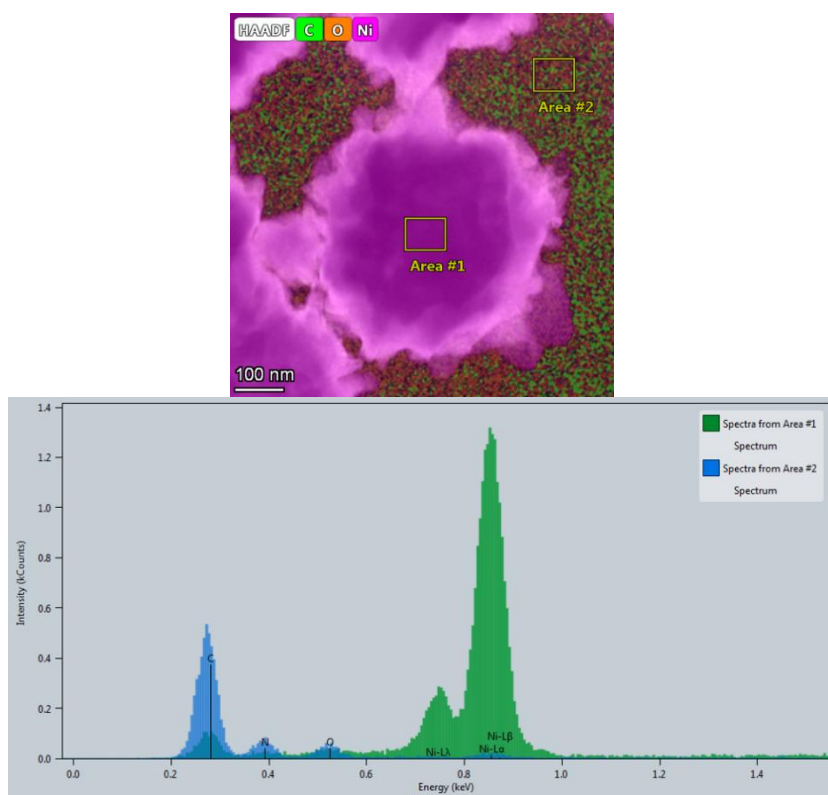


Fig.III.14 EDS spectrum of Ni-cat2.

X-Ray Diffraction (XRD) is a powerful technique for analyzing materials structure. Various aspects of materials structure can be analyzed using XRD. The phase structure and purity of the as-synthesized **Ni-cat2** were examined by powder XRD to evaluate the presence of metallic Ni or Ni oxide. The XRD patterns of the **Ni-cat2** (**Fig.III.15**) showed the typical diffraction peaks of the metallic state of Ni at a 2θ value of 44.7° which is referred to the plane [111] and at 2θ value of 51.9° assigned to the plane [200], respectively.²⁴² No characteristic peaks due to the presence of the oxide of nickel are observed.

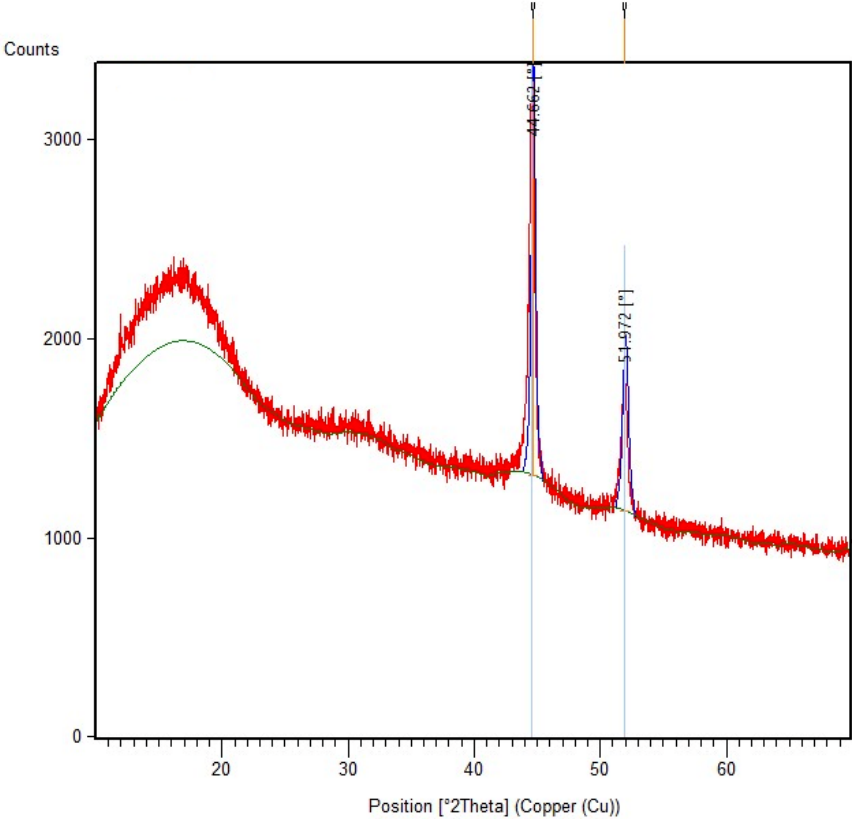


Fig.III 15 XRD spectrum of Ni-cat2.

3.3.3.2 Magnetism study

Recovery and reusability are very important factors to consider when evaluating the performance of an heterogenous catalysts. **Ni-cat2** unlike **Ni-cat** is also magnetic, and its magnetic characteristics was preliminary noticed by checking whether a neodymium magnet was able to attract the powder.

Next, the magnetic properties of the Ni-cat2 catalyst were characterized by measuring the magnetic hysteresis loop (M-H) at 300 K. The obtained hysteresis loop is shown in Fig. III 16.

The sample exhibit typical ferromagnetic behavior, and the loop is well symmetrical of its shape over the field H, with a coercivity $H_c \sim 0.4$ KOe and an effectively saturation magnetization $M_s \sim 2,2$ emu/g.

A slight decrease of M_s values compared to 2,5 emu/g in bulk nickel is probably due to the presence of polymeric matrix surface which are either spin disordered or magnetically dead.²⁴³

Thus, this magnetic property will facilitate the separation of **Ni-cat2** from the reaction mixture as well as its recyclability saving energy process.

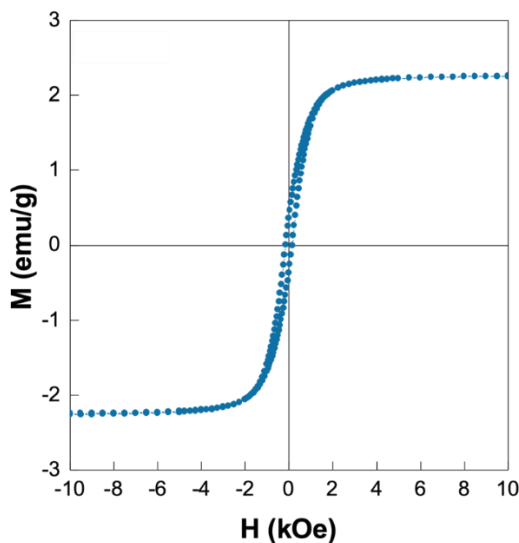
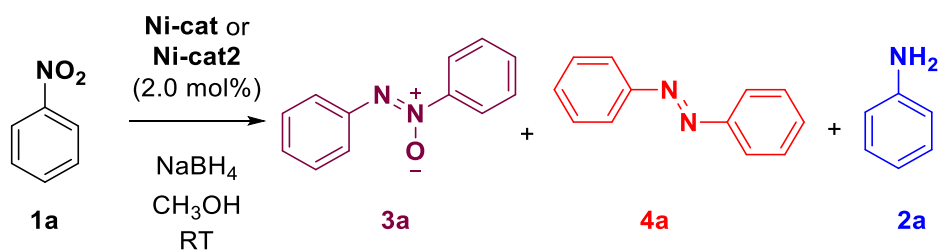


Fig.III 16 Normalized magnetization loop measured at 300 K of Ni-cat2.

3.3.4 Catalytic activity of Ni-cat and Ni-cat2 in the selective reduction of nitrobenzenes towards azoxybenzenes

Taking in account the previous results obtained with **Ni-res.1** and **Ni-res.2**, we started our study testing the catalytic activity of **Ni-cat** and **Ni-cat2** in the selective reduction of nitrobenzene towards azoxybenzene (**Schme III.10**) using NaBH₄ as reducing agent and CH₃OH as solvent, and fixing the substrate/catalyst ratio equal to 50 (namely a 2.0 mol % of catalyst)



Scheme III.10

In **Table III.2**, the preliminary tests for achieving the optimum reaction conditions are summarized.

Table III.2

Entry ^{a)}	Catalyst	NaBH ₄ (mmol)	Time [h]	Conv. [%]	Selectivity [%]		
					3a	4a	2a
	Ni-cat	1.5	2.5	>99	-	-	>99
	Ni-cat2	1.5	3	80	>99	-	-
	Ni-cat	1.7	2	>99	-	-	>99
	Ni-cat2	1.7	3	>99	99.5	0.5	-

^{a)} Reaction conditions: 0.5 mmol of nitrobenzene (**1a**), 2.0 mol% of Ni catalyst (16.1 mg of **Ni-cat** (Ni%_w = 5,46) or 13.3 mg of **Ni-cat2** (Ni%_w = 4,47)), 5 mL of CH₃OH,

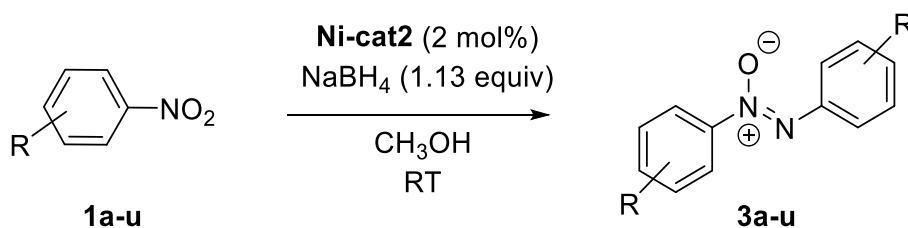
With the same amount of NaBH₄ (1.5 mmol with respect to 0.5 mmol of **1a**) employing in catalysis with **Ni-res.1** and **Ni-res.2**, **Ni-cat** was completely selective towards the

formation of aniline within 2.5 h (Entry 1, **Table III.2.**) whereas with **Ni-cat2** an 80% conversion of nitrobenzene was achieved with a high selectivity (>99%) in azoxybenzene. By slightly raising the amount of NaBH₄ up to 1.7 mmol, **Ni-cat** completely converted **1a** to **2a** in 2 h and, with our delight, **Ni-cat2** completely converted **1a** to azoxybenzene (**3a**) within 3 h with a selectivity higher 99%. Thus, a switchable preparation of **aniline** or **azoxybenzene** is easily possible using respectively **Ni-cat** or **Ni-cat2**.

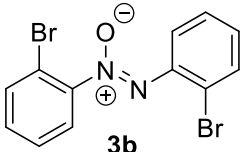
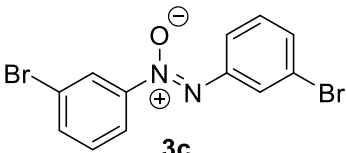
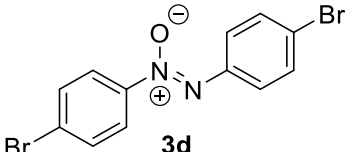
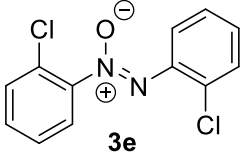
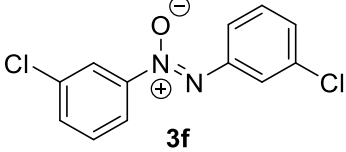
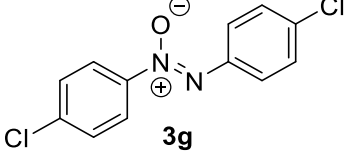
Once again, as in the case of **Ni-res.1** and **Ni-res.2**, we have shown how the calcination method for the preparation of catalyst is important for achieving a different kind of selectivity in the reduction of nitrobenzene. Indeed, the selectivity achieved with **Ni-cat2** towards azoxybenzene is remarkable and this prompted us to study how this catalyst could mediated the reduction of others nitroarenes versus the corresponding azoxyarenes.

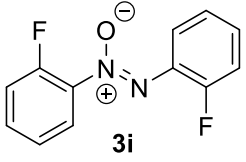
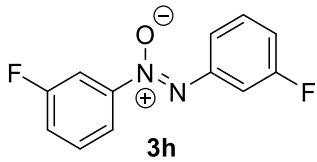
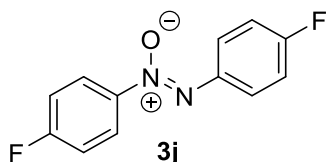
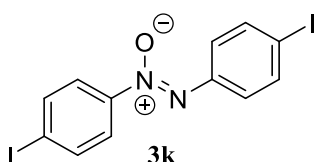
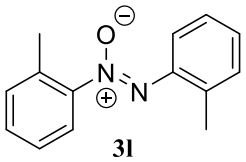
With the optimized reaction conditions in our hand, we passed to explore the scope and general applicability of **Ni-cat2** catalytic system in the selective reduction of various substituted nitroarenes towards the corresponding azoxyarenes (**Table III.3**).

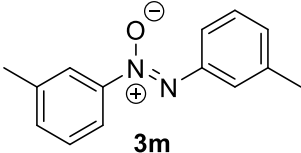
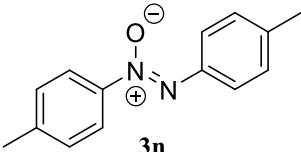
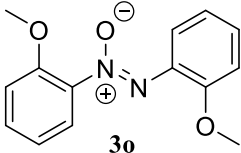
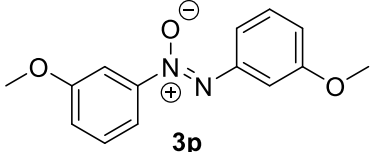
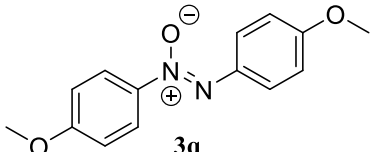
Table III.3 Reduction of different nitrobenzenes (**1a-u**) towards corresponding azoxyarenes (**3a-u**) catalyzed by **Ni-cat.2**

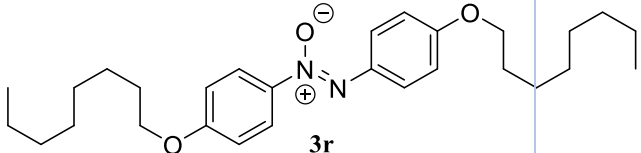
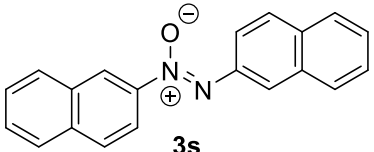
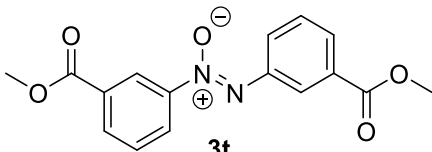
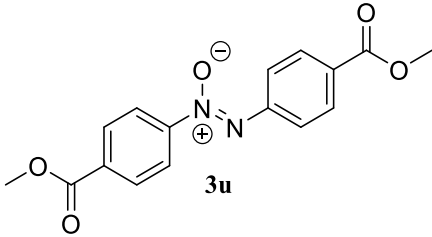


Entry ^{a)}	Product	Time (h)	Yields (%) ^{b)}
1	<p style="text-align: center;">3a Azoxybenzene</p>	3	98

2	 <p>3b 2,2'-Dibromoazoxybenzene</p>	2	85
3	 <p>3c 3,3'-Dibromoazoxybenzene</p>	2	88
4	 <p>3d 4,4'-Dibromoazoxybenzene</p>	1	95
5	 <p>3e 2,2'-Dichloroazoxybenzene</p>	3	83
6	 <p>3f 3,3'-Dichloroazoxybenzene</p>	2	87
7	 <p>3g</p>	1	93

	4,4'-Dichloroazoxybenzene		
9	 <p>3i</p> <p>2,2'-Difluoroazoxybenzene</p>	1	90
8	 <p>3h</p> <p>3,3'-Difluoroazoxybenzene</p>	2	96
10	 <p>3j</p> <p>4,4'-Difluoroazoxybenzene</p>	2	92
11	 <p>3k</p> <p>4,4'-Diiodoazoxybenzene</p>	6	65 ^{c)}
12	 <p>3l</p> <p>2,2'-Dimethylazoxybenzene</p>	4	65

13	 <p style="text-align: center;">3m</p> <p style="text-align: center;">3,3'-Dimethylazoxybenzene</p>	4	85
14	 <p style="text-align: center;">3n</p> <p style="text-align: center;">4,4'-Dimethylazoxybenzene</p>	3	75
15	 <p style="text-align: center;">3o</p> <p style="text-align: center;">2,2'-Azoxyanisole</p>	2	85
16	 <p style="text-align: center;">3p</p> <p style="text-align: center;">3,3'-Azoxyanisole</p>	2	88
17	 <p style="text-align: center;">3q</p> <p style="text-align: center;">4,4'-Azoxyanisole</p>	1	95
18		6	80

	 <p style="text-align: center;">3r</p> <p style="text-align: center;">4,4' octyloxyazoxybenzene</p>		
19	 <p style="text-align: center;">3s</p> <p style="text-align: center;">4,4'-Azoxy-naphthalin</p>	6	70
20	 <p style="text-align: center;">3t</p> <p style="text-align: center;">Dimethylazoxybenzene-3,3'-dicarboxylate</p>	5	70
21	 <p style="text-align: center;">3u</p> <p style="text-align: center;">Dimethylazoxybenzene-4,4'-dicarboxylate</p>	5	75

^{a)} Reaction conditions: 0.5 mmol of nitroarenes, 13.3 mg of **Ni-cat2** (2 mol %_{of Ni}), 5 mL of MeOH, 1.7 mmol of NaBH₄ were stirred at room temperature for the appropriate amount of time.

^{b)} Unless otherwise indicated, all conversions were higher than 98% and yields were determined by GC-MS.

We started to study the reduction of nitroarenes bearing electron-withdrawing groups such as p-halo-nitroarenes. With substrates such as bromo-nitrobenzenes (**1b-d**) and

chloro-nitrobenzenes (**1e-g**), the same trends in selectivity and activity were obtained (Entries 2-7, **Table III.3**): the yields were excellent and ranged from 83% for azoxy compound **3e** (Entry 5) to 95% for azoxy compound **3d** (Entry 5). The time reaction with this electron-withdrawing groups were significantly decreased with respect to nitrobenzene: the substituent in meta or para position lowered the time reaction to 2 and 1 h respectively. However, the steric effect of orto position slightly affects reaction yields (Entries 2 and 5, **Table III.3**). It is noteworthy that with both bromo- and chloro-nitrobenzenes no hydrodehalogenation reaction of corresponding azoxy compounds was observed. In the case of fluoro-nitrobenzenes (**1h-j**), again excellent yields in **3h-j** (90-86%) and lower time reactions compared to **1a** (1-2 h) were achieved (Entries 8-10, **Table III.3**). In the case of o-fluoronitrobenzene (**1h**), the reaction yield (90%) in corresponding azoxy **3h** (Entry 9, **Table III.3**) was not affected to the potentially steric hindrance of fluorine in orto position and the reaction was even faster (1 h) than m-fluoronitrobenzene (2 h) or p-fluoronitrobenzene (2 h). Among the iodo-nitrobenzenes, which are challenge substrates due to hydrodehalogenation, we tested only the p-iodo-nitrobenzene (**1k**) reaching an acceptable yield (65%) in corresponding azoxy compound **3k** (Entry 9, **Table III.3**). However, the obtained yield is by far higher than those reported in the literature for similar catalytic systems.²³⁴

The reduction of nitroarenes bearing electron-donating groups such as methyl-nitrobenzenes (**1l-n**) gave lower yields (65-85%) in azoxy compounds **3l-n** (Entries 12-14, **Table III.3**) and higher time reactions (3-4 h) with respect to halo-nitrobenzenes. However, with a stronger electron-donating substituent such as methoxy-nitrobenzenes (**1o-q**) the same behaviour in yields and time reactions observed in halobenzenes was achieved: 85-95% yields in **3o-q** within 1-2 h (Entries 15-17, **Table III.3**). The excellent results obtained with methoxy-nitrobenzenes prompted us to explore the preparation of a liquid crystalline compound such as 4,4'-octyloxyazoxybenzene.²⁴⁴ With our catalytic protocol, starting from substrate 1-nitro-4-(octyloxy) benzene (**1r**) an 80% yield in 4,4'-octyloxyazoxybenzene (**3r**) was obtained (Entry 18, **Table III.3**).

Next, with a sterically hindered substrate such as 2-nitronaphthalene (**1s**) a moderate yield (70%) in corresponding azoxy compound **3k** (Entry 19, **Table III.3**) were obtained. Last but not least, the reduction of substrates with a potentially reducible moiety such as methyl 3-nitrobenzoate (**1t**) and methyl 4-nitrobenzoate (**1u**) was

explored achieving acceptable yields (70-75%) in corresponding azoxy compounds **3t** and **3u**.

3.3.5 Recyclability

The selective reduction of nitrobenzene (**1a**) to azoxybenzene (**3a**) was chosen as a test reaction to demonstrate reusability of **Ni-cat2** under optimized conditions. To handle and study with a greater quantity of **Ni-cat2** the reaction scale-up was even raised up to 3.0 mol of **1a**.

The **Ni-cat2** recyclability was maintained up to five times without any substantial decrease in catalytic activity (**Fig. III. 17**) and after each reaction cycle **Ni-cat2** was easily recovered from the reaction mixture by magnetic separation (**Fig. III.18**) and washed thoroughly with acetone.

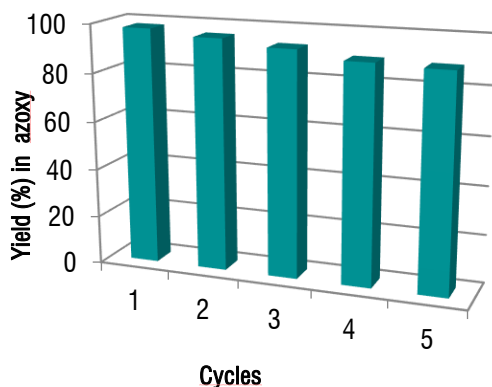


Fig. III.17 Recyclability of Ni-cat2 over five cycle.

A TEM study of **Ni-cat2** recovered after (a) the first cycle; (b) the fifth reaction was also carried out (**Fig. III.19**) and it was possible to underline that, during the reaction recycles, the nickel(0) NPs of **Ni-cat2** remained embedded in the polymer bulk substantially maintaining the urchin-like nanostructure with the same NPs distribution as well as no further particle aggregation.

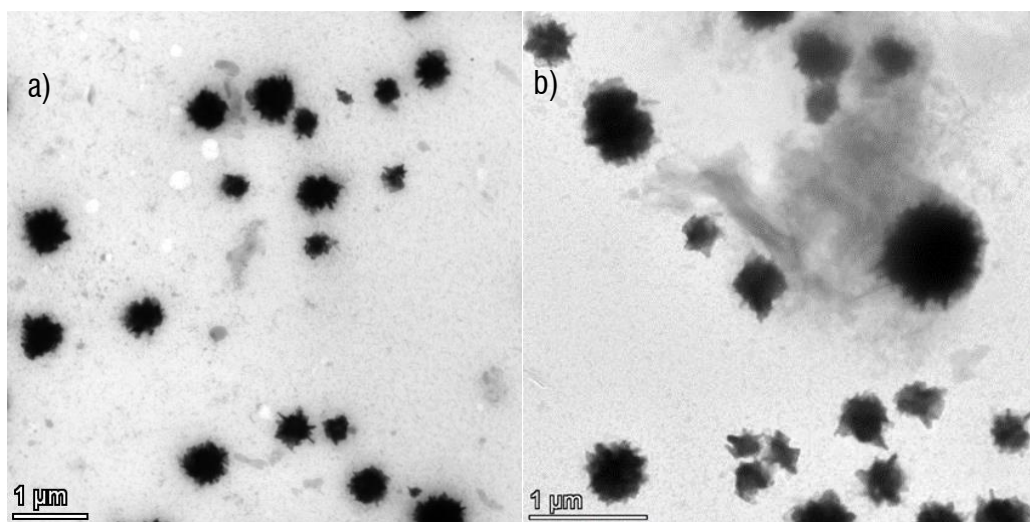


Fig.II 16 a) Ni-cat recovered after the first run of the reduction of nitrobenzene; (b) Ni-p recovered after the fifth run of the reduction of 4-bromonitrobenzene.

3.4 Conclusions

Two new nickel nanoparticles based heterogeneous catalysts (**Ni-cat** and **Ni-cat2**) were prepared from a methacrylic polymer supported Ni(II)-containing acrylamide polymer depending on the cooling step of the calcination procedure. Thanks to their different morphologies of the Ni NPs, **Ni-cat** and **Ni-cat2** have been shown an opposite selectivity in the reduction of nitrobenzene: **Ni-cat** completely converted the nitrobenzene to aniline whereas **Ni-cat2** completely converted the nitrobenzene to azoxybenzene. The peculiar selectivity of **Ni-cat2** is due to its uncommon urchin-like shape for Ni NPs as widely demonstrated by TEM studies. **Ni-cat2** unlike **Ni-cat** is also magnetic, and its magnetic characteristics have facilitated its separation from the reaction mixture. Next, **Ni-cat2** was found to be an efficient catalyst for the selective reduction of a wide range of structurally different nitroarenes towards the corresponding azoxyarenes in good to excellent yields using a small amount of NaBH_4 as reducing agent under very mild conditions. The **Ni-cat2** catalyst also showed true heterogeneity as its effectiveness remains almost same after five cycles of reuse. Moreover, thanks to the magnetic properties of **Ni-cat2** it can be removed easy from the reaction mixture minimizing the use of auxiliary substances and energy.

CHAPTER IV

Experimental section

4.0 Experimental section

4.1 Materials for the synthesis of Co-pol and Ni-pol

All chemicals were purchased from commercial sources and used as received. All manipulations were carried out under inert dinitrogen atmosphere using standard Schlenk techniques unless otherwise specified.

FT-IR spectra (in KBr pellets) were recorded on a Jasco FT/IR 4200 spectrophotometer. Elemental analyses were obtained on a Euro Vector CHNS EA3000 elemental analyzer using acetanilide as analytical standard material. Melting points were determined on a Büchi B-545 melting point apparatus and are uncorrected. The high-resolution mass spectrometry (HRMS) analysis was performed using a Bruker micro TOF QII mass spectrometer equipped with an electrospray ion source operated in positive ion mode. The sample solutions (CH₃OH) were introduced by continuous infusion with a syringe pump at a flow rate of 180 $\mu\text{L min}^{-1}$. The instrument was operated with endplate off set and capillary voltages set to -500 V and -4500 V respectively. The nebulizer pressure was 0.4 bar (N₂), and the drying gas (N₂) flow rate was 4.0 L min⁻¹. Capillary exit and skimmer voltages were 90 V and 30 V, respectively. The drying gas temperature was set at 180 °C. The calibration was carried out with a sodium formate solution (10 mM NaOH in isopropanol/water 1:1 (+0.2% HCOOH) and the software used for the simulations was Bruker Daltonics Data Analysis (version 4.0). Tap water was deionized before use by ionic exchange resins (Millipore). Cobalt and nickel weight percentage in nickel and cobalt catalysts (Co_{%w}, Ni_{%w}) were evaluated after sample mineralization by Graphite Furnace Atomic Absorption Spectroscopy (GFAAS) using a Perkin–Elmer 3110 instrument. The experimental error on the metal percentage was ± 0.3 . Before cobalt and nickel catalysts analyses, mineralization of corresponding polymers were carried by microwave irradiation with an ETHOS E-TOUCH Milestone applicator, after addition of HCl/HNO₃ (3:1 v/v) solution (12 mL) to each weighted sample. Microwave irradiation was used up to 1000 W, the temperature being ramped from room temperature to 220 °C in 10 minutes and the sample being held at this temperature for

10 min. After cooling to room temperature, the digested solution of cobalt or nickel catalyst was diluted to 1000 mL before submitting to GFAAS analysis. Thermogravimetric analyses (TGA) were performed in a nitrogen flow (40 mL min^{-1}) with a Perkin Elmer Pyris 6 TGA in the range from 30 to 800 °C with a heating rate of 10 °C min^{-1} . Triplicate TGA runs have been performed to ensure reproducibility.

Surface morphology was investigated on a selected part of Co and Ni-supported catalyst considered to be representative of the material. Nova Nano SEM 450 manufactured by FEI Company, USA, was used to perform FESEM analysis on the selected samples, equipped with Energy Dispersive X-ray Spectroscopy (X-EDS; Bruker QUANTAX-200) and Electron Backscatter Diffraction (EBSD) detectors (Nordlys with Channel 5 software). Each dried sample of cobalt and nickel catalysts was finely ground and a suspension in water of the fine powder was dropped on common Formvar® coated copper grids. To enhance the resolutions of the scanning micrograph obtained, each grid was coated with gold-palladium alloy (sputtering machine: K550, Emitech Ltd, United Kingdom). The coating thickness was set-up to about 8 nm to avoid alteration of the sample morphology. The stability of the specimen material under the scanning electron beam of the Scanning Transmission Electron Detector (STEM) mode was checked comparing the surface morphology before and after the focusing process; this assured that the originality of the structure, pattern, contour, and texture of the catalyst were not affected by any physical and chemical distortion before and during the FESEM analysis, since low voltage (30 kV) STEM mode was adopted. The STEM allowed transmission images to be taken at a resolution of about 1 nm @300,000x in our samples when observed in high vacuum mode. The particle sizes were analyzed by STEM image analysis using the Image J software (free ware software: <http://rsb.info.nih.gov/ij/>). The dried powder for Ni-cat sample was analyzed by a computer assisted X-ray powder diffractometer (Model X'Pert PRO Philips, Eindhoven, Netherlands) using $\text{CuK}\alpha$ radiation. The X-ray diffraction (XRD) patterns were collected in a 2θ range of 5 to 80° at room temperature, with a step size of 0.02° and a time per step of 6 s.

The magnetic behavior of the annealed materials was preliminarily ascertained by checking whether a neodymium magnet was able to attract the powders. For samples exhibiting magnetic behavior magnetization curves were recorded. For samples exhibiting magnetic behavior field-dependent magnetization loops were recorded at room temperature by using a commercial vibrating sample magnetometer (MicroSense Model 10) with a maximum magnetic field of 2 T.

4.1.1 *Co(AAEMA)₂*

To 6.88 mL of a 1.0 M aqueous solution of NaOH 1.48 g di HAAEMA (6.88 mmol) were added under stirring and within 15 min a clear solution was obtained. 20 mL of water solution containing a mixture of and was left under stirring in nitrogen atmosphere until the formation of an emulsion. Then, 6th the solution of NaAAEMA was added dropwise, at room temperature and within 1 h, to a solution of 1.00 g of $\text{Co}(\text{NO}_3)_2 \cdot 6\text{H}_2\text{O}$ (3.44 mmol) in 20 mL of water causing the precipitation of a violet-pink precipitate, which was recovered by filtration and washed with deionized water (3×10 ml) and with cold $\text{H}_2\text{O}/\text{EtOH}$ (1:1) (3×5 ml). The solid obtained was dried for 12 h under vacuum and rewashed with diethyl ether and acetone Eventually, the pink complex **Co(AAEMA)₂** was dried two days under vacuum. HRMS: (ESI, CH_3OH , positive ion mode) m/z : calc. for $\text{CoC}_{20}\text{H}_{27}\text{O}_{10} [\text{M} + \text{H}]^+$ 486.0947; found 486.0931. IR (cm^{-1}): 1720 (s), 1634 (s), 1619 (s), 1530 (s), 1296 (vs), 1163 (vs), 945 (m), 786 (m). UV-vis (CH_2Cl_2): $\lambda_{\text{max}} = 273$ nm ($\epsilon = 17300 \text{ L mol}^{-1} \text{ cm}^{-1}$). Anal. Calc: C, 49.49; H, 4.40; Co, 12.14. Found: C, 49.55; H, 5.63; Co, 12.48. m.p = 200 ± 0.4 °C. Yield: 62%.

4.1.2 *Co(AAEMA)₂-pol*

$\text{Co}(\text{AAEMA})_2$ (4.0 mmol, 2.0 g) [AAEMA^- = deprotonated form of 2-(acetoacetoxy) ethyl methacrylate] was dissolved in *N,N*-dimethylformamide (DMF, 8 mL) and the resulting solution was added to a mixture of *N,N'*-methylenebisacrylamide (2.4 mmol, 0.36 g) and *N,N*-dimethylacrylamide (33.4 mmol, 3.0 g) in DMF (8 mL), subsequently 5 mg of azaisobutyronitrile were added, and the system heated at 50 °C under vigorous stirring. After 2h, the stirring was blocked by a pink jelly solid, which was filtered off, washed with cold acetone and diethyl ether, dried under vacuum at 50 °C, and then

grinded with a mortar to give a pink powder. IR (cm^{-1}): 3477 (bs), 2923 (bs), 1720 (s), 1622 (s), 1527 (s), 1256 (vs), 1144 (vs), 1355 (s), 780 (m). Elemental analysis (found): C, 56.89; H, 9.39; N, 12.21; Co, 4.15%w.

4.1.3 Co-pol catalyst

The polymers obtained $\text{Co}(\text{AAEMA})_2\text{-pol}$ were put in a tube furnace inserted in A 50 mL stainless steel autoclave equipped with a transducer for online pressure monitoring under nitrogen stream. The autoclave was purged three times with hydrogen then pressurized at 5 Bar. and heated at $10\text{ }^\circ\text{C min}^{-1}$ up to $300\text{ }^\circ\text{C}$, and kept at this temperature for 30 min. Afterwards, the heating was turned off and the whole system was kept closed overnight until it reached room temperature, yielding a black powder referred to as **Co-pol**. Yield: 4.52 g. IR (cm^{-1}): 3480 (bs), 2927 (bs), 1710 (s), 1626 (s), 1490 (m), 1407 (m), 1260 (m), 1144 (s), 1053 (m). Elemental analysis (found): Co, 5.17%w.

4.1.4 Ni(AAEMA)₂

To a solution of KOH (579 mg, 10.3 mmol) in ethanol (10 mL), 2-(acetoacetoxy) ethyl methacrylate (HAAEMA) (2.211 g, 10.3 mmol) was added and left under stirring at room temperature for 5 min. The resulting solution was added to a solution of $\text{Ni}(\text{NO}_3)_2 \cdot 6\text{ H}_2\text{O}$ (1.5 g, 5.16 mmol) in ethanol (15 mL), causing the sudden precipitation of **Ni(AAEMA)₂** as a pale green solid. After 1 h stirring, the solid was filtrated and washed with water ($3 \times 5\text{ mL}$), ethanol ($3 \times 5\text{ mL}$) and pentane ($3 \times 5\text{ mL}$), and dried overnight under vacuum. Anal. Calc. for $\text{NiC}_{20}\text{H}_{26}\text{O}_{10}$: C, 45.00; H, 4.92; Ni, 19.97. Found: C, 44.50; H, 4.99; Ni, 19.76. HRMS: (ESI, CH_3OH , positive ion mode) m/z: calc. for $\text{NiC}_{20}\text{H}_{27}\text{O}_{10} [\text{M} + \text{H}]^+$ 485.0952; found 485.0954. IR (cm^{-1}): 1720 (s), 1635 (s), 1623 (s), 1521 (s), 1385 (vs), 1259 (vs), 1161 (vs), 977 (m), 785 (m). UV-vis (CH_2Cl_2): 280 nm ($\epsilon = 10660\text{ mol L}^{-1}\text{cm}^{-1}$), 227 nm ($\epsilon = 4800\text{ mol L}^{-1}\text{cm}^{-1}$). m.p. = $120.3 \pm 0.4\text{ }^\circ\text{C}$. Yield: 2.01 g, 80%.

4.1.5 Ni(AAEMA)₂-res

Ethyl methacrylate (2.4803 g, 21.6 mmol), ethylene glycol dimethacrylate (119 mg, 0.6 mmol), and azaisobutyronitrile (5 mg) were added to a solution containing Ni(AAEMA)₂ (511 mg, 1.06 mmol) in DMF (2.5 mL) and the resulting green solution was warmed up to 110°C under vigorously stirring for 1 h. The recovered green gel was washed with acetone and left under vacuum for an hour at 110°C to remove residual DMF, and overnight in an oven at 90°C. The dried green solid was then crushed with a mortar. Yield: 2.88 g of methacrylic polymer (**Ni(AAEMA)₂-res**). Elemental analysis (found): Ni, 3.18%w. IR (KBr): (cm⁻¹): 2960(s), 1724(s), 1605 (s), 1506 (s), 1481(vs), 1266 (vs), 1145 (s).

4.1.6 Ni(AAEMA)₂-res1

Ni(AAEMA)₂-res (0.375) was put in a 50 mL stainless steel autoclave under initial dihydrogen pressure of 5 bar, ramped at 10°C min⁻¹ and kept at the final temperature of 300°C for 30 min. Afterwards, the heating was turned off and the whole system was kept closed overnight until it reached room temperature, yielding a black powder referred to as **Ni-res1**. Yield: 0.256 g. Elemental Analysis (found): Ni 5.46%w.

4.1.7 Ni(AAEMA)₂-res2

Ni(AAEMA)₂-res (2.501) was put in a 50 mL stainless steel autoclave under initial dihydrogen pressure of 5 bar, ramped at 10°C min⁻¹ and kept at the final temperature of 300°C for 30 min. Afterwards, the heating was turned off and the autoclave valve was opened, letting air go inside the system. After the autoclave reached room temperature, a black powder was collected and referred to as **Ni-res2**. Yield: 1.704 g. Elemental Analysis (found): Ni 5.71%w.

4.1.8 Ni(AAEMA)₂-cat

Ni(AAEMA)₂ (4.0 mmol, 2.0 g) [AAEMA⁻ = deprotonated form of 2-(acetoacetoxy) ethyl methacrylate] was dissolved in N,N-dimethylformamide (DMF, 5 mL) and the resulting solution was added of a mixture of N,N'-methylenebisacrylamide (1.2 mmol, 0.186 g)

and N,N-dimethylacrylamide (43.2 mmol, 4.434 g) in DMF (6 mL) and heated at 120 °C under vigorous stirring. After 1 h from the addition of azaisobutyronitrile (5 mg), the green jelly solid, which formed in the reaction vessel, was filtered off, washed with acetone and diethyl ether, dried under vacuum, kept overnight in oven at 95 °C and grinded with a mortar to give a pale green powder. Yield: 4.04 g of polymer supported Ni(AAEMA)₂ [Ni(AAEMA)₂-pol]. Elemental Analysis (found): Ni 3.69; C 57.06; H 7.94; N 9.91%. IR(cm⁻¹): 3477 (bs), 2923 (bs), 1720 (s), 1622 (s), 1527 (s), 1256 (vs), 1144 (vs), 1355 (s), 780 (m).

4.1.9 Ni-cat

Ni(AAEMA)₂-cat was put in a 50 mL stainless steel autoclave under initial dihydrogen pressure of 5 bar, ramped at 10°C min⁻¹ and kept at the final temperature of 300°C for 30 min. Afterwards, the heating was turned off and the whole system was kept closed overnight until it reached room temperature, yielding a black powder referred to as **Ni-cat**. Yield: 3.83 g. Elemental Analysis (found): Ni 5.35; C 56.66; H 9.20; N 11.54%. IR (cm⁻¹): 3482 (bs), 2930 (bs), 1720 (s), 1631 (s), 1495 (m), 1402 (m), 1258 (m), 1144 (s), 1053 (m).

4.1.10 Ni-cat2

Ni(AAEMA)₂-pol was put in a 50 mL stainless steel autoclave under initial dihydrogen pressure of 5 bar, ramped at 10°C min⁻¹ and kept at the final temperature of 300°C for 30 min. Afterwards, the heating was turned off and the autoclave valve was opened, letting air go inside the system. After the autoclave reached room temperature, a black powder was collected and referred to as **Ni-cat2**. Yield: 2.013 g. Elemental Analysis (found): Ni 5.35; C 56.66; H 9.20; N 11.54%. IR (cm⁻¹): 3482 (bs), 2930 (bs), 1720 (s), 1631 (s), 1495 (m), 1402 (m), 1258 (m), 1144 (s), 1053 (m).

4.2 Materials and procedure for catalytic reaction

Nitrobenzene was distilled under inert atmosphere before use. All other chemicals were purchased from commercial sources and used as received. All glassware and magnetic stirring bars used in catalytic reactions were kept in an oven at 60 °C for at least two

hours and allowed to cool before use. Monitoring of the reactions was carried out using the technique of thin layer chromatography (TLC) or gas chromatography (GC). For thin layer chromatography silica gel plates Supelco (Aldrich) were used and compounds were visualized by irradiation with UV light source of 254/365 nm. Unless otherwise stated the products were identified by comparison of their GC–MS features with those of authentic samples. Gas chromatography (GC) data were acquired on a HP 6890 instrument equipped with an FID detector and a HP-1 (Crosslinked Methyl Siloxane) capillary column (60.0 m x 0.25 mm x 1.0 μ m). GC–MS data (EI, 70 eV) were acquired on a HP 6890 instrument using a HP-5MS cross-linked 5% phenyl methyl siloxane (30.0 m \times 0.25 mm \times 0.25 m) capillary column coupled with a mass spectrometer HP 5973. GLC analysis of the products was performed using a HP 6890 instrument equipped with an FID detector and a HP-1 (Crosslinked Methyl Siloxane) capillary column (60.0 153 m \times 0.25 mm \times 1.0 m). Conversions and yields were calculated by GLC analysis by using biphenyl as internal standard, or by column chromatography. Column chromatography was performed using Merck® Kieselgel 60 (230–400 mesh) silica gel.

4.2.1 Typical experimental procedure for the reduction of nitroarenes with Co-pol catalyst

0.5 mmol of nitroarene, 11.4 mg of **Co-pol** ($\text{Co}_{\%w} = 5.17$) and 15.0 mmol of sodium borohydride were stirred under nitrogen at room temperature in 2.5 mL of double deionized water and 2.5 mL of diethyl ether for the appropriate amount of time, using a Schlenk tube equipped by a gas bubbler to discharge the hydrogen excess produced during reaction. The progress of the reaction was monitored by GLC. After completion of the reaction, the reaction mixture was centrifuged to separate the catalyst. The solid residue was first washed with deionized water and then with acetone and diethyl ether to remove any traces of organic material. The filtrate containing the reaction mixture was extracted with ethyl acetate (3 \times 5 mL) and then dried over anhydrous Na_2SO_4 . The solvent was evaporated under reduced pressure to yield the crude product, which was then purified by column chromatography using silica gel and n-hexane/ethyl acetate as an eluent to afford the pure product. The products were characterized by GC–MS by comparison with authentic samples. For the assessment of the chromatographic yields, biphenyl (50.0 mg) was used as the internal standard.

4.2.2 Recycling of Co-catalysts

Co-pol (34.2 mg, $\text{Co}_{\%w} = 5.17$), nitrobenzene (1.5 mmol), 15 ml of a mixture $\text{H}_2\text{O}/\text{Et}_2\text{O}$ (1:1=v:v), and NaBH_4 (30 mmol) were introduced in a 100 mL three-necked round flask (equipped with a magnetic stirrer and a gas bubbler), and the mixture was stirred under magnetic stirring at 25 °C until aniline formed (12 h). The reaction mixture was then diluted with 20.0 mL of methanol and centrifugated for separating **Co-pol**, which was washed with methanol (3 × 25.0 mL), water (2 × 25.0 mL) and rinsed in n-hexane (20 mL). The methanol phase was dried (Na_2SO_4) and concentrated under reduced pressure to get the crude product, which was then purified by column chromatography using a short plug of silica gel and eluted with petroleum ether 40–60 °C/dichloromethane in a volume ratio of 7:3 and evaporation of solvents afforded the desired aniline. The recovered **Co-pol** was dried in air at 60 °C for 2 h, and then brought to room temperature, re-weighed, re-calcinated, and then used for the subsequent catalytic cycle. Iteration of this procedure was repeated for five reuses of the catalyst.

4.2.3 Typical experimental procedure for the reduction of nitrobenzene with Ni-res₁ and Ni-res₂

0.50 mmol of nitrobenzene, the catalyst (**Ni-res₁** or **Ni-res₂**, 0.010 mmol of Ni) and 1.7 mmol of sodium borohydride were stirred under nitrogen at room temperature in 5 mL of methanol for the appropriate amount of time, using a three-necked flask equipped by a gas bubbler to discharge the hydrogen excess produced during reaction. The progress of the reaction was monitored by GLC. Chromatographic yields were assessed by using biphenyl as the internal standard.

4.2.4 Typical experimental procedure for the selective reduction of nitroarenes by using Ni-cat2

Ni-cat2 (13.1 mg, $\text{Ni}_{\%w} = 4.47$, 10.0 μmol of Ni), the desired nitroarene (0.50 mmol), methanol (5.0 mL) and NaBH_4 (1.7 mmol) were introduced in a 25 mL Schlenk tube (equipped with a gas bubbler to discharge the dihydrogen excess produced during reaction) and the mixture was stirred under magnetic stirring at 25°C for the time necessary to form the corresponding azoxyarene (monitoring by TLC and/or GC and

GC-MS). The reaction mixture was then diluted with 5.0 mL of dichlorometane and filtered. The solid (**Ni-cat2**) was washed with methanol (3×3.0 mL) and the combined organic layers were dried (Na_2SO_4) and concentrated under reduced pressure to get the crude product, which was then purified by flash column chromatography using silica gel and eluted with the appropriate solvent mixture. Evaporation of solvents afforded the desired azoxyarene. All obtained azoxyarenes were characterized by MS (EI, 70 eV) and the spectra obtained were compared with the standard spectra reported in literature. [rif]

4.2.5 Recycling of catalyst Ni-cat2

Ni-cat2 (66.0 mg, Ni %w = 4.47, 60.0 μmol of Ni), nitrobenzene (3.0 mmol), methanol (30.0 mL) and NaBH_4 (5.1 mmol) were introduced in a 100 mL three-necked round flask (equipped with a magnetic stirrer and a gas bubbler), and the mixture was stirred under magnetic stirring at 25°C until azoxybenzene quantitatively formed (3 h). The reaction mixture was then diluted with 20.0 mL of dichlorometane, and the catalyst was easily removed thanks to its magnetic features by a small neodymium magnet. It was washed with methanol (3×25.0 mL), water (2×25.0 mL) and rinsed in *n*-hexane (20 mL). The organic phase was dried (Na_2SO_4) and concentrated under reduced pressure to get the crude product, which was then purified by flash column chromatography using silica gel and eluted with petroleum ether 40-60°C/dichloromethane in a volume ratio of 7:3 and evaporation of solvents afforded the desired aniline. The recovered Ni-cat1 was dried in air at 60 °C for 2 h, and then brought to room temperature, re-weighed, and used for the subsequent catalytic cycle. Iteration of this procedure was repeated for four reuses of the catalyst.

Conclusions

Conclusions

In conclusion, catalysts to use for sustainable reactions should be active, selective under mild conditions and easily and effectively reusable. A deep investigation about the performance of our cobalt and nickel-based catalysts demonstrated that the developed systems fulfill the aims proposed in this research thesis.

In the first part of the work, the synthesis of the cobalt catalyst **Co-pol** was improved, and its activity was underlined in the reduction of aromatic nitroarenes in aqueous medium at room temperature in the presence of a safe and mild reduction agent like the NaBH_4 .

This heterogeneous catalytic system avoids the formation of dehalogenation side products and can be easily recovered after the reaction occurred and reused at least five times by maintaining good selectivities.

In the second part, new polymers supported Ni(II) complex were synthesized as precursors of Ni(0) NPs obtained from calcination under dihydrogen. Following two different calcination procedures and using various matrices, materials with different morphologies have been obtained.

The different morphologies lead to catalysts that showed an opposite selectivity in the reduction of nitrobenzene.

In particular, a highly selective reduction system was achieved with **Ni-cat2**. It was prepared by copolymerizing Ni(AAEMA)₂ with N,N-dimethylacrylamide and N,N'-methylenebisacrylamide and submitting it to calcination at 300°C under H₂, followed by natural cooling under air at room temperature.

Thanks to its uncommon urchin-like shape for Ni NPs, **Ni-cat2** converted completely the nitrobenzene to azoxybenzene by requiring less time than the other and was found to be active for the selective reduction of a wide range of different nitroarenes towards corresponding azoxyarenes.

Moreover, thanks to its magnetic properties, it can be removed easily from the reaction mixture. Magnetic separation eliminates the necessity of centrifugation, filtration, or other procedures and decreases the costs of the entire catalytic process.

Curriculum vitae

Curriculum vitae



PERSONAL DETAILS:

Name: Valentina Petrelli

Place and date of birth:
Taranto, 22/07/1991

Phone: +39 3423597205

E-mail:
valentina.petrelli@poliba.it

EDUCATION

Polytechnic University of Bari - DICATECh 2018 – 2022
Phd in risk and environmental, territorial, and building development.

Research activity: “Synthesis of metal nanoparticles supported on polymeric matrix and evaluating of their catalytic activity in reaction with low environmental impact”

University of Bari “Aldo Moro” - Department of Pharmacy
2010-2017

Master’s degree in Pharmaceutical Chemistry and Technology
Vote 110/110
Thesis research in Organic Chemistry, titled
“Development of sustainable pyrrolidine supported catalysts”
Performed to Universidad Autonoma de Madrid
Supervisor: Prof. Renzo Luisi
Co-Supervisor: Belen Cid de la Plata

SCHOOLS and COURSE

- **SCI-Puglia** (on-line course) From 24 to 26 November 2021
Scuola di monitoraggio ambientale.
- **S-IN Soluzioni Informatiche S.r.l.** (on-line course)
From 27 September to 1 October 2021
Corso base DOE-Quality by design.
- **S-IN Soluzioni Informatiche S.r.l.** (on-line course) 8-10 June 2021
Analisi Multivariata di dati.
- **GIDRM** (on-line school) 20-23 July 2020
Scuola biennale di risonanza magnetica nucleare (XXII edizione) - Corso avanzato.
- **Bruker Italia S.r.l.** (on-line course) 30 June and 1 July 2021
“NMR quantitativo”.
- **Bruker Italia S.r.l.** (on-line course) 23-24 June 2020
“NMR in campo alimentare e clinico”.

- **University of Bologna** 10-15 June 2019
“The VIII Ciamician Photochemistry School”.

WORK EXPERIENCE

Polytechnic University of Bari - 2018-2022

Supporting for the Chemistry and Chemistry complements course, in degree course of Mechanical Engineering and common courses.

SCIENTIFIC PRODUCTION

A Study of Graphene-Based Copper Catalysts: Copper(I) Nanoplatelets for Batch and Continuous- Flow Applications. De Angelis, S., Franco, M., Trimini, A., González, A., Sainz, R., Degennaro, L., Romanazzi, G., Carlucci, C., Petrelli, V., de la Esperanza, A., Goni, A., Ferritto, R., Cid, M. B. (2019). *Chemistry - an Asian Journal*, 14(17), 3011-3018. doi:10.1002/asia.201900781.

Stable mixed-valence diphenylphosphanido bridged platinum(ii)-platinum(iv) complexes. Fortuño, C., Martín, A., Mastroilli, P., Latronico, M., Petrelli, V., & Todisco, S. (2020). *Dalton Transactions*, 49(15), 4935-4955. doi:10.1039/d0dt00712a.

How the calcination procedure could affect the morphology and the catalytic activity of polymer supported Nickel nanoparticles. Fiore, A.M., Nefedova, D., Dell'Anna, M.M., Petrelli, V., Mali, M., Leonetti, C., Mortarò, C., Catauro, M., Mastroilli, P., Romanazzi, G. (2021) *Macromolecular Symposia*, 395(1) doi:10.1002/masy.202000195.

Metal-based heterogeneous catalysts for one-pot synthesis of secondary anilines from nitroarenes and aldehydes. Romanazzi, G., Petrelli, V., Fiore, A. M., Mastroilli, P., & Dell'Anna, M. M. (2021). *Molecules*, 26(4) doi:10.3390/molecules26041120.

Microwave-Assisted Treatment of Waste Wood Biomass with Deep Eutectic Solvents. Colella, M., Romanazzi, G., Petrelli, V., Baldassarre, F., Ciccarella, G., Catauro, M., Mastroilli, P., Dell'Anna, M. M. *Macromolecular Symposia*. (in course of publication).

CONFERENCES

Poster Presentation:

- VIII AICIng Workshop: Advanced materials for sustainable energy, environmental and sensing applications". Synthesis of polymer supported cobalt nanoparticles and evaluating of their catalytic activity in the reduction of nitroarenes under mild conditions, Lipari, Italy, 27-29 June 2019.
 - Merck Young Chemists' Symposium 2021: Urchin-like Ni-nanoparticles for reduction of nitroarenes towards azoxyarenes under mild conditions. Rimini, 22-24 November 2021.
-

Oral Presentation:

- Workshop Chimica sotto l'albero 2021: ^{13}C CP/MAS NMR: a key to evaluate the dominant conformation of silk materials. Bari, Italy 20 December 2021.
- XII Congresso Nazionale AICing 2021: Efficient and selective reduction of nitroarenes towards azoxyarenes catalyzed by Ni nanoparticles supported on an acrylamide-based resin". Reggio Calabria, Italy, 05-09 September 2021.

References

References

1. J.K.Smith, History of Catalysis. In Encyclopedia of Catalysis. I. Horváth, (2010).
2. J. J. Berzelius, *Reseanteckningar*, P. A. Norstedt & Söner, Stockholm, (1903).
3. H. Heinemann, A brief history of industrial catalysis, in: J. Anderson, M. Boudart (Eds.), *Catalysis Science & Technology*, vol. 1, Springer-Verlag, Berlin, (1981).
4. A. Zecchina and S. Califano, *Development of Catalysis: A History of Key Processes and Personas in Catalytic Science and Technology*, John Wiley & Sons, Inc., Hoboken, NJ, (2017).
5. J.N.Armor, A history of industrial catalysis, *Catalysis Today* 163, 3–9, (2011).
6. P. Sabatier, *La Catalyse en Chimie Organique*, Librairie Polytechnique, Paris, (1913).
7. J. Wisniak, The History of Catalysis. From the Beginning to Nobel Prizes. *Educación Química* 21, 60–69, (2010).
8. F. Haber and R. Le Rossignol, *Ber. Dtsch. Chem. Ges.*, 40, 2144–2154, (1907).
9. J. Hagen, *Industrial Catalysis*, Wiley-VCH, Weinheim, Germany, (2006).
10. C. Bartholomew, R. Farrauto, *Industrial Catalytic Processes*, 2nd ed., Wiley-Interscience, Hoboken, NJ, (2006).
11. E. Mejía, The Royal Society of Chemistry, pp. 1–15, (2020).
12. P. T. Anastas and J. C. Warner, *Green Chemistry: Theory and Practice*, Oxford University Press, New York, (1998).
13. I. Horvath and P. T. Anastas, *Chem. Rev.* 107(6), 2169–2173, (2007).
14. A. Roger Sheldon, Isabel W. C. E. Arends, and Ulf Hanefeld. *Green Chemistry and Catalysis*, Wiley-VCH Verlag GmbH & Co. KGaA: Weinheim. (2007).
15. P. T. Anastas, M.M. Kirchoff, and T.C. Williamson, *Catalysis as a foundational pillar of green chemistry*, *Applied Catalysis a General*, 221, 3, (2001).
16. R. A. Sheldon, in *Industrial Environmental Chemistry*, D. T. Sawyer, A. E. Martell (Eds.), Plenum, New York, pp. 99– 119, (1999).
17. B.M. Trost, *Angew. Chem. Int. (1995). Ed.*, 34, 259–281.
18. Q.-L. Zhou. *Angew. Chem. Int. (2016). Ed.* 55, 5352–5353.
19. F. Hartwig, *Organotransition Metal Chemistry – From Bonding to Catalysis*, University Science Books, (2010).
20. D. Astruc, *Nanoparticles and Catalysis*. Wiley-VCH Verlag GmbH & Co. KGaA, Weinheim, (2008).
21. C. Descorme, P. Gallezot, C. Geantet, C. George, *ChemCatChem*(2012) 4, 1897– 1906.
22. M. Beller, A. Renken, R.A. Van Santen, *Catalysis: From Principles to Applications*, Wiley VCH-Verlag, (2012).
23. H.-J. Arpe, *Industrial Organic Chemistry*, Wiley-VCH, (2010).
24. R. Bates *Organic Synthesis Using Transition Metals*, Second Edition. John Wiley & Sons, Ltd, (2012).
25. D. Wang, D. Astruc, *Chem. Soc. Rev. (2017)* 46, 816–854.
26. M., Lancaster, *Principles of Sustainable and Green Chemistry*, in: *Handbook of Green Chemistry and Technology*. John Wiley & Sons, Ltd, pp. 10–27, (2002).
27. K. Martin., *Green Catalysts for Industry*, in: *Handbook of Green Chemistry and Technology*. John Wiley & Sons, Ltd, pp. 321–337, (2002).
28. B. Cornils, W. A. Herrmann, *Applied Homogeneous Catalysis with Organometallic Compounds*, Wiley-VCH, Weinheim, Germany, (2002).

29. J. Hagen, *Industrial Catalysis: A Practical Approach*, Wiley, (1999).
30. A. Jess and P. Wasserscheid, *Chemical Technology: An Integral Textbook*, Wiley- VCH Verlag GmbH, (2013).
31. K., Tanabe., M., Misono, Y., Ono, H., Hattori, *Catalytic Activity and Selectivity*, in: *New Solid Acids and Bases, Studies in Surface Science and Catalysis*. Elsevier, pp. 215–337, (1989).
32. Ross A. Widenhoefer, *Journal of the American Chemical Society* (2005)127 (25), 9309–9310.
33. G.V., Smith, F., Notheisz, Chapter 1 - Introduction to Catalysis, in: Smith, G.V., Notheisz, F. (Eds.), *Heterogeneous Catalysis in Organic Chemistry*. Academic Press, San Diego, pp. 1–28, (1999).
34. D. J. Cole-Hamilton, *Science*, (2003) 299, 1702–1706.
35. S., Bhaduri, D., Mukesh, *Homogeneous Catalysis: Mechanisms and Industrial Applications*, (2000).
36. S., Bhaduri and D. Mukesh, *Basic Chemical Concepts*. In *Homogeneous Catalysis*, (2014).
37. D. J Cole-Hamilton and R. P. Tooze (eds.), *Catalyst Separation, Recovery and Recycling*, Springer, 1–8, (2000).
38. A.M., Trzeciak, and J.J. Ziolkowski, *Perspectives of rhodium organometallic catalysis. Fundamental and applied aspects of hydroformylation*. *Coord. Chem. Rev.*, (1999)190–192, 883.
39. J.A., Dumesic, G.W. Huber, and M. Boudart. *Principles of Heterogeneous Catalysis*. In *Handbook of Heterogeneous Catalysis* (eds G. Ertl, H. Knözinger, F. Schüth and J. Weitkamp), (2008).
40. G. A., Somorjai. *Introduction to Surface Chemistry and Catalysis*, 2nd ed.; Wiley: New York, (2010).
41. L.M., Rossi, N.J.S., Costa, F.P., Silva, R., Wojcieszak, *Green Chem.* (2014)16, 2906–2933.
42. H.S. Taylor, *A theory of the catalytic surface*. *Proc. R. Soc. Lond.*, A108, 105–111, (1925).
43. G. Rothenberg, *Catalysis: Concepts and Green Applications*. Wiley-VCH Verlag GmbH & Co. KGaA, Weinheim, (2008).
44. J.C., Védrine, *Catalysts* 7(11), 341, (2017).
45. J. Junyong Zhang, C. Gong, X. Zeng, J. Xie *Coord. Chem. Rev.* (2016) 324, 39.
46. R. A. Sheldon and H. van Bekkum, *Fine Chemicals through Heterogeneous Catalysis*. Wiley–VCH: Weinheim, (2001).
47. W. Hunt, (2004) *Journal of the Minerals Metals & Materials Society* 56-13.
48. K. B. Sharpless, *Angew. Chem. Int.* (2002) Ed., 41, 2024-2032.
49. N., Sharma, H., Ojha, A., Bharadwaj, D.P., Pathak, R.K., Sharma, *RSC Adv.* (2015) 5, 53381–53403.
50. M., Nasrollahzadeh, S.M., Sajadi, M., Sajjadi, Z., Issaabadi, (2019) Elsevier, pp. 113–143.
51. P. Khanna, A. Kaur and D. Goyal, *J. Microbiol. Methods*, (2019). 163, 105656.
52. N., Baig, I., Kammakakam, W., Falath, *Mater. Adv.* (2021) 2, 1821–1871.
53. A. C. Jones and M. L. Hitchman, *Royal Society of Chemistry, Cambridge*, (2008) pp. 1–36.

54. P., Iqbal, J.A. Preece, and P.M. Mendes, Nanotechnology: The “Top-Down” and “Bottom-Up” Approaches. In *Supramolecular Chemistry* (eds P.A. Gale and J.W. Steed), (2012).
55. J., Jeevanandam, A., Barhoum, Y. S., Chan, A., Dufresne, M. K. Danquah, Beilstein J. Nanotechnol. (2018) 9, 1050–1074.
56. S., Oliveira, S., Forster, S., Seeger, Nanocatalysis: Academic Discipline and Industrial Realities. *Journal of Nanotechnology* (2014) 1–19.
57. K.J. Klabunde, Introduction to nanotechnology, in *Nanoscale Materials in Chemistry* (ed. K.J. Klabunde), John Wiley & Sons, Inc., Hoboken, USA, pp. 1–13, (2001).
58. M., Boudart, A., Aldag, J.E., Benson, N., Doughart, and C.G. Harkins, *J. Catal.*, (1966).6 (1), 92–99.
59. Van Santen, R.A. *Acc. Chem. Res.*, (2009) 42 (1), 57–66.
60. V. Polshettiwar, *Nanomaterials in Catalysis. Angew. Chem. Int.* (2013) Ed., 52: 11199–11199.
61. B., Corain, G., Schmid, Toshima, *Metal nanoclusters in catalysis and materials science.* Elsevier, (2008).
62. M. Che, C.O. Bennett, in: *Adv. Catal.*, (1989) pp. 55–172.
63. L. D. Rapino, F. F. Nord, *J. Am. Chem. Soc.* (1941) 63, 2745.
64. D. Y. Cha, G. Parravano, *J. Catal.* (1970) 18, 320.
65. M. Haruta, N. Yamada, T. Kobayashi, and S. Lijima, *J. Catal.*, (1989) vol. 115, pp. 301–309.
66. M. L. Toebes, J. A. van Dillen, K. P. de Jong, *J. Mol. Catal. A: Chem.* (2001) 173, 75.
67. S., Shukla, R., Khan, A., Daverey, *Environmental Technology & Innovation* (2021) 24, 101924.
68. C. B. Murray, C. R. Kagan, M. G. Bawendi. *Ann. Rev. Mater. Sci.* (2000) 30, 545.
69. Schmid, G. Metals, in *Nanoscale Materials in Chemistry* (ed. K.J. Klabunde), John Wiley & Sons, Inc., Hoboken, USA, pp. 15–59 (2001).
70. D., Astruc, F. Lu, and J.R. Aranzaes, *Angewandte Chemie International* (2005) Edition, 44: 7852–7872.
71. S., Mourdikoudis, R.M., Pallares, N.T.K., Thanh, *Nanoscale* (2018) 10, 12871–12934.
72. D. Astruc, *Nanoparticles and Catalysis.* WILEY-VCH Verlag GmbH & Co. KGaA, Weinheim, (2008).
73. J. Kiwi, M. Grätzl, *J. Am. Chem. Soc.* (1979) 101, 7214.
74. N. Madhavan, C. W. Jones, and M. Weck, *Accounts of Chemical Research* (2008) 41 (9), 1153–1165.
75. M.J., Ndolomingo, N. Bingwa, & R. Meijboom, *J Mater Sci* (2020) 55, 6195–6241.
76. L. Liu and A. Corma, *Chemical Reviews.* (2018)118 (10), 4981–5079.
77. N. E. Leadbeater and M. Marco, *Chemical Reviews.* (2002) 102 (10), 3217–3274.
78. M. Trueba, and S.P., Trasatti, *Eur. J. Inorg. Chem.*, (2005) 3393–3403.
79. P.S., Shinde, P.S., Suryawanshi, K.K., Patil, V.M., Belekar, S.A., Sankpal, S.D., Delekar, S.A., Jadhav, *J. Compos. Sci.* (2021) 5, 75.
80. S., Bagheri, N., Muhd Julkapli, S., Bee Abd Hamid, *The Scientific World Journal*, (2014), 727496.
81. A. Dobrzyniecka and P. J. Kulesza, *ECS Journal of Solid-State Science and Technology*, (2013) vol. 2, no. 12, pp. M61–M66.
82. D., Wang, D., Astruc, *Chem. Soc. Rev* (2017) 46, 816–854.
83. Y.; Li, X.M.; Hong, D.M.; Collard, El-Sayed, M.A. *Org. Lett.*, (2000) 2, 2385–2388.
84. Narayanan, R.; El-Sayed, M.A. *J. Am. Chem. Soc.* (2003) 125, 8340–8347.

85. Y., Li, M.A. El-Sayed, J. Phys. Chem. B, (2001) 105, 8938–8943.
86. Y., Liu, C., Khemtong, Hu, J. Chem. Commun. 2004.
87. C. Wang, R. Ciganda, L. Salmon, D. Gregurec, J. Irigoyen, S. Moya, J. Ruiz and D. Astruc, *Angew. Chem., Int.* (2016) Ed.55, 3091–3096.
88. M., Benaglia, A., Puglisi, F. Cozzi, *Chem. Rev.* (2003) 103, 3401–3429.
89. J., Lu, P.H., Toy, *Chem. Rev.* (2009) 109, 815–838.
90. A., Zulauf, M., Mellah, X., Hong, E. Schulz. *Dalton Trans.* (2010), 39, 6911–6935.
91. B.M.L., Dijos, I.F.J., Vankekecom, P.A., Jacobs, *Adv. Synth. Catal.* (2006) 348, 1413–1446.
92. D.E., Bergbreiter, *Chem. Rev.* (2002) 102, 3345–3384
93. T.J., Dikerson, N.N., Reed, K.D., Janda, *Chem. Rev.* (2002) 102, 3325–3344.
94. D.E., Bergbreiter, S.D., Sung, *Adv. Synth. Catal.* (2006) 348, 1352–1366.
95. C.G., Frost, L., Mutton, *Green Chem.* (2010) 12, 1687–1703.
96. M., Lamblin, L., Nassar-Hardy, J.-C., Hierso, E., Fouquet, F.-X., Felpin, *Adv. Synth. Catal.* 352, 33 – 79, (2010).
97. J., Lu, P.H., Toy *Chem. Rev.*, (2009) 109, 815–838.
98. B.M.L., Dijos, I.F.J., Vankekecom, P.A, Jacobs. *Adv. Synth. Catal.* (2006) 348, 1413–1446.
99. N.E., Leadbeater, M., Marco. *Chem. Rev.* (2002) 102, 3217–3274.
100. F. R. Hartley *Carbon Bond: Volume 4* John Wiley & Sons, Inc., Chichester, UK, (1987).
101. W.O. Haag, D.D. Whitehurst, German Patent 1,800, 371; *Chem. Abs.* 71 (1969) 114951.
102. H. Sajiki, T. Ikawa, H. Yamada, K. Tsubouchi, K. Hirota, *Tetrahedron Lett.* 44 (2003) 171.
103. K. Huang, L. Xue, Y.-C. Hu, M.-Y. Huang, Y.-Y. Jiang, *React. Funct. Polym.* 50 (2002) 199.
104. K. Huang, L. Xue, Y.-C. Hu, M.-Y. Huang, Y.-Y. Jiang, *Polym. Adv. Technol.* 13 (2002) 165.
105. T., Kaliyappan, P., Kannan. *Coordination polymers, Prog. Polym. Sci.*, (2000) 25, 343–370.
106. M.M., Dell’Anna, G., Romanazzi, P., Mastrorilli. *Curr. Org. Chem.*, (2013) 17, 1236–1273.
107. A., Zoller, K.B., Kockler, M., Rollet, C., Lefay, D., Gignes, C., Barner-Kowollik, Y., Guillaneuf. *Polym. Chem.*, (2016) 7, 5518–5525.
108. H., Schlaad, T., Krasia, M., Antonietti *J. Am. Chem. Soc.*, (2004) 126, 11307–11310.
109. D., Pospiech, D., Jehnichen, S., Starke, F., Müller, T., Bünker, A., Wollenberg, L., Häußler, F., Simon, K., Grundke, U., Oertel, M., Opitz, R., Kruspe. *Appl. Surf. Sci.*, (2017) 399, 205–214.
110. J.J., Wu, P.N., Shek. *J. Biomed. Mater. Res. B Appl. Biomater.* (2009) 90B, 738–44.
111. I., González, G., Arzamendi, J.M., Asua, J.R., Leiza. *Macromol. Mater. Eng.*, (2006) 291, 1185–1193.
112. S.S., Dinachali, M.S.M., Saifullah, R., Ganesan, E.S., Thian. *HeC.*, *Adv. Funct. Mater.* (2013) 23, 2201–2211.
113. W., Zhou, Q., Qu, W., Yu, Z., *An. ACS Macro Lett.*, (2014) 3, 1220–1224.
114. P., Papaphilippou, L., Loizou, N.C., Popa, A., Han, L., Vekas, A., Odysseos, T., Krasia-Christoforou. *Biomacromolecules* (2009) 10, 2662–2671.
115. G., Romanazzi, P., Mastrorilli, M., Latronico, M., Mali, A. Nacci and M.M. Dell’Anna, *Open Chemistry*, (2018) Vol. 16 (Issue 1), pp. 520–534.
116. P., Mastrorilli, A., Rizzuti, G., Romanazzi, G.P., Suranna, R., Gobetto, C.F., Nobile. *J. Mol. Catal. A-Chem.* (2002) 180, 177–185.

117. M.M., Dell'Anna, P., Mastrorilli, A., Rizzuti, G.P., Suranna, C.F., Nobile. *Inorg. Chim. Acta* (2000) 304, 21–25.
118. M.M., Dell'Anna, M., Gagliardi, P., Mastrorilli, G.P., Suranna, C.F., Nobile. *J. Mol. Catal. Chem.* (2000) 158, 515–520.
119. M.M., Dell'Anna, P., Mastrorilli, F., Muscio, C.F., Nobile, G.P., Suranna. *Eur. J. Inorg. Chem.* (2002) 1094–1099.
120. M.M., Dell'Anna, M., Mali, P., Mastrorilli, P. Cotugno, A. Monopoli. *J. Mol. Catal. A-Chem.*, (2014) 386, 114–119.
121. M.M., Dell'Anna, P., Mastrorilli, A., Rizzuti, C., Leonelli. *Appl. Catal. Gen.* (2011) 401, 134–140.
122. M.M., Anna, G., Romanazzi, P., Mastrorilli. *Curr. Org. Chem.* (2013) 17, 1236–1273.
123. M.M., Dell'Anna, P., Mastrorilli, C.F., Nobile, G.P., Suranna. *Journal of Molecular Catalysis A: Chemical* (1995) 103, 17–22.
124. A.M., Fiore, G., Romanazzi, M.M., Dell'Anna, M., Latronico, C., Leonelli, M., Mali, A., Rizzuti, P., Mastrorilli. *Mol. Catal.* (2019) 476, 110507.
125. M.S. Holzwarth, and B. Plietker, *ChemCatChem* (2013) 5: 1650–1679.
126. A.G. Blackman, A.G. *Encyclopedia of Inorganic Chemistry*, First Edition. (2006).
127. H. Beyer, *Lehrbuch der organischen Chemie*, Vol. 24, Hirzel, Stuttgart, (1968) 617.
128. W.A. Herrmann, and B. Cornils, *Applied Homogeneous Catalysis with Organometallic Compounds*, (2017) vol. 1, 1–21. Weinheim: Wiley-VCH.
129. a) M. Hapke, and G. Hilt, *Cobalt Catalysis in Organic Synthesis* (2020) 1:1-23. b) J. Waser, B.Gaspar, H. Nambu, E. M. Carreira *Journal of the American Chemical Society* (2006)128 (35), 11693-11712.
130. a) M.R., Friedfeld, M., Shevlin, J.M. Hoyt, et al. *Science* (2013). 342: 1076–1080. b) P., Jungk, F., Fischer, I., iel, M. J. Hapke. *Org. Chem.* (2015). 80:9781–9793.
131. Xiao-Le Zhou, Fan Yang, Han-Li Sun, Yun-Nian Yin, Wei-Ting Ye, and Rong Zhu, *Journal of the American Chemical Society* (2019) 141 (18), 7250-7255.
132. a) M. Arndt, A. Reinhold, G. Hilt, *J. Org. Chem.* (2010), 75, 5203; b) M. M. P. Grutters, J. I. van der Vlugt, Y. Pei, A. M. Mills, M. Lutz, A. L. Spek, C. Müller, C. Moberg, D. Vogt, *Adv. Synth. Catal.* (2009), 351, 2199. c) Gläsel, T. and Hapke, M. *Cobalt Catalysis in Organic Synthesis*, (2020), 287-335.
133. a) J. Park, and S. Chang, *Angew. Chem. Int. Ed.* (2015) 54: 14103–14107. b) X., Wang, A., Lerchen, and F., Glorius. *Org. Lett.* (2016) 18: 2090–2093. c) A. Baccalini, S. Vergura, P. Dolui, G. Zanon, D. Maiti, *Organic & Biomolecular Chemistry* (2019) vol.17(48) 10119-10141.
134. a) G.G., Melikyan, and E. Artashyan. *Cobalt Catalysis in Organic Synthesis* (2020), 207-234. b) B P. C. B. Widger, S. M. Ahmed, W. Hirahata, R. M. Thomas, E. B. Lokovsky, G. W. Coates, *Chem. Commun.* (2010) 46, 2935.
135. G. Cahiez, A. Moyeux, *Chem. Rev.* (2010) 110, 1435.
136. Ociepa, M. nd Gryko, D. In *Cobalt Catalysis in Organic Synthesis*, (2020) 417-451.
137. a) M.-Y. Lee, Y. Chen, X. P. Zhang, *Organometallics* (2003) 22, 4905. b) F. Denes, A. Perez-Luna, F. Chemla, *Chem. Rev.* (2010) 110, 2366.
138. P. Chirik, R. Morris. *Accounts of Chemical Research* (2015) 48 (9), 2495-2495.
139. Mahmoudi, H., Mahmoudi, M., Doustdar, O., Jahangiri, H., Tsolakis, A., Gu, S., & LechWyszynski, M. *Biofuels Engineering*, (2017) 2, 11 - 31.
140. H.Sohn and U.S. Ozkan *Energy & Fuels* (2016) 30 (7), 5309-5322.
141. V., Andrei, B. Reuillard & E. Reisner. *Nat. Mater.* (2020)19, 189–194.
142. M. Zhen, *Current Catalysis* (2014) 3(1), 15-26.

143. C., Casadevall, H., Zhang, S., Chen, D.J., Sommer, D.-K., Seo, G., Ghirlanda. *Catalysts* (2021) 11, 626.
144. J., Wang, W., Cui, Q., Liu, Z., Xing, A.M., Asiri, and X., Sun, *Adv. Mater.* (2016) 28: 215-230.
145. S., Gao, Y., Lin, X., Jiao et al. *Nature* (2016). 529: 68–71.
146. a) Y., Ohtsuka, K., Koyasu, T., Ikeno, and T., Yamada. *Organic Letters* (2001) 3 (16), 2543-2546. b) M. North, D. L. Usanov, C. Young, *Chem. Rev.* (2008) 108, 5146. c) J. Waser, B. Gaspar, H. Nambu, E. M. Carreira, *J. Am. Chem. Soc.* (2006) 128, 11693.
147. a) D. Wang, and D. Astruc, *Chem. Soc. Rev.* (2017). 46: 816–854.
148. I. Yoshida, H. Kobayashi and K. Ueno, *Bull. Chem. Soc. Jpn.*, 45 (1972) 1411.
149. I. Yoshida, H. Kobayashi and K. Ueno, 45 (1972) 2768.
150. F.A. Cotton and R.C. Elder, *Inorg. Chem.*, 8 (1965) 1145 and reference therein.
151. G., Romanazzi, A.M., Fiore, M., Mali, A., Rizzuti, C., Leonelli, A., Nacci, , P. Mastrorilli & M.M. Dell'Anna. *Molecular Catalysis* (2018) vol. 446, pp. 31-38.
152. a) H. Ma, H. Wang, T. Wu, C. Na, *Appl. Catal. B: Environ.* 180 (2016) 471–479. b) X. Wang, Y. Li, *J. Mol. Catal. A: Chem.* 420 (2016) 56-65 c) P. Zhang, C. Yu, X. Fan, X. Wang, Z. Ling, Z. Wang and J. Qiu, *Phys. Chem. Chem. Phys.*, 2015, 17, 145-150.
153. M.M., Dell'Anna, G., Romanazzi, P., Mastrorilli. (2013). *Current Organic Chemistry* 17, 1236–1273.
154. F. A., Westerhaus, R. V., Jagadeesh, G., Wienhöfer, M.- M., Pohl, J., Radnik, A.-E., Surkus, J., Rabeah, K., Junge, H., Junge, M., Nielsen, et al. *Nat. Chem.* (2013) 5, 537–543.
155. R. V., Jagadeesh, T., Stemmler, A.-E., Surkus, M., Bauer, M.-M., Pohl, J., Radnik, K., Junge, H., Junge, A., Bruckner, M. Beller. *Nat. Protoc.* (2015) 10, 916–926.
156. P. F., Vogt, J. J., Gerulis. In *Ullmann's Encyclopedia of Industrial Chemistry*; Wiley-VCH: Weinheim, Germany, (2000) p.699.
157. H. K., Porter in *Organic Reactions*; John Wiley & Sons, Inc.: Hoboken, NJ, (2011), p.455.
158. Z. Wang in *Comprehensive Organic Name Reactions and Reagents*; Wang, Z., Ed.; Wiley-VCH: Weinheim, Germany, (2010) p.284.
159. H.-J., Arpe. *Industrial Organic Chemistry*; Wiley-VCH, (2010).
160. H.-U., Blaser, H., Steiner, M. Studer. *Selective Catalytic Hydrogenation of Functionalized Nitroarenes: An Update.* *Chem- CatChem* (2009) 1, 210–221
161. B., Amini, S. Lowenkron, In *Kirk-Othmer Encyclopedia of Chemical Technology*; John Wiley & Sons, Inc.: Hoboken, NJ, (2003) p. 783.
162. P., Baumeister, H. U., Blaser, W., Scherrer. In *Studies of Surface Science Catalysis*; Elsevier, (1991) p. 321.
163. H. U., Blaser, U., Siegrist, H., Steiizer, M., Studer. *Aromatic Nitro Compounds.* In: *Fine Chemicals Through Heterogeneous Catalysis*, Sheldon, R. A.; Bekkum, H. v., Eds. Wiley-VCH, 2001.
164. Y., Chen, C., Wang, H., Liu, J., Qiu, X., Bao. *Chem. Commun.* (2005) 5298–5300.
165. a) Corma, A.; Serna, P. *Science* (2006) 313, 332–334. b) Boronat, M.; Concepción, P.; Corma, A.; González, S.; Illas, F.; Serna, P. *J. Am. Chem. Soc.* (2007) 129, 16230–16237.
166. R., Raja, V. B., Golovko, J. M., Thomas, A., Berenguer-Murcia, W., Zhou, S., Xie, B. F. G., Johnson. *Chem. Commun.* (2005) 2026–2028.
167. D., Formenti, F., Ferretti, F.K. Scharnagl and M., Beller. *Chemical Reviews* (2019) 119 (4), 2611-2680.

168. S.C. Amendola, S.L. Sharp-Goldman, M.S. Janjua, N.C. Spencer, M.T. Kelly, P.J. Petillo, M. Binder, (2000) *Int. J. Hydrogen Energy*, 25.
169. M.M., Dell'Anna, S., Intini, G., Romanazzi, A., Rizzuti, C., Leonelli, F., Piccinni, P., Mastroilli. *J. Mol. Catal. Chem.* (2014) 395, 307–314.
170. F. Lo, K. Karan, B. R. Davis, *Ind. Eng. Chem. Res.* 48 (2009) 5177–5184 and references therein.
171. F. Haber, Über Stufenweise Reduktion Des Nitrobenzols Mit Begrenztem Kathodenpotential. *Z. Elektrochem.* (1898) 4, 506–51.
172. P., Serna, A. Corma. *ACS Catal.* (2015) 5, 7114– 121 and references therein.
173. H.I. Schlesinger, H.C. Brown, A.E. Finholt, J.R. Gilbreath, H.R. Hoekstra, E.K. Hyde J. *Am. Chem. Soc.*, 75 (1953), pp. 215-219.
174. J. Wang, L. Hu, X. Cao, J. Lu, X. Li, H. Gu, *RSC Adv.*, 3 (2013), pp. 4899-4902.
175. M. R., Pietrowski. *Curr. Org. Synth.* (2012) 9, 470–487.
176. T., Schwob, R., Kempe. *Angew. Chem., Int. Ed.* (2016) 55, 15175–15179.
177. M., Eckardt, M., Zaheer, R., Kempe. *Sci. Rep.* (2018) 8, 2567.
178. L. Mond, C. Langer, F. Quincke, *J. Chem. Soc.* 1890, 749.
179. P. Sabatier, *Catalysis in Organic Chemistry*; D. Van Nostrand Company: New York, (1922) p 15.
180. Z., Ahmad, 2006. CHAPTER 9 in: Butterworth-Heinemann, Oxford, pp. 479–549.
181. S., Tasker, E. Standley & T., Jamison, (2014) *Nature* **509**, 299–309.
182. Z. Zhuang, S. A. Giles, J. Zheng, G. R. Jenness, S. Caratzoulas, D. G. Vlachos and Y. Yan, *Nat. Commun.*, (2016) 7, 10141.
183. A. Modi, S. Singh and N. Verma, *Electrochim. Acta*, (2016) 190, 620–627.
184. E. J. Park, J. H. Lee, K.-D. Kim, D. H. Kim, M.-G. Jeong and Y. D. Kim, *Catal. Today*, (2016) 260, 100–106.
185. Y. Y. Tong, C. D. Gu, J. L. Zhang, H. Tang, X. L. Wang and J. P. Tu, *Int. J. Hydrogen Energy*, (2016) 41, 6342–6352.
186. I. Buslov, F. Song and X. Hu, *Angew. Chem., Int. Ed.*, (2016) 55, 12295–12299.
187. M. Zhiani and S. Kamali, *Electrocatalysis*, (2016) 7, 466–476.
188. M., Holzwarth, B., Plietker. 2013. *Chem Cat Chem* 5.
189. W. Brenner, P. Heimbach, H. Hey, E. W. Müller, G. Wilke, *Liebigs Ann. Chem.* (1969) 727, 161.
190. Y. Nakao, N. Kashiwara, K. S. Kanyiva, T. Hiyama, *Angew. Chem.* (2010) 122, 4553.
191. K., Tamao, K., Sumitani, M., Kumada (1972) *J Am Chem Soc* 94:4374.
192. R.J.P., Corriu, J.P., Masse. (1972) *J Chem Soc Chem Commun* 3:144.
193. D. Astruc, *Anal Bioanal Chem* 399 (2011)1811–1814.
194. T. Mesganaw & N. K. Garg. (2013) *Org. Process Res. Dev.* 17, 29–39.
195. J. J., Garcia, N. M. Brunkan, & W. D. Jones, (2002) *J. Am. Chem. Soc.* 124, 9547–9555.
196. M., Tobisu, T., Xu, T. Shimasaki, & N. Chatani, *J. Am. Chem. Soc.* 133, 19505–19511(2011).
197. a) A. S. Dudnik & G. C.,Fu. (2012) *J. Am. Chem. Soc.* 134, 10693–10697; b) S. L., Zultanski & G. C., Fu. (2013) *J. Am. Chem. Soc.* 135, 624–627.
198. J.P. Klelman, M. Dubeck, *J. Am. Chem. Soc.* 85 (1963) 1544–15459.
199. N.D., Clement, and K.J. Cavell. (2004) *Angew. Chem. Int. Ed.* 43, 3845–3847.
200. N., Matsuyama, K., Hirano, T., Satoh, and M. Miura. (2009). *Org. Lett.* 11, 4156–4159.
201. T., Yao, K., Hirano, T., Satoh, and M. Miura, (2010). *Chemistry* 16, 12307–12311.
202. K., Muto, J., Yamaguchi, and K. Itami. (2012). *J. Am. Chem. Soc.* 134, 169–172.

203. S. Li, A. Tuel, D. Laprune, F. Meunier and D. Farrusseng, *Chem. Mater.* (2015) 27, 276–282.
204. Z. Zhu, X. Guo, S. Wu, R. Zhang, J. Wang and L. Li, *Ind. Eng. Chem. Res.*, (2011) 50, 13848–13853.
205. S. Pisiewicz, D. Formenti, A.-E. Surkus, M. M. Pohl, J. Radnik, K. Junge, C. Topf, S. Bachmann, M. Scalone and M. Beller, *ChemCatChem*, (2016) 8, 129–134.
206. V. S. Marakatti and S. C. Peter, *New J. Chem.*, (2016) 40, 5448–5457.
207. M.M.Dell'Anna, G.Romanazzi, S.Intini, A.Rizzuti, C.Leonelli, A.F.Piccinni, P. Mastroilli, *J. Mol. Catal. A Chem.* (2015) 402, 83.
208. J.E. Dander, N.K.Garg, *ACS Catal.* (2017) 7, 1413.
209. X.Zhang, J.Yao, X.Ke, *Catal.Lett.* (2018) 148, 1124.
210. J.Weil, H.Yao, Y.Wang, G.Luo, *Ind. Eng. Chem. Res.* (2018) 57, 15039.
211. E. Buncel, *Can. J. Chem.* 78 (2000) 1251 and reference therein.
212. CL, Folcia, I, Alonso, J, Ortega, J, Etxebarria, I, Pintre, MB, *Ros. Chem Mater.* (2006) 18:4617.
213. S. Sakuae, T., Tsubakino, Y., Nishiyama, Y., Ishii, *J. Org. Chem.* (1993) 58, 3633–3638.
214. E. Buncel. *Acc. Chem. Res.* 8 (1975) 132–139.
215. O. H., Wheeler, D., Gonzalez. *Tetrahedron* (1964) 20, 189–193.
216. H. E. Baumgarten, A. Staklis and E. M. Miller, *J. Org. Chem.* (1965) 30, 1203.
217. E. Wenkert and B. Wickberg, *J. Am. Chem. Soc.* (1962) 84, 4914.
218. H. E. Baumgarten, A. Staklis and E. M. Miller, *J. Org. Chem.* (1965) 30, 1203.
219. E. Wenkert and B. Wickberg, *J. Am. Chem. Soc.* (1962) 84, 4914.
220. C. F. Chang and S. T. Liu, *J. Mol. Catal A: Chem.*, (2009) 299, 121
221. G.R. Howe and R.R. Hiatt, *J. org. chem.*, (1970) 35, 4007.
222. K. Kosswig, *Justus Liebigs Ann. Chem.* (1971) 749, 206–208.
223. G. Barak, Y. Sasson, *J. Org. Chem.* (1989) 54, 3484–3486.
224. E. Voutyritsa, A. Theodorou, M. G. Kokotou, C. G. Kokotos, *Green Chem.* (2017) 19, 1291–1298.
225. A. Grirrane, A. Corma and H. Garcia, *Science* (2008) 322, 1661
226. S. Han, Y. Cheng, S. Liu, C. Tao, A. Wang, W. Wei, H. Yu, Y. Wei, *Angew. Chem. Int. Ed.* (2021) 60, 6382.
227. S. Acharyya, S. Ghosh, and R. Bal *ACS Sustainable Chemistry & Engineering* (2014) 2 (4), 584-589.
228. C. F. Chang, S. T. Liu *Journal of Molecular Catalysis A: Chemical* 299 (2009) 121–126.
229. H.Y. Zhu, X.B. Ke, X.Z. Yang, S. Sarina, H.W. Liu, *Angew. Chem. Int. Ed.* 49 (2010) 9657.
230. B. Zhang, H. Asakura, J. Zhang, J. Zhang, S. De, N. Yan, *Angew. Chem. Int. Ed.* 55 (2016) 8319–8323.
231. A., Shukla, R.K., Singha, T., Sasaki, S., Adak, S., Bhandari, V.V.D.N., Prasad, A., Bordoloi, R., Bal, (2020) *Molecular Catalysis* 490, 110943.
232. Z. Liu, Y. Huang, Q. Xiao, H. Zhu, *Green Chem.* 18 (2016) 817–825.
233. Q., Xiao, Z., Liu, F., Wang, S., Sarina, H., Zhu. (2017) *Applied Catalysis B: Environmental* 209
234. F. Ferlin, M. Cappelletti, R. Vivani, M. Pica, O. Piermatti, L. Vaccaro, *Green Chem.* 21 (2019) 614–626.
235. B., Zhou, J., Song, T., Wu, H., Liu, C., Xie, G., Yang, B., Han. (2016) *Green Chem.* 18, 3852–3857.

236. N., Sakai, K., Fujii, S., Nabeshima, R. Ikeda, & T. Konakahara, (2010) *Chem. Commun.* 46, 3173–3175.
237. Z.-P. Zhang, X.-Y. Wang, K. Yuan, W. Zhu, T. Zhang, Y.-H. Wang, J. Ke, X.-Y. Zheng, C.-H. Yan, Y.-W. Zhang, *Nanoscale* 8 (2016) 15744–15752.
238. M.N. Pahalagedara, L.R. Pahalagedara, J. He, R. Miao, B. Gottlieb, D. Rathnayake, S.L. Suib, *J. Catal.* 336 (2016) 41–48.
239. T. Hou, Y. Wang, J. Zhang, M. Li, J. Lu, M. Heggen, C. Sievers, F. Wang, *J. Catal.* 353 (2017) 107–115.
240. L. Liu, P. Concepción, A. Corma, *J. Catal.* 369 (2019) 312–323.
241. B., Liu, L., Liu, X., Liu, M., Liu, Y., Xiao. (2009) *Materials Science and Technology* 28, 1345–1348.
242. J., Richardson, R., Scates, M., Twigg. (2003) *Applied Catalysis A: General* 246, 137–150.
243. X., He, H., Shi, (2012). *Particuology* 10, 497–502.
244. a) P. Das, A. N. Biswas, S. Acharya, A. Choudhury, P. Bandyopadhyay, P. K. Mandal, S. Upreti. (2009) *Molecular Crystals and Liquid Crystals* 501:1, pages 53–61; b) Das, P., Neogi, D., Upreti, S., Mandal, P., Bandyopadhyay, P., (2005) *Acta Crystallographica Section E* 61.

